

© 2025 by Nathan Sean Ryan. All rights reserved.

LEU+ TO HALEU NUCLEAR FUEL CYCLE TRANSITIONS AND DYNAMIC REACTOR MODELS

BY

NATHAN SEAN RYAN

THESIS

Submitted in partial fulfillment of the requirements
for the degree of Master of Science in Nuclear, Plasma, Radiological Engineering
in the Graduate College of the
University of Illinois at Urbana-Champaign, 2025

Urbana, Illinois

Master's Committee:

Assistant Professor Madicken Munk, Advisor
Associate Professor Kathryn D. Huff, Co- Advisor
Professor Rizwan Uddin

Abstract

Understanding the nuclear fuel cycle is crucial when designing sustainable and efficient nuclear energy systems. This thesis studies timely transition scenarios for fleets of Micro Modular Reactors (MMRs), X-Energy Xe-100s (Xe-100s), and AP1000s where low-enriched uranium plus (LEU+) fuel delays the demand for high-assay low-enriched uranium (HALEU) for the TRi-structural ISOtropic (TRISO) fueled reactors through a greedy, random, and initially random then greedy deployment scheme to meet energy demand growths from the U.S. Department of Energy (DOE) and U.S. Energy Information Administration (EIA). Using the open-source code Cyclus to model fuel cycles and the Monte Carlo code Serpent to perform neutronics calculations for the Xe-100 and USNC MMR, the results show that the reactor deployment scheme impacts the separative work units (SWU) required to meet energy demand. The greedy scheme, which prefers the highest capacity reactors, leads to the most significant increase in SWU for AP1000 low-enriched uranium (LEU), while the random and initially random then greedy schemes result in more consistent increases across fuel types. By evaluating the masses of fresh and used fuel, SWU, the number of reactors, and how well each simulation meets the projected energy demand, this thesis provides a comprehensive understanding of the impact of reactor deployment schemes on the nuclear fuel cycle.

Additionally, this thesis examines the computational complexity of reactor fuel trading and removes assumptions about reactor power. The Trading On-Demand (TOD) reactor reduces the number of instructions in a simulation by trading fuel only when needed, while the Dynamic Power Reactor (DPR) allows for flexible power output to mirror historical or projected capacity factors. The results show that improving reactor models and simulating fuel cycle transitions leads to more efficient reactor deployment and fuel cycle design.

Keywords: Cyclus, TRISO, HALEU, LEU+, LEU Plus, Serpent, Nuclear Fuel Cycle, Memory Efficiency, Dynamic Power, Fuel Trading, Reactor Deployment, Advanced Reactors

Acknowledgments

I would like to thank Prof. Madicken Munk, who mentored me as a student and who constantly inspires me to think big and find the impact in my work. Relatedly, I would like to thank Prof. Kathryn Huff, who has been a mentor to me at every step of my collegiate education and who shows me how to be a happy warrior.

I want to thank my fellow graduate students and the members of Advanced Reactors and Fuel Cycles (ARFC); particularly Dr. Amanda Bachmann, Sam Dotson, Nataly Panczyk, Olek Yardas, Zoë Richter, Dr. Gwendolyn Chee, Dr. Sun Myung Park, Rhys MacMillian, and Ceser Zambrano. I would like to especially thank Luke Seifert for his assistance in running the Serpent simulations in this thesis.

Throughout the years, I have learned much from my group mates, advisors, and mentors, but I would be remiss not to acknowledge that I went to the school of open source and learned much from countless developers who work openly to better science. Particularly the CYCLUS community, especially Prof. Paul P.H. Wilson, Dr. Katie Mumma, Jin Whan Bae, and Dr. Eva Davidson.

I owe many thanks to my parents, brother, grandparents, family, partner, and friends who have reminded me—sometimes to my chagrin—that life keeps going outside the walls of my office. To my cousin Matthew, I can not wait to explain this part of my life to you someday when we are reunited because I know you will have questions.

This research was performed, in part, using funding received from the DOE Office of Nuclear Energy's Nuclear Energy University Program (Project 23-29656 DE-NE0009390) 'Illuminating Emerging Supply Chain and Waste Management Challenges'.

This research was supported in part by an appointment to the Oak Ridge National Laboratory Research Student Internships Program, sponsored by the U.S. Department of Energy and administered by the Oak Ridge Institute for Science and Education.

Table of Contents

Chapter 1 Introduction	1
Chapter 2 Background & Motivation	5
2.1 Energy System Modeling	5
2.2 The Nuclear Fuel Cycle	7
2.3 CYCLUS	11
2.4 Fuel Enrichment	14
2.5 TRISO Fuel	16
2.6 Reactor Models	17
Chapter 3 Deployment Scenarios	24
3.1 Transition Scenarios	24
3.2 Metrics	28
3.3 Greedy Deployment	30
3.4 Random Deployment	38
3.5 Initially Random, Greedy Deployment	46
Chapter 4 Reactor Power and Market Interactions	55
4.1 Archetypes and Time Management	55
4.2 Trading On-Demand Reactor	56
4.3 Dynamic Power Reactor	59
Chapter 5 Conclusions	62
5.1 Transition Scenarios Conclusions and Limitations	62
5.2 Reactor Power and Market Interaction Conclusions and Limitations	64
References	66
Appendix A LWRs Simulated	71
Appendix B Considered Deployment Schemes	77
B.1 Capped Deployment	77
B.2 Pre-Determined Distribution Deployment	79

Chapter 1

Introduction

While the world grapples with the effects of climate change, the demand for clean and firm power continues to increase. Utilities and decision-makers face rising energy demands of machine learning and data center companies, which require a constant and reliable energy source. The escalation of data center demand and electrification in the economy has led the U.S. Energy Information Administration (EIA) to forego publishing its annual energy outlook report in 2023 as it evaluates its models under emergent market pressures [1]. New nuclear reactors—designed to be more efficient, flexible, and resilient than the reactors that have come before them—can provide clean energy to meet these demands.

Since 1959, the United States (U.S.) has commercially operated large Light Water Reactor (LWR) designs at nuclear power plants. These reactors use light water as a coolant and moderator; commercial designs are either Pressurized Water Reactors (PWRs) or Boiling Water Reactors (BWRs). As shown in Figure 1.1, the LWR fleet in the U.S. expanded power capacity over roughly 20 years before achieving just over 99 GWe in 1990 and remained roughly constant in the years since then. With the recent connection of Vogtle Units 3 and 4 to the grid, the U.S. has seen the first new LWR units come online in 8 years—following the completion of Watts Bar-2 in 2016.

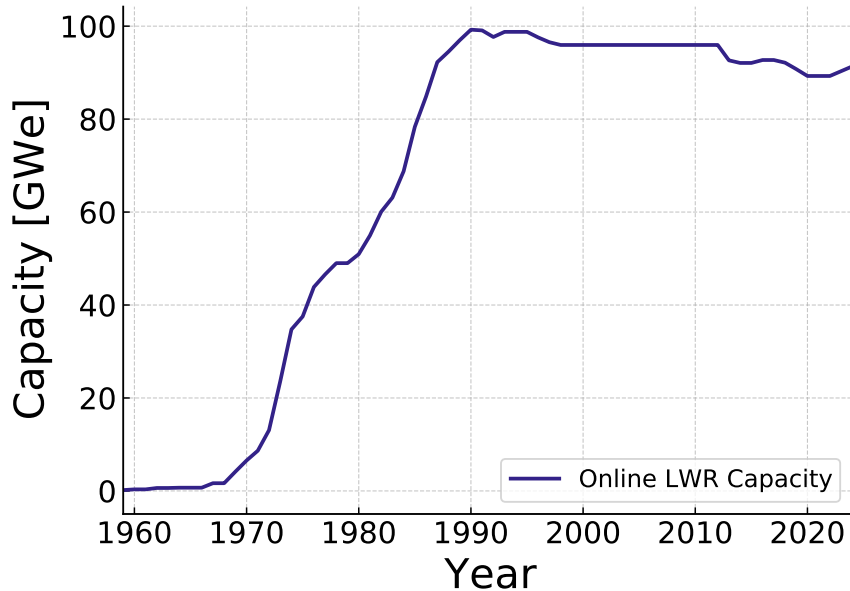


Figure 1.1: US LWR capacity through 2024. Reproduced from [2].

According to the EIA, nuclear power plants produced 18% of utility-scale electricity generation in 2023 [3], meaning nuclear energy was 46.5% of total clean energy generation and the largest clean energy source in the country. The last license in the fleet will now expire in 2063 following the completion of Vogtle Unit 4. However, to meet growing energy demands, the U.S. will need to replace and expand the current fleet as it retires over that time; deploying new reactors at a rate that has not been seen since the 1970s. The U.S. Department of Energy (DOE) has published a liftoff report on how nuclear energy can expand to meet future demands and has outlined myriad scenarios that could lead to a 100% net zero carbon by 2050 [4]. One of the striking takeaways from the liftoff report is the necessity of tripling nuclear energy demand by 2050 due to new capacity demand, the retirement of fossil fuels, electrification of the economy, and other behind-the-meter applications of nuclear technologies. The future that the DOE outlines is complicated by the decrease in uranium concentrate production in the U.S. (highlighted in the EIA 2023 Domestic Uranium Production Report) and the increasing number of decommissioned or dormant fuel cycle facilities [5] as suppliers have optimized services for our existing fleet.

Despite these declines, the DOE liftoff report asserts that high-value propositions in low land use, firm power generation, direct heat applications, local economic benefits, and the low transmission build-out associated with nuclear energy make it a compelling choice. Some of these benefits can be reflected in the 73% increase in U.S. uranium production workers from 2022 to 2023, the 4x increase in exploration of uranium resources, and a \$20 million increase in resource investment [5]; the private sector is starting to move on the value proposition of nuclear

energy.

The current fleet of LWRs has been the backbone of the commercial nuclear industry, but the industry is on the precipice of a different generation of reactor technologies. The fleet of LWRs uses a ceramic uranium oxide fuel that is enriched to 3-5% ^{235}U , but there is a panoply of advanced reactor designs at various stages of deployment using decades of experience with generating nuclear energy. These reactors vary in size from large gigawatt-scale reactors to smaller reactors designed to fit on the back of a truck. The design space is vast, but one innovation that has been a focus of the nuclear industry is the TRi-structural ISOtropic (TRISO) fuel particle. This fuel particle is a small sphere of uranium fuel coated in carbon and silicon carbide layers. TRISO is designed to be more robust than traditional fuel and has been the proposed fuel form for higher-enrichment designs that require high-assay low-enriched uranium (HALEU) (5-20%).

The nuclear fuel cycle (NFC) describes the steps nuclear fuel goes through from mined uranium to eventual disposal. Figure 1.2 outlines a simple *once-through* fuel cycle (so-called because the fuel goes through the cycle once in its lifetime). The fuel cycle begins with mining uranium ore, typically from uraninite or pitchblende deposits. Then, the ore must be milled and refined into yellowcake, which can then be converted into uranium hexafluoride. To power the reactors in the U.S., the uranium hexafluoride is then enriched to the desired percentage of ^{235}U and converted into uranium dioxide. Reactor operators receive the fuel in rods after it has been fabricated into fuel pellets from uranium dioxide. Upon receiving the fuel, workers load the rods into the reactor to generate heat. The heat generates steam, which drives a turbine and generates electricity. After years of operation, workers remove the used fuel from the reactor and store it in a spent fuel pool. After cooling, transporters move the used fuel to dry cask storage, where it will remain until policymakers act to enable a long-term solution.

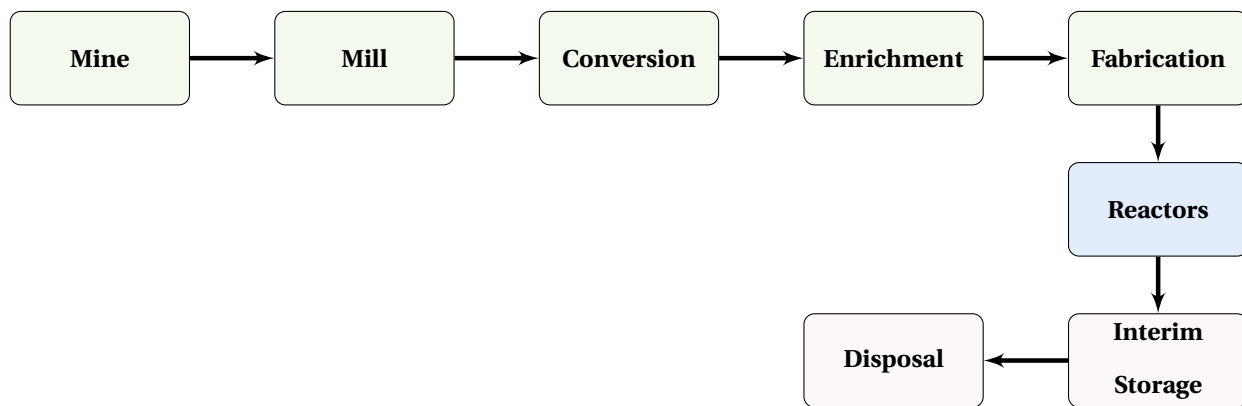


Figure 1.2: Hypothetical once-through fuel cycle, akin to the U.S., where the front end of the fuel cycle (the top row in green) supplies fuel to a fleet of reactors (the middle row in blue), and the back end of the fuel cycle disposes of the Used Nuclear Fuel (UNF) (bottom line in purple).

Although linear in 1.2, in reality these steps are interwoven with multilateral relationships and long-term

purchasing agreements that complicate the establishment of new supply chains. Consequently, the multiplicity of facilities and availability of services at each step in the fuel cycle is difficult to model; this is where the CYCLUS [6] tool is valuable. CYCLUS is a nuclear fuel cycle simulator that allows users to model the material movement between facilities in discrete-event simulations. These facilities are run by agents that make decisions and interact with other agents. Because CYCLUS is designed to be technology agnostic, it can model a variety of fuel cycles and reactor types—although it is not primarily a physics engine, so coupling it with physics software can be necessary for some problems.

Partners in industry, academia, and government are building the body of literature surrounding TRISO fuel cycles. This thesis is a timely evaluation of various energy-demand scenarios and an optimization of the deployment of advanced reactors building off of the method established by Bachmann et al. [7] for HALEU fuel, incorporating a phased enrichment demand that advanced reactor companies could explore as the HALEU supply chain develops. This thesis presents the potential for advanced reactor deployment in the U.S. and the implications of the fuel cycle on the deployment of these reactors, as some designs adopt a staggered enrichment demand for various TRISO fuels. Metrics used to evaluate the scenarios include: separative work units (SWU), energy output, mass of fuel, and reactor deployment timeline. In service of this goal, this thesis will also examine the computational efficiency of the Dynamic Resource Exchange (DRE) in CYCLUS to contribute to a robust tool for future analysis.

The structure of this thesis is as follows:

- Chapter 2 provides background information relevant to the work. This includes an outline of energy system modeling, key information about the reactors investigated in this thesis, the types of fuel, and the CYCLUS tool as pertinent.
- Chapter 3 discusses deployment schemes, the metrics used to evaluate the scenarios, and presents the results of each.
- Chapter 4 outlines two new reactor archetypes, and compares them to the CYCLOMOR reactor.
- Chapter 5 concludes the work, discusses the assumptions and limitations, and presents directions for future work.
- Appendix A shows the details for each reactor in the "existing fleet."
- Appendix B discusses the reactor deployment schemes that were not used in this thesis.

Chapter 2

Background & Motivation

The United States (U.S.) contributed over 12.5% of 2020 global carbon emissions [8]. Local, state, and national governmental bodies have announced myriad programs to support clean energy projects in response to growing climate concerns. Elisa Papadis and George Tsatsaronis set out to characterize and identify a well-designed policy framework for decarbonization in their 2020 paper, surmising that should consist of "carefully introduced targeted investment subsidies, performance standards and mandates, communication and education campaigns and a CO₂ tax for global aviation and shipping" [9]. This approach will require geographically bespoke solutions that draw in stakeholders to focus on serving the needs of the future. They advocate for expansion and maintenance investments in the complex U.S. power grid to accommodate flexibly generated capacity.

Flexibility is a ubiquitous goal of decarbonizing industries, like producers of large volume/low-profit goods [10], or farm researchers who highlight the growing importance of human intervention as climate change impacts their crop in a negative feedback cycle [11]. Focusing efforts where investment can have the largest impact in the shortest time would further this goal of flexibility. This thesis characterizes nuclear fuel cycle (NFC) options and improvements to existing fuel cycle models to support further flexibility and fidelity in NFC and nuclear power plant models.

2.1 Energy System Modeling

Nations such as the U.S. and the United Kingdom (UK) centralized their electrical infrastructure as it developed, which Dieter Helm from the University of Oxford describes as prevailing until the end of the 1970s [12]. Evidence of this style of centralized energy system planning can be found in 1967 in nationalized industry reports from the UK [13] and was a top-of-mind consideration in the U.S. and other countries.

In 1973, Michael Posner from the University of Cambridge published his book *Fuel Policy A Study In Applied Economics* [14], which describes methods large institutions could use to make energy decisions. In connection with the 1973 oil crisis, many countries enhanced their predictive capabilities for energy markets. The crisis led to the development of energy planning models that could be used to evaluate the impact of different policies on energy

systems as disruptions tend to do [15]. The International Institute for Applied Systems Analysis (IIASA), founded in 1972, and the International Energy Agency (IEA), founded in 1974, have served international communities with Energy System Model (ESM) tools since the 1973 oil crisis. The resulting models were used to develop long-term energy plans to help countries increase their energy security, facilitate economic development, and better legislate with increasingly complex energy systems.

Today, utilities, countries, and other organizations use ESMs to preempt behavior under different economic conditions, such as the cost of energy, the price of carbon, and the availability of financing. The goal can be any combination of developing favorable conditions for new technologies, understanding the relationship between actors, predicting future trends, and the impact of different policies on energy systems. Decision-makers compare the behavior of energy systems in various scenarios to a baseline, such as business-as-usual scenarios compared with low-carbon or high-renewable scenarios. These are effective across regulated, deregulated, and hybrid markets. As ESMs have evolved, they have become more sophisticated. Now, they can model the behavior of energy systems in different sociotechnical contexts, such as the adoption of energy efficiency measures, the acceptance of energy technologies, and the resistance to new energy projects.

Pfenninger et al. [16] describe four paradigms of energy system modeling: optimization, simulation, econometric, and hybrid models. In the optimization paradigm, the modeler seeks a normative solution to a problem by minimizing or maximizing an objective function subject to constraints. In the simulation paradigm, the modeler aims to predict the behavior of the energy system by simulating the interactions between different system components. In the econometric, or market, paradigm, the modeler seeks to understand the relationship between different operational variables in the energy system by estimating the parameters of a statistical model. The hybrid paradigm is a catch-all for narrative scenarios that combine the paradigms to develop a more comprehensive understanding of the energy system.

Although there are myriad paradigms of ESM, two philosophies (top-down and bottom-up) to their construction dictate the restrictions a model will place on the type of questions it can answer. In the top-down approach, the modeler starts with a high-level view of the energy system and then drills into the details. This approach aids in understanding the overall behavior of the energy system and the impact of different policies on the system [17]. In the bottom-up approach, the modeler starts with the details of the energy system and then builds up to a high-level view. This approach is useful for understanding the behavior of individual components of the energy system and the impact of different technologies on the system [18, 17].

2.2 The Nuclear Fuel Cycle

Starting with President Eisenhower's Atoms for Peace speech in 1953 [19], the international community has been working toward the peaceful use of nuclear energy while reducing proliferation routes. Nuclear safeguards were formally introduced with the creation of the International Atomic Energy Agency (IAEA) in 1957, which conducts inspections and verifies compliance with safeguards agreements and supports states building facilities to meet its standards [20]. Compliance is verified through regular inspections, data analysis, and cooperation between the IAEA and member states. Countries must declare their nuclear activities, and inspectors perform unannounced visits to nuclear facilities to ensure compliance. As of November 2024, the IAEA has 180 member states, with the addition of the Cook Islands and Somalia.

The nuclear fuel cycle (NFC) is present in various IAEA member states and is a series of industrial processes that produce and consume nuclear fuel. Commonly, the fuel cycle is discussed with two categories, the front end and back end. The U.S. keeps these facilities separate, in the front end of the fuel cycle, in a "collect and wait" pathway [21]. Without a long-term or interim solution for the Used Nuclear Fuel (UNF), the back end of the NFC is collocated with the reactors that burn the fuel (with the minor exception of the consolidated storage facility in Morris, Illinois). This thesis will restrict discussion of the fuel cycle to fuel alone.

Companies can reprocess and recycle nuclear fuel into a different fuel type that can produce usable power for several cycles, called a "closed" fuel cycle. As outlined in Figure 1.2, the "open" fuel cycle is a one-time use of fuel that is then stored in a repository. The closed fuel cycle is a more sustainable option, as it reduces the amount of waste stored in a repository by adding an extra step for reprocessing and recycling the used fuel into new fuel—as shown in Figure 2.1. However, a closed fuel cycle is currently more expensive and may pose proliferation risks associated with reprocessing fuel. The open fuel cycle is less costly and has fewer proliferation risks, but it produces more waste that must be stored in a repository. Choosing an open or closed fuel cycle is a policy decision for the country using nuclear technology.

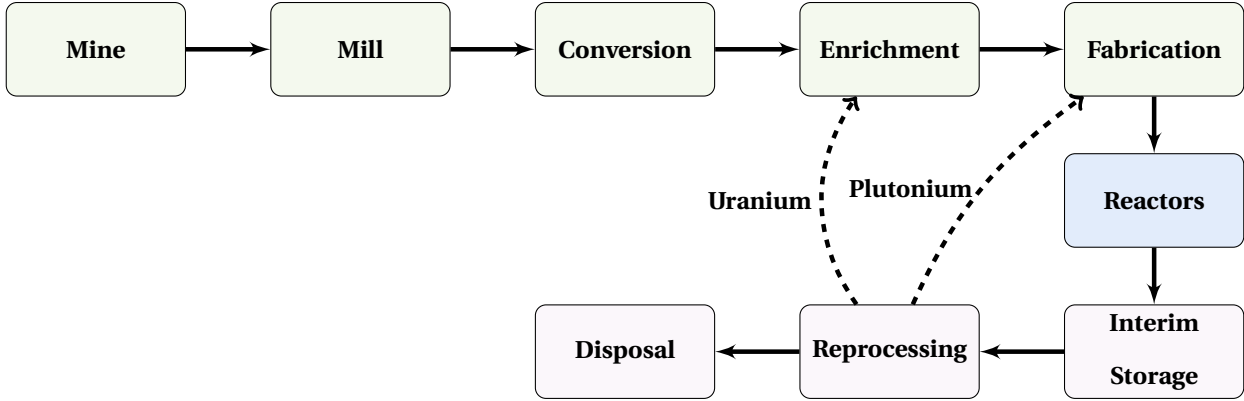


Figure 2.1: Hypothetical closed fuel cycle where the front end of the fuel cycle results in an initial fuel form, which moves to the reactor before entering the back end of the fuel cycle for reprocessing and disposal. The top row in green represents the front end of the fuel cycle, the middle row in blue represents the reactor fleet, and the bottom row in purple represents the back end of the fuel cycle.

2.2.1 Front End of the Fuel Cycle

The Nuclear Energy Agency (NEA) and IAEA publish a biennial report on the state of the global uranium market, called the *Red Book*. At the time of writing the 2024 *Red Book* is not public; however, interested parties can extrapolate trends from the 2022 *Red Book* report on global Uranium availability, which covers January 2019 to January 2021 and updates the projections from 54 countries of their uranium supply and resources through 2040 [22].

Globally, Australia holds the most significant reasonably assured resources of uranium at roughly 28% of the world's total. However, total identified recoverable resources declined 2% from 2019 to 2021—in contrast with slight increases reported in previous versions of the report—as countries increased mining efforts, reclassified economic viability of inferred resources, and currency values fluctuated with inflation. Among the most well-established uranium exporters like Australia, Canada, and Kazakhstan, re-evaluations of inferred resources accounted for decreases in nearly every quality category, while relatively new exporters, Mongolia and Niger, reported increases in inferred resources [22]. This thesis focuses on the U.S. explicitly and does not incorporate geospatial information, as such it does not present the real limitations of an international fuel cycle.

The U.S. imports more uranium than it produces domestically, as shown in Figure 2.2, from countries with large uranium deposits like Canada, Australia, and Kazakhstan. This trend is expected to continue as investments from the U.S. in new uranium mines could change the domestic availability of uranium ores.

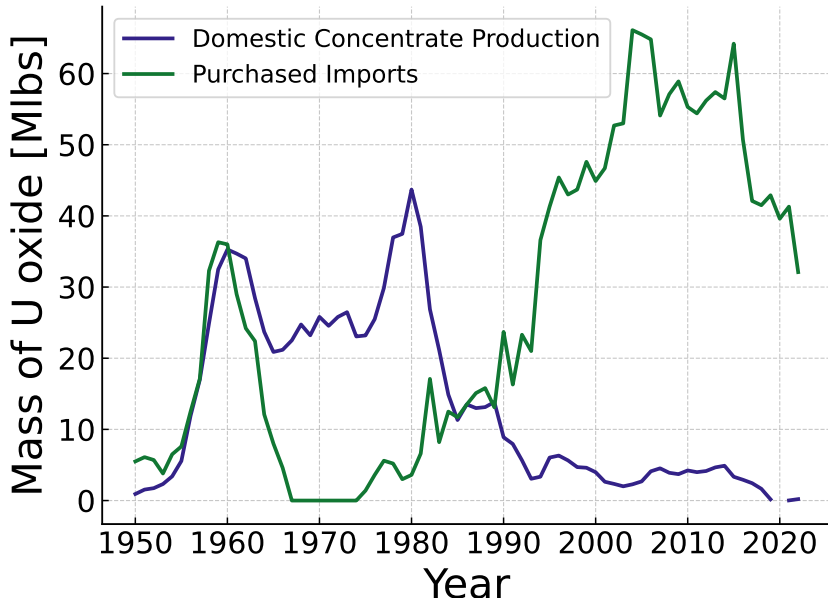


Figure 2.2: Foreign and domestic uranium purchases over time. Reproduced from [23].

As the 2022 *Red Book* notes, the literature surrounding the understanding of best practices for environmental stewardship and remediation of mines is growing. Once-common practices of strip, pit, and underground mining are beginning to be replaced with more sustainable practices that minimize the environmental impact of mining. One method that has garnered interest in the uranium mining community is in-situ leaching, wherein automatic pumps inject a leaching solution into the ground to dissolve the uranium and then pump the solution to the surface for processing [24]. In-situ leaching is limited to areas with favorable permeabilities, but the reduced labor intensity, simplified infrastructure requirements, and lower environmental impact make it an attractive option for uranium mining where applicable.

In-situ leaching also reduces the extent of the milling process as the ratio of desirable material to non-desirable material is higher in the leaching solution than in the resultant material from traditional mining. The milling process generally involves crushing the ore into a fine powder and then leaching the uranium from the ore with a sulfuric acid solution. Workers then extract the uranium from the solution and convert it into yellowcake (U_3O_8), a concentrated form of uranium oxide [25]. The yellowcake is then shipped to a conversion facility, where it is converted into uranium hexafluoride (UF_6), a gas that cools to a liquid and then a solid before it is transported to be enriched. Uranium hexafluoride is attractive in the enrichment process because fluorine has only one naturally occurring isotope and is easy to ensure isolation from the uranium.

Up to the enrichment stage of the fuel cycle, the process is almost entirely agnostic to the end use of the uranium

fuel. Leaving the conversion stage, UF_6 enters the enrichment process aims to achieve a specific concentration or weight percent of ^{235}U relative to the other uranium isotopes. Today, enrichment relies on centrifuges, which separate the isotopes based on their mass; however, historical gaseous diffusion technology could potentially use laser enrichment if it becomes economically viable. This thesis does not distinguish between enrichment services; instead, using separative work units (SWU), which Section 3.2.1 expands on, to quantify the enrichment delivered.

The enriched UF_6 is then converted into uranium dioxide (UO_2) and fabricated into fuel. For the U.S. fleet of large Light Water Reactors (LWRs), the fuel is made into pellets, stacked into rods, and collected into assemblies. This is not the case for every reactor design, as some reactors use prismatic, pebble, or liquid fuel elements. As with enrichment, the fabrication stage of the fuel cycle is simplified in this thesis, and this thesis does not incorporate explicit details of the fabrication process.

2.2.2 Reactor Operation

Up to now, this section has laid out the front end of the fuel cycle. The part of the NFC where the fuel is used in the reactor is neither at the front nor back of the fuel cycle. Inside the reactor core, the fuel generates heat through fission, which produces steam, thereby driving a turbine to generate electricity. The fuel remains in the reactor for several years, depending on the reactor design and fuel enrichment, after which possesses different properties leading to new storage and transportation challenges.

2.2.3 Back-End of the Fuel Cycle

After the fuel has been in the reactor for several years, it is removed and stored in a spent fuel pool. After cooling, the fuel is moved to dry cask storage, where it will remain until a long-term solution is implemented. This thesis does not focus on closed-fuel cycles, therefore it does not consider fuel reprocessing in this description of the NFC. Instead, it examines the masses of different used fuels to characterize how the current U.S. NFC would perform over time with the deployment of new reactors.

When considering a long-term repository for the used fuel, maintainers must consider the macroscopic and microscopic effects of the environment on the repository. On a macroscopic level, climate change will drive shoreline erosion, permafrost recession, and congenital ice sheet melting. Translating these well-known effects into chemical consequences that dictate the design of a repository will require site-specific adaptations on several fronts. Special attention must be given to the impact in the first few thousand years, as this period will exhibit the highest activity. In the case of meltwater exposure, water saturated with dissolved O_2 could infiltrate a repository, potentially altering the oxidizing conditions [26]. Consequently, regulators considering the 100,000-year perspective of a potential repository must account for proximity to such meltwater sources to meet the demands imposed by a

changing climate.

Sites experiencing reducing conditions may continue to do so; however, the changing climate will also influence the salinity of groundwater. Changes in salinity affect density, which could either exacerbate or mitigate the spread of contaminants in the event of exposure outside the repository [26]. This change in salinity also has the potential to interact differently with canisters, necessitating that proactive regulators ensure containment is designed to withstand a changing environment over the repository's lifetime.

An additional layer of microscopic consideration for these regulatory concerns is the imminent deployment of new nuclear fuels with different compositions and forms. Some fuels are designed with pyrolytic carbon matrices that can immobilize decay products for much longer than current fuel forms. As new fuel technologies are deployed, NFC facilities will need to adapt their capacities, production timelines, and regulatory compliance. These changes, although seemingly slight (the fuel will likely still be uranium-based), can have significant consequences over 100,000 years of storage [27].

2.3 CYCLUS

CYCLUS [6] is an agent-based NFC simulator that is versatile, open-source, and modular. The software achieves this versatility through a series of generic *archetypes* that are primarily transaction-based. In the CYCLUS ecosystem, archetypes are generic models that are not tied to any specific reactor technology, and the user community and developer community have created many nuclear facility archetypes for everything from proliferation assessment to fuel burnup. Many standard fuel cycle facility archetypes have been implemented in the CYCLOPS repository [28], which holds technology-agnostic archetypes for material sources, material sinks, enrichment services, separations capabilities, storage services, and a generic reactor.

The architecture of CYCLUS is designed to facilitate the simulation of complex interactions between various agents in a nuclear fuel cycle. Figure 2.3 provides an illustration of the architecture, highlighting the core components of the CYCLUS kernel and the Agent API. The kernel manages the simulation's overall state and handles the scheduling and execution of events, while the Agent API allows users to define custom agents (e.g., regions, institutions, and facilities) that can interact with each other through the Dynamic Resource Exchange (DRE). Facilities are the primary agents in the simulation, and they can represent various types of nuclear facilities, such as reactors, enrichment plants, and waste repositories. Each facility can have its own internal logic for managing resources and making decisions based on the interactions with other agents in the simulation. The interactions between facilities can be modified by grouping them in institutions, which are analogous to real-world organizations (like utilities) that manage multiple facilities. The interactions between institutions can be modified by grouping them into regions,

which can represent larger geographical areas or regulatory jurisdictions. This hierarchical structure allows for a more organized and manageable way to model complex fuel cycles with multiple layers of interaction.

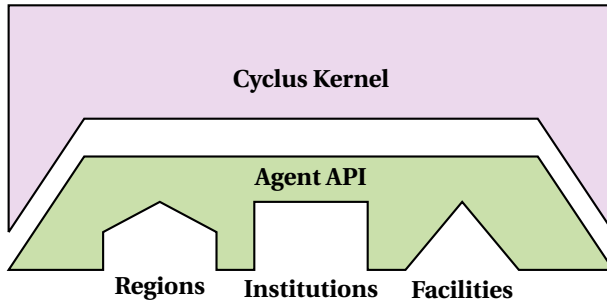


Figure 2.3: CYCLUS architecture overview. The Cyclus kernel manages the simulation, while the Agent API allows for the creation of regions, institutions, and facilities. Facilities are the primary agents that interact with each other through the Dynamic Resource Exchange (DRE).

CYCLUS treats each facility, institution, and region as an agent that can interact with other agents in the simulation. These agents are defined by their capabilities and the resources they can provide or consume. The agents are connected through a unique market mechanism, called the DRE, that allows agents to request resources and respond to requests from other agents. The DRE is responsible for matching resource requests with offers from suppliers and ensuring that the resources are exchanged.

Commodities, in the parlance of the CYCLUS ecosystem, are passed by agents through the DRE in recorded transactions. A commodity can be anything, from raw materials (like uranium ore) to contextual concepts (e.g., money or permits). The transactions are recorded in a database that can be queried to determine the flow of materials through the simulation. As Huff et al. outline in their 2016 paper [6], treating facilities and materials independently allows for flexibility in the level of fidelity for both.

As CYCLUS is a transactions code and not necessarily a physics code, the reactors incorporate depletion physics through pre-defined *recipes*, where the user specifies the concentration of isotopes in a fuel form. Pre-defining recipes build in the assumption that the fuel is being actively managed such that the utilization of each assembly is the same, but it dramatically increases computational efficiency for simulations of complex fuel cycles. For example, depending on how fuel is discharged from a core at the end of a reactor's lifetime, there are instances when the model will over or under-predict the concentration of isotopes, thereby injecting a level of error into calculations. Users approximate the burnup of each fuel element using the same input recipe to be the same. This thesis incorporates a cascading enrichment from low-enriched uranium plus (LEU+) to high-assay low-enriched uranium (HALEU) to investigate the deferred demand for Category II enrichment facilities. LEU+ is used in the short term, while reactor vendors and fuel suppliers work with the government to establish the supply chain for HALEU.

In CYCLUS, the user defines the simulation by specifying the regions, institutions, and facilities that will be present. Regions are collections of institutions, where institutions are collections of facilities, while facilities are the primary agents interacting in the simulation. The user can define the relationships between regions, institutions, and facilities to model the flow of materials and resources through the simulation. Through initial conditions, the user can tailor their simulation for any historical or imagined starting point based on the expected facilities and resources available from the outset.

2.3.1 Fuel Depletion

Fuel depletion is a critical aspect of fuel cycle simulations, as it directly influences the characteristics and behavior of UNF. The composition of this fuel, shaped by factors like decay heat, the quantity of fissile material, and the volume of UNF, has profound implications for various stages of the nuclear fuel cycle. The effects of depletion on these properties are the thermal and physical characteristics of the fuel, as well as the practical considerations such as the transportation of UNF, the limits of repository storage, and the potential for reprocessing and recycling of materials. Thus, any comprehensive fuel cycle simulation must account for fuel depletion, ensuring that the resulting data reflect realistic conditions and constraints.

In many fuel cycle simulators, fuel depletion is managed using pre-defined compositions, which allow for rapid calculations and straightforward modeling of fuel cycles. Tools such as VISION [29], the CYCAMORE Reactor archetype in CYCLUS—which uses the aforementioned *recipes*—and ORION utilize this methodology. In these frameworks, the compositions of UNF are established in advance and derived from separate depletion modeling efforts. This approach is particularly effective for once-through fuel cycles, where fresh fuel compositions remain constant across refueling periods, leading to no variation in the characteristics of discharged fuel. While this method offers simplicity and speed, it may not capture scenarios where external events prevent reactors from uniform operation over time, or fuel cycles that adopt recycling strategies over time.

Users have developed several archetypes to further expand the capabilities of CYCLUS in modeling fuel depletion. Bright-lite [30], for instance, introduces a comprehensive framework for evaluating fuel compositions based on burnup and criticality. This archetype offers two operational modes—forward and blending mode—allowing users to tailor depletion modeling to specific scenarios. The initial recipe is depleted based on a given fluence in forward mode. In blending mode, the reactor is connected to a fabrication facility that mixes material streams to meet a burnup criticality or conversion ratio. The burnups and material definitions need to be given, which is the first step in implementing this archetype. CyBORG [31], another CYCLUS archetype, integrates CYCLUS with ORIGEN by generating a problem-specific cross section library (which it then feeds to ORIGEN to perform a single depletion calculation for the core), enabling a more nuanced approach to modeling fuel cycles. Although CyBORG

requires access to the export-controlled ORIGEN, it enhances the accuracy of UNF compositions. The ann_pwr [32] archetype employs neural networks trained on historical data to predict fuel compositions based on burnup and initial enrichment. While achieving results with less than 1% error 0.23% of the time as ORIGEN, ann_pwr's applicability is limited to Pressurized Water Reactor (PWR) designs, highlighting a need for broader models that can encompass diverse reactor types.

Dynamic modeling of fuel depletion represents an evolution in fuel cycle simulations, allowing for real-time updates to fuel compositions as material properties evolve. This approach is crucial for accurately reflecting the influences of fuel depletion on material properties. Various simulators outside the CYCLUS ecosystem, including ORION [33], DYMOND [34], and NFCSim [35], are capable of dynamic modeling. For instance, ORION allows users to define initial material compositions using recipes and autonomously model decay and depletion. DYMOND enhances accuracy by coupling with ORIGEN2, enabling criticality searches that refine fresh fuel compositions based on updated UNF data [34]. NFCSim's coupling with the Los Alamos Criticality Engine (LACE) further exemplifies this trend by employing fluence-dependent calculations to ascertain the evolving nature of nuclear materials. These advancements in dynamic modeling are essential for improving the fidelity and reliability of fuel cycle simulations, particularly as the nuclear industry moves toward more intricate and sustainable fuel management strategies.

The OpenMCyclus archetype [36] enhances the CYCLUS ecosystem by introducing an open-source real-time fuel depletion tool for CYCLUS simulations, building off of the concept of CyBORG. Unlike traditional approaches that rely on pre-defined recipes for fuel compositions, OpenMCyclus integrates with OpenMC [37] to dynamically update spent fuel compositions throughout the simulation, allowing for greater accuracy and flexibility in modeling various reactor designs. This real-time depletion capability is valuable for assessing the impacts of different fuel cycle strategies, as it accommodates changes in fuel composition and operational conditions without the need for restrictive licensing agreements associated with other depletion tools.

2.4 Fuel Enrichment

In 2020, a HALEU workshop report led by Monica Regalbuto [38] highlighted the unique regulatory challenges of establishing a HALEU fuel cycle in the U.S.. It noted that part of enriching HALEU is first to produce LEU+, defined as between 5% and 10% ^{235}U enrichment. The report notes that LEU+ facilities would fall under a similar category of regulations as the existing low-enriched uranium (LEU) fuel cycle, allowing existing enrichment servicers to leverage their experience and infrastructure before taking on the increased regulatory burden of producing HALEU. If a reactor could be redesigned to accommodate it, using LEU+ could delay the demand for HALEU. Table 2.1 shows the various levels of enrichment for uranium fuel in the U.S.

Table 2.1: Enrichment levels and their ranges.

Enrichment Level	Range [% ^{235}U]
Natural	< 0.711
LEU	0.711-5
LEU+	5-10
HALEU	10-20
high-enriched uranium (HEU)	≥ 20

One of the primary advantages of a fuel cycle containing LEU+ is that the facility to produce it would fall under the same licensing category as LEU fuel. The U.S. Nuclear Regulatory Commission (NRC) defines a *special nuclear material of low strategic significance* as meeting one of three criteria, the most notable of which for the purposes of this thesis is "(3) 10,000 grams or more of uranium-235 (contained in uranium enriched above natural but less than 10 percent in the U-235 isotope)," [39]. This facility definition is where the upper limit of the LEU+ range arises.

Facilities like Centrus in Piketon, Ohio enrich HALEU fuels compliant with regulations for *special nuclear material of moderate strategic significance* (Category II), but the commercial facilities in the U.S. do not have contemporary experience enriching HALEU fuels and this demonstration will need to be expanded to support a fleet of higher enriched reactors. Additionally, Category II facilities come with increased construction and operation costs that would increase the barriers to establishing these facilities before a consistent demand has been established. Thus, LEU+ is an attractive intermediary step for servicers wishing to minimize the size of a Category II facility (thereby reducing costs) as it is the same category as historically licensed enrichment facilities for LEU.

Traditional LWRs could receive benefits from using LEU+ fuel; as outlined by López-Luna et al. [40], incorporating such fuel rods would allow for a 24-month cycle in the Boiling Water Reactor (BWR) design they studied and would reduce the levelized cost of the nuclear fuel cycle they simulated. In October 2024, Framatome announced that their 6 wt% ^{235}U GAIA fuel assemblies completed their third 18-month fuel cycle at the Vogtle plant in Georgia [41], with the eventual goal of this process being commercialization of new accident-tolerant fuels that can potentially support LEU+.

Increased prevalence of higher enrichment fuels will require modifications to the existing supply chain, particularly to ensure the continued safety of workers and the public. A 2022 report from Shaw and Clarity out of Oak Ridge National Laboratory (ORNL) highlighted that existing nuclear fuel vault configurations at BWRs and PWRs did not have sufficient margins to satisfy regulatory requirements when fully flooded [42]. Their report only studied the impacts of 6.5 wt% and 8 wt% fuel, but they concluded that HALEU fuel would similarly require significant changes to existing fuel storage infrastructure.

2.5 TRISO Fuel

This thesis adapts the approach of Bachmann et al. [7] to focus on TRi-structural ISOtropic (TRISO) fueled reactor designs alongside current commercial fuel forms at various enrichments. The TRISO fuel form can accommodate any classification of enrichment; several reactor designs use different fuel enrichments that are all TRISO. This section will distinguish the production of TRISO from the traditional metallic fuels used in LWRs outlined in Section 2.2.

Coating the fuel particles is a critical step in the fabrication of TRISO fuel, and the idea has existed in nuclear fuel design spaces since the 1950s [43] with the Dragon project. In 1957, the Harwell facility began coating spherical fuel particles, and in 1961, researchers modified the particle coating to include a silicon carbide layer to trap cesium, strontium, and barium—which diffused through the single pyrolytic carbon layer. Concurrently, in 1958, a report to the Atomic Energy Commission (AEC) introduced the concept of a pebble bed pile (first proposed by Daniels [44]) to the broader nuclear community. Researchers in Germany, China, and the UK have proposed, built, and operated similar designs since then, with companies in the U.S. looking to deploy modern versions of the technology.

In a 2019 paper, authors Demkowicz, Liu, and Hunn [45] authors describe the fuel as a particle encapsulated in layers of pyrolytic carbon and silicon carbide; a fluidized-bed chemical vapor deposition system (FB-CVD) applies each of these layers. The fuel kernel, shown by Figure 2.4, is typically composed of uranium dioxide, and it is surrounded by a porous carbon buffer using acetylene in the FB-CVD as it has a relatively low density. The silicon carbide layer encapsulates the pyrolytic carbon layers and provides a barrier to fission products. A mix of methyltrichlorosilane and hydrogen is sufficient for SiC deposition without argon. The inner and outer pyrolytic carbon layers isolate the silicon carbide layer and provide a barrier to the coolant; the FB-CVD applies these layers using a mix of propylene, acetylene, and argon.

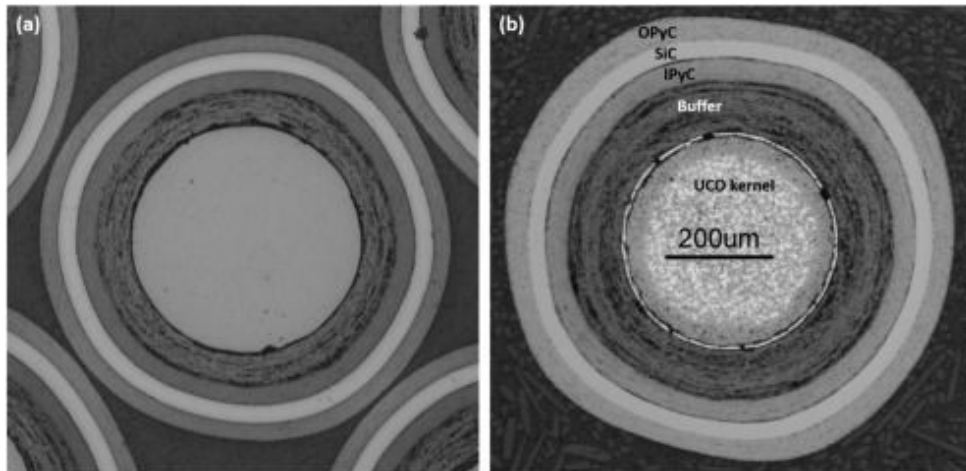


Figure 2.4: TRISO fuel particle layers [45].

Through a heat and pressure setting process, fabricators create a graphite matrix that accepts the coated particles. The resulting fuel type is incredibly robust and can reduce proliferation concerns due to the difficulty of separating the particles from the matrix and the fuel from the particles. The fuel can withstand high temperatures and burnups, which can be advantageous in reactor designs that require high temperatures for efficient operation.

2.6 Reactor Models

This thesis explores various transition scenarios for the deployment in the U.S. of the: 1) X-Energy Xe-100 (Xe-100) High-Temperature Gas-cooled Reactor (HTGR); 2) Ultra Safe Nuclear Corporation (USNC) Micro Modular Reactor (MMR) HTGR; and 3) and Westinghouse AP1000 PWR. To accommodate the assumption that the HALEU-fueled TRISO reactors will first accept LEU+ fuel, this thesis adapts Bachmann's MMR-like Serpent model [46] and Richter's Xe-100-like Serpent model [47] to accept LEU+ fuel. These reactor models are constructed from publicly available data to approximate their aggregate behavior.

Table 2.2 shows the design specifications for the advanced reactors in this thesis. The MMR and Xe-100 reactors are HTGRs that use TRISO fuel, while the AP1000 is a PWR that uses UO₂ fuel. The enrichment distinguishes the versions of the MMR and Xe-100 as the only distinguishing variable between the two versions of the reactors. The cycle length, discharge burnup, and reactor lifetime are the same for both versions of the reactors. The AP1000 is assumed to use LEU fuel throughout the simulation. The MMR is the smallest power output reactor in this thesis, and can serve as a representative of mix of small, TRISO-fueled reactors. The Xe-100 reactor is an order of magnitude larger in power output, and can be considered a representative of larger, TRISO-fueled reactors. The AP1000 is the largest reactor in this thesis and is a representative of gigawatt-scale reactors.

Table 2.2: Advanced reactor design specifications.

Design Criterion	MMR-Like [48]	Xe-100-Like [49]	AP1000
Reactor type	HTGR	HTGR	PWR
Power Output [MWe]	15	100	1000
Fuel Type	TRISO	TRISO	UO ₂
Enrichment [% ²³⁵ U]	9.95, 19.75	9.95, 15.5	5
Cycle Length	20 [yrs]	Online Refuel	18 [months]
Discharge Burnup [GWd/MTU]	82	168	65
Reactor Lifetime [yrs]	20	60	60

The following subsections discuss the reactors in greater detail. These models approximate that the LEU+-fueled

reactors achieve the same burnup, power level, and core lifetime as the HALEU-fueled version. These assumptions are sufficient for the metrics outlined in Section 3.2 as this thesis does not perform UNF isotopic analysis, but could stretch the UNF temporal profile.

2.6.1 MMR-like Reactor

In 2021, University of Illinois Urbana-Champaign (UIUC) submitted a notice of intent to the NRC detailing their plans to apply for a construction permit of the MMR reactor from USNC [50]. Activities have continued as UIUC continues the project, they reached the pre-licensing phase with the NRC and were planning on commencing operation of an on-campus reactor in the 2030s. This MMR is an HTGR that uses TRISO fuel, has an electrical output of 15 MW_e , and a cycle length of 20 years. The fuel is enriched to 9.95% ^{235}U for LEU+ and 19.75% for HALEU. As modeled, both have a discharge burnup of 82 GWd/MTU, which coincides with the 20-year lifetime of the reactor. In this thesis, the MMR is based on the model developed by Bachmann et al. [46] and is implemented here as-is for the HALEU version of the reactor, while the LEU+ version updates the fuel composition from the HALEU version.

Figure 2.5 shows a rendering of the MMR core and reactor vessel. As indicated by the figure, the design is intended to be underground, with an estimated total reactor footprint less than 5 acres. The primary coolant is helium gas, which heats up in the core and deposits its heat in a heat exchanger to generate electricity to the side of the reactor [51]. Helium is transparent to many nuclear interactions and is inert, making it an attractive choice for a coolant.

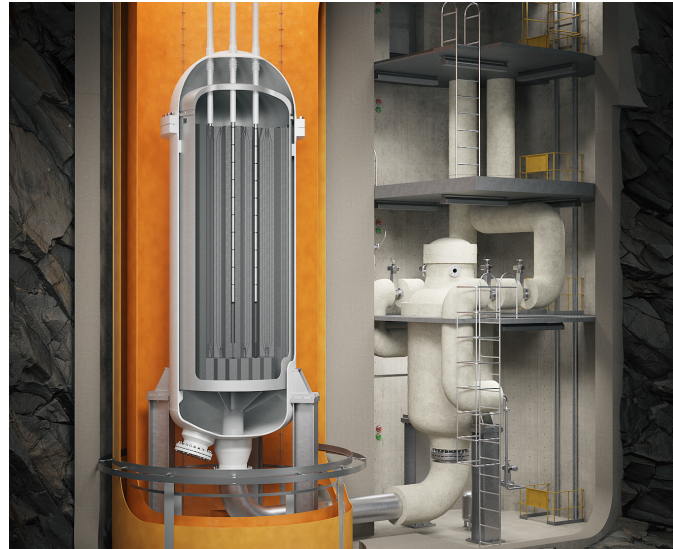


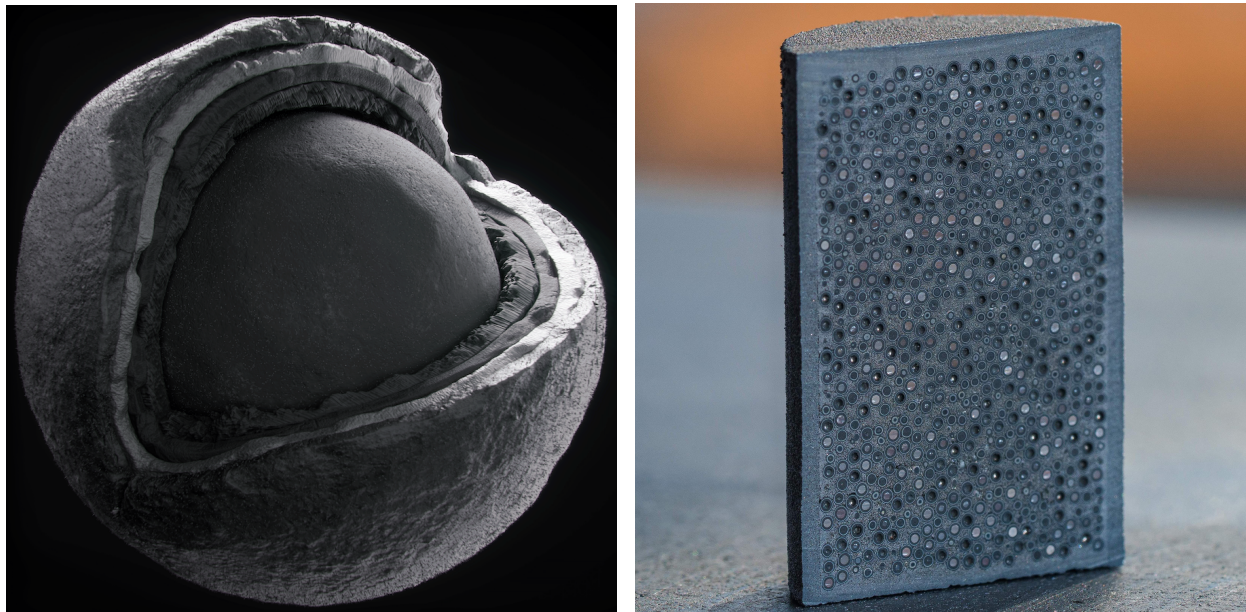
Figure 2.5: USNC MMR design [48].

The proposed deployment of this reactor concept includes an operational *MMR Energy System* consisting of two plants: the *Nuclear Plant* and the *Adjacent Plant*. The *Nuclear Plant* contains multiple MMR units, including all

the equipment required to transport the heat to the *Adjacent Plant*. The *Adjacent Plant* consists of the equipment that converts heat to electricity or process heat as needed. The *MMR Energy System* will theoretically store up to 10 hours of power plant thermal output and can be supplemented with hydrogen burners. Auxiliary molten salt thermal storage allows for a flexible electricity and process heat supply.

Electricity and heat would be delivered on demand from the power plant while the MMR unit operates at constant power. The MMR's high-temperature heat has many uses beyond the generation of electricity. District heating, desalination, and chemical or industrial heat highlight the broader point of how fourth generation (GENIV) nuclear reactors are not solely intended for electricity generation as with the current domestic fleet. An MMR could deliver steam temperatures of 660 °C, and they estimate that temperatures up to 950 °C could be possible in future MMR variants [48].

The fuel for this reactor is inspired by the TRISO fuel developed in the 1960s and 1970s. A small sphere of uranium fuel is coated in carbon and silicon carbide layers. As shown in Figure 2.6, the fuel is composed of kernels arranged into a larger fuel pellet. They call their fuel form Fully Ceramic Microencapsulated (FCM) fuel. They additively manufacture each element, allowing for a high packing fraction of fuel, which means their fuel could be adapted to other reactor designs.



(a) Fuel element layers.

(b) Fuel pellet profile.

Figure 2.6: USNC MMR fuel renderings [52].

Figure 2.7 shows a top-down and side view of the MMR Serpent model [46], modified in fuel composition alone. As Bachmann describes [53], the radius of the fuel channel is based on the publicly available size of the FCM pellets

(1.15 cm), and the coolant channel has an arbitrarily chosen radius of 3 cm. The entire core is assumed to be in an isothermal state at 800 K. There is a 20 cm thick graphite reflector above and below the stacks of graphite and a 10 cm thick beryllium-oxide reflector on the outside of the graphite blocks of the core, illustrated by the green material in Figure 2.7. The model does not contain control rods or burnable poisons, so the control rod tubes are filled with helium. Five layers of graphite fuel blocks are stacked to form the entire core to approximate the number of fuel blocks described in the publicly available data [48]. The fuel does not move through the core, as the model is designed to use the same fuel for the entire reactor lifetime.

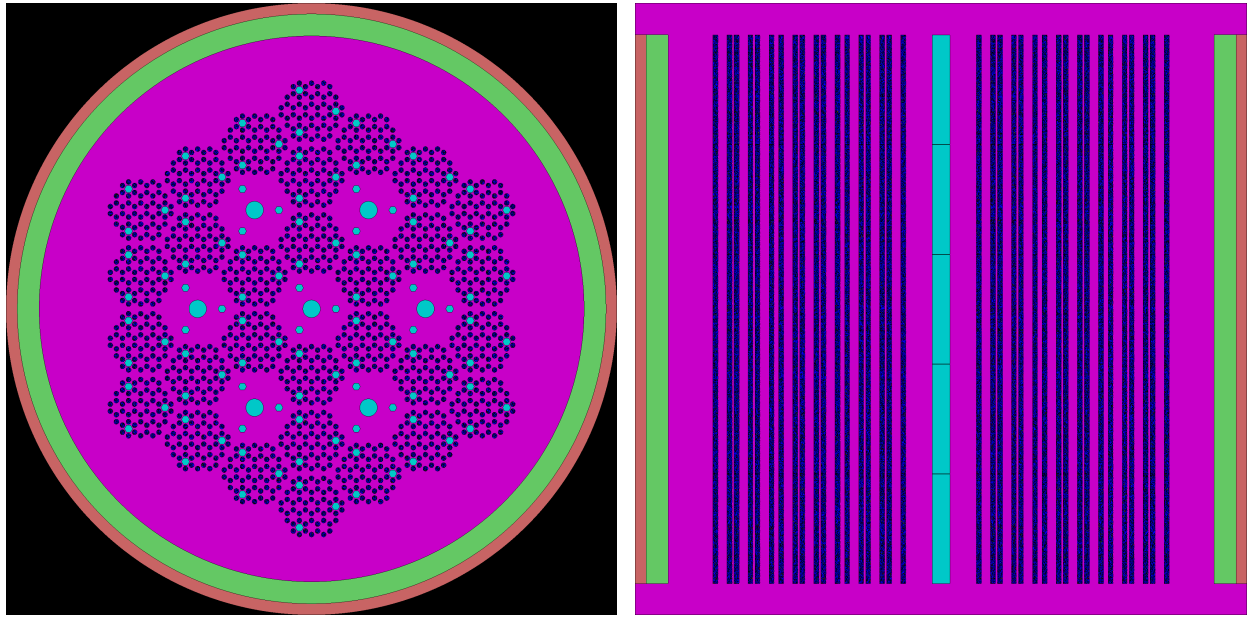


Figure 2.7: Serpent model of the USNC MMR core.

2.6.2 Xe-100-like Reactor

X-Energy has entered into a cooperative agreement with U.S. Department of Energy (DOE) to deploy their Xe-100, is in the pre-licensing phase with the NRC for projects in Texas and Washington, and is expected to be operational in the 2030s. There are similar projects in the early stages in Canada and the UK. The X-Energy Xe-100 is an HTGR that uses TRISO fuel and is expected to operate for 60 years. The reactor has an electrical output of 100 MW and uses online refueling. The fuel is enriched to 9.95% ^{235}U for LEU+ and 15.5% ^{235}U for HALEU and a discharge burnup of 168 GWd/MTU. The reactor in this thesis is an approximation based on publicly available data and is not based on confidential or proprietary information. The model was developed by Richter et al. [47] and is implemented herein as-is for the HALEU-fueled reactor, while the LEU+ version has a modified fuel composition.

Figure 2.8 shows a rendering of the Xe-100 core and reactor vessel. The Xe-100 reactor is designed to be a small modular reactor that can be deployed in various locations and will be gas-cooled. This design differs from the MMR as the reactor features online refueling.

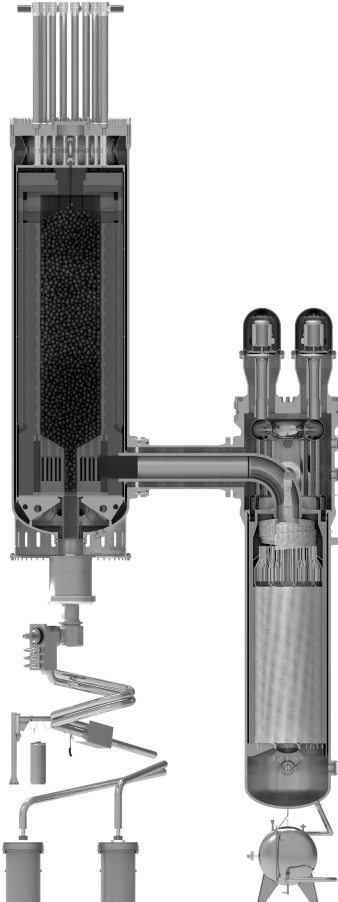


Figure 2.8: X-Energy Xe-100 rendition [54].

Unlike the MMR's annular fuel elements, the Xe-100 pebbles are composed of a spherical graphite matrix that contains the TRISO fuel particles. These TRISO particles are similar to those in the MMR, as shown in Figure 2.9.

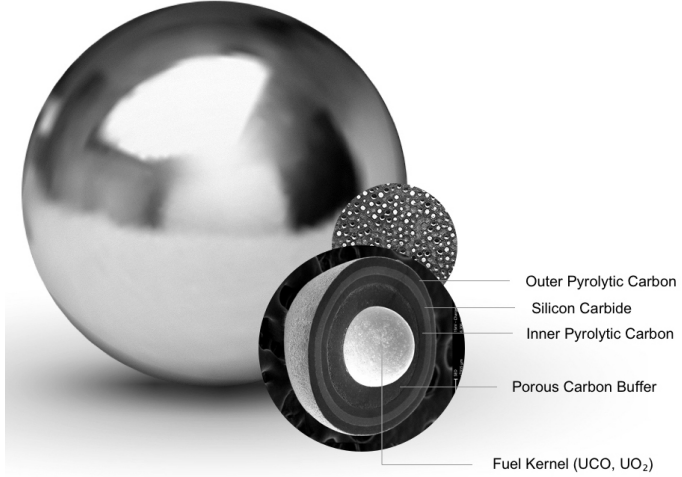
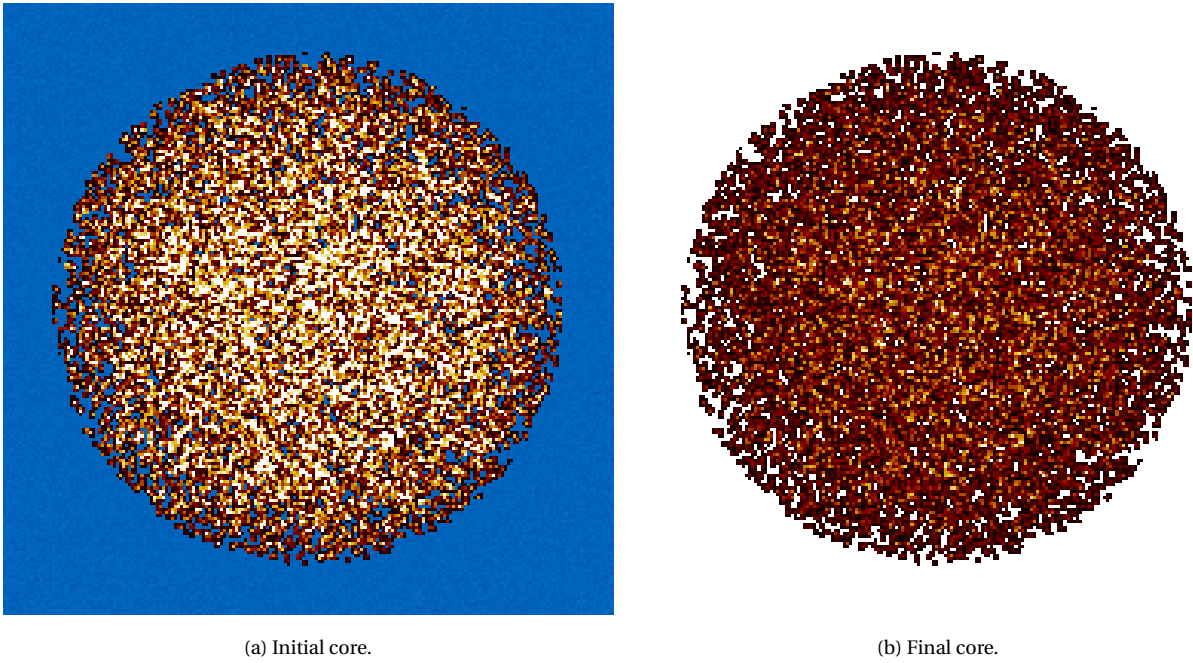


Figure 2.9: X-Energy Xe-100 fuel pebble [55].

This thesis modifies the fuel composition of Richter's Xe-100-like reactor model to accept LEU+ fuel. The LEU+ fuel is assumed to have the same burnup and power level as the HALEU fuel. This assumption, as with the MMR-like reactor, would impact the UNF isotopic calculations. I will explore the implications in future work. Figure 2.10 shows the top-down view of the LEU+ Xe-100 core as the HALEU version has been established by Richter [56].



(a) Initial core.

(b) Final core.

Figure 2.10: Top-down view of the LEU+ X-Energy Xe-100 core model where darker shading corresponds to higher burnup, and lighter shading corresponds to lower burnup.

Figures 2.10a and 2.10b are shaded based on the burnup of the fuel, with darker pebbles indicating higher burnup. The pebbles are inserted into the core at the top, and gravity pulls them down through the core. After a brief holding time outside the core, the pebbles are reinserted at the top of the core. In CYCLUS, we approximate the core as containing 6 batches in the core and one batch is removed when they reach the end of their life. This process is repeated until the pebbles reach their targeted number of passes, at which point they are removed from the core and stored.

2.6.3 AP1000 Reactor

AP1000s are operational in the U.S. and China, and the UK and India plan to deploy more. The Westinghouse AP1000 is a PWR that uses UO_2 fuel. The reactor has an electrical output of 1000 MW, a cycle length such that every 18 months 80 fuel assemblies are replaced, and an expected lifetime of 60 years. The fuel is enriched to approximately 5% ^{235}U and has a discharge burnup of 65 GWd/MTU. The reactor in this thesis is an approximation based on publicly available data about the units currently operating at the Vogtle Plant in Georgia, and is not based on confidential or proprietary information. As this thesis does not anticipate LEU+ being used in the AP1000, there is no such neutronics model of the reactor herein, and this work adapts the generic CYCLOMOR reactor archetype to represent the AP1000 in number of fuel assemblies, power output, core mass, and cycle length.

Chapter 3

Deployment Scenarios

This chapter discusses transition scenarios for reactor deployment of the X-Energy Xe-100 (Xe-100), Ultra Safe Nuclear Corporation (USNC) Micro Modular Reactor (MMR), and the AP1000 in the United States (U.S.) and the reactor models used to simulate them. It also discusses transition scenarios broadly, the schemes used to set deployment schedules, and the results for each deployment scheme. The input files and analysis scripts are available on GitHub [57].

3.1 Transition Scenarios

As the energy landscape evolves, compounding factors will drive the actual deployment of these reactors in ways this thesis does not capture. The value of energy system modeling and *transition scenarios* is to understand the deployment implications compared with and measured relative to business-as-usual cases with similar approximations. In this work, a *transition scenario* refers to a modeled system wherein, when the existing Light Water Reactor (LWR) fleet is decommissioned, a deployment scheme selects new reactors to meet an objective. The objective in this thesis is to meet a projected demand growth.

This chapter explores the deployment schemes implemented in this thesis—outlined in Table 3.1—and the demand growth scenarios that this thesis considered—outlined in Table 3.2. Appendix B will discuss two additional deployment schemes that I implemented but did not leverage, as they are more useful for problems not considered herein.

Table 3.1: Deployment schemes.

Status	Scheme	Description
Incorporated	Greedy Deployment	Deploy reactors to fill demand, preferring to deploy larger capacity units first.
	Random Deployment	Uses a date and hour as seed to sample the reactors list randomly.
	Initially Random then Greedy Deployment	Randomly deploy reactors until a reactor bigger than the remaining capacity is proposed for each time step, then fills the remaining capacity with the greedy algorithm.
Not Incorporated	Capped Deployment	There is a single-number capacity for one or more of the reactor models.
	Pre-Determined Distribution	One or more reactors have a preset distribution, and a smaller capacity model fills in the gaps.
	Deployment	

The deployment schemes shown in Table 3.1 choose reactors to fill demand growth based on two predictions of future. The U.S. Energy Information Administration (EIA) publishes demand expansion projections for the totality of the U.S. [58]. The administration has refrained from publishing AEO 2024 in light of recent accelerations in demand growth. The assumptions for the low-growth scenarios are that the relative percentage of nuclear power remains constant and that the relative performance of the various fuel cycle metrics will remain constant. The high-growth scenarios come from the U.S. Department of Energy (DOE) Liftoff Report [4], which does not reflect this constant percentage assumption for nuclear power in their demand scenarios. Their growth projections are specific to nuclear energy deployment increases, and the number is agnostic to the total increase.

Table 3.2: Demand growth scenarios.

Demand Growth	Year-to-Year Increase	Source
No Growth	0.0%	N/A
Low Growth	0.17%	[58]
Low Growth	0.5%	[58]
Low Growth	1.0%	[58]
High Growth	3.5%	[4]
High Growth	5.6%	[4]

As shown in Table ??, each growth scenario has two enrichment deployments: 1) the reactors are never fueled with low-enriched uranium plus (LEU+); 2) the MMR and Xe-100 reactors are fueled with LEU+ until 2040, when they move to high-assay low-enriched uranium (HALEU). MMRs deployed before this fuel transition will continue to use LEU+ fuel until the end of their lifetime as they do not refuel; however, the Xe-100 reactors will refuel with LEU+ until 2040, at which point they will refuel with HALEU. The AP1000 reactors will continue to use low-enriched uranium (LEU) fuel throughout the simulation.

Under each enrichment deployment, each demand projection is met by deploying reactors using the schemes outlined in Table 3.1. The following sections will discuss the results of these deployment schemes, their limitations, and propose future work. Regardless of the enrichment deployment, each run will attempt to deploy reactors to meet the capacity outlined in Figure 3.1. The results will focus on the *no growth* and 3.5% growth (corresponding to doubling nuclear by 2050) scenarios.

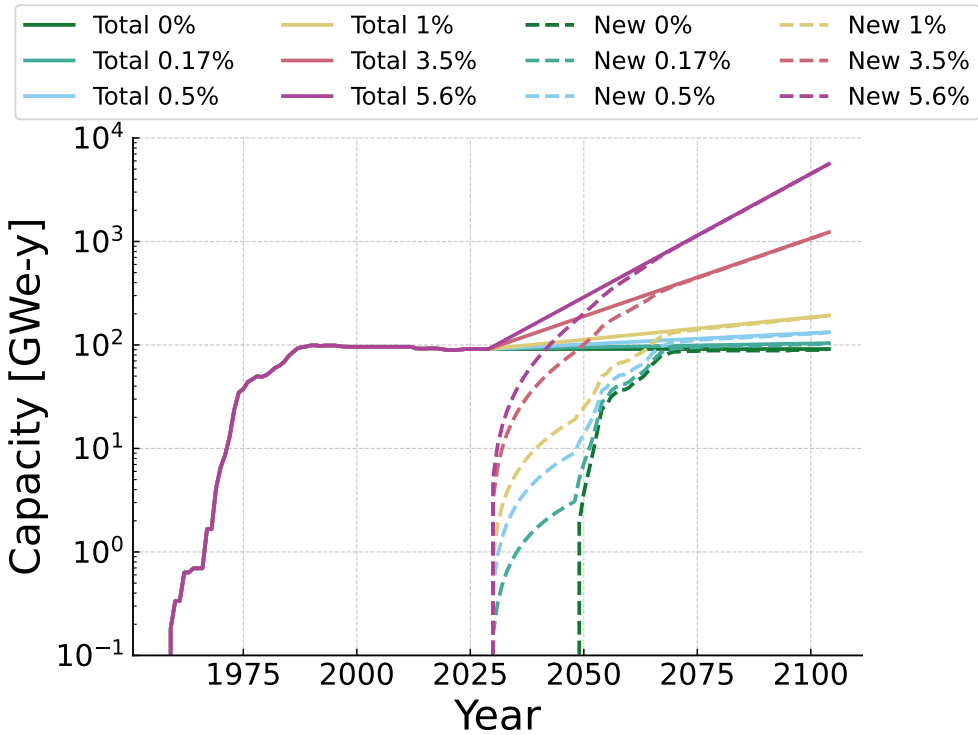


Figure 3.1: Total and new nuclear capacity deployed in each scenario.

As shown in Figure 3.1, advanced reactors (for this thesis, the designs are the MMR, Xe-100, and AP1000) begin deployment in 2030. While this is an aggressive deployment schedule, [53] established that the precise deployment start did not significantly impact the total results for this type of analysis and could reasonably serve as an upper bound of deployment. The business-as-usual, or *no growth*, scenario does not require the deployment of a new nuclear reactor until just before 2050, whereas the other scenarios understandably commence deployment in 2030.

As it is on a logarithmic plot, the linear appearance of the data belies the compounding effect that the year-to-year percentage growth requires.

Comparing these projected deployments with the results from the *no growth* and *double by 2050* scenarios, Table 3.3 consolidates the over- and under- deployments of capacity into Table to show that the random deployment scheme had the least total difference between the results and the projection. The initially random, then greedy deployment scheme showed the largest total difference between the results and the projection, while the greedy deployment scheme was between the two.

Table 3.3: Capacity difference between results and projection.

Scenario	Deployment Scheme	Total Difference [GWe]
No Growth	Greedy	19.46
	Random	-15.21
	Initially Random Then Greedy	47.26
Double	Greedy	103.54
	Random	6.65
	Initially Random Then Greedy	151.86

Figure 3.2 shows the difference in energy capacity between the results and the projection for the *no growth* and *double by 2050* scenarios over time. The difference curves in Figure 3.2b show a tightly perturbed oscillation as more reactors are deployed to meet the increasing demand in the random and the initially random, then greedy schemes. Closer to the start of advanced reactor deployment, the greedy scheme shows a consistently smaller difference than the other schemes, but the difference continues to grow as time progresses.

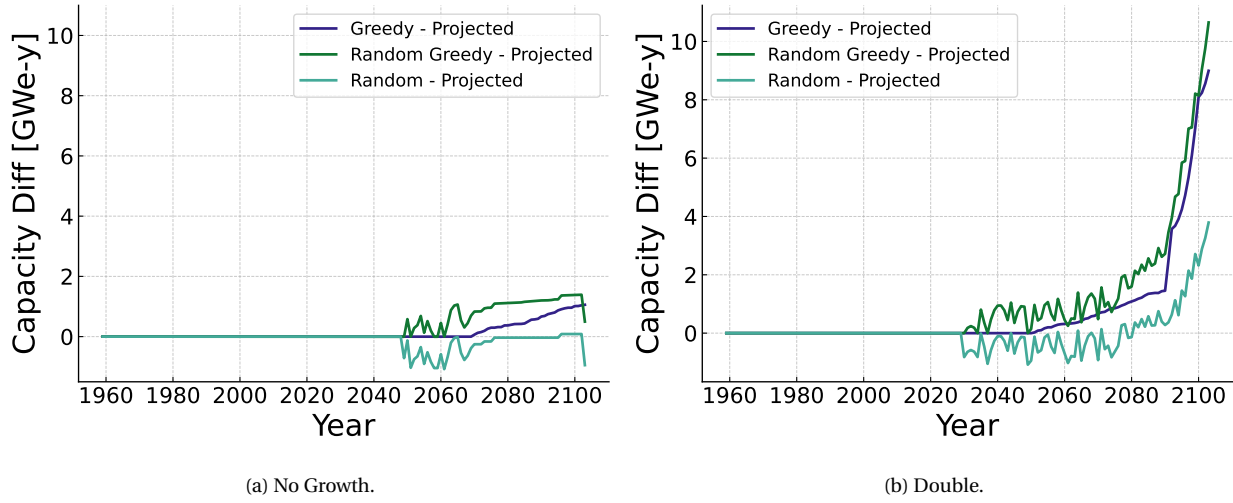


Figure 3.2: Energy capacity difference between projection and scheme predictions.

3.2 Metrics

This thesis develops a nuclear energy model of the U.S. using concepts from Energy System Models (ESMs) on scenarios that compare the transition from the current fleet to incorporate advanced reactor technologies not currently deployed. To compare these scenarios, I have focused on a few key metrics: separative work units (SWU), energy capacity, mass of fuel, and reactor deployment.

3.2.1 Separative Work Units

The process of enriching uranium is a crucial step in the nuclear fuel cycle, and is expected to be a bottleneck in the deployment of advanced reactors. The Separative Work Unit (SWU), is a ubiquitous measure of effort that goes into separating isotopes. It is simplified as:

$$SWU = (PV(x_p) + TV(x_t) - FV(x_f)) t$$

where:

$$V(x_i) = (2x_i - 1) \ln\left(\frac{x_i}{1 - x_i}\right)$$

and

SWU = Separative Work Units [kgSWU]

P = Product mass flow rate [kg/d]

F = Feed mass flow rate [kg/d]

T = Tails mass flow rate [kg/d]

$V(x)$ = Separation Potential [-]

x_p = Weight fraction of ^{235}U in the product stream [-]

x_f = Weight fraction of ^{235}U in the feed stream [-]

x_t = Weight fraction of ^{235}U in the tails stream [-]

t = Time [d]

This thesis compares the SWU required for each scenario to understand the relative effort required to deploy the reactors and provide a stable precursor to economic calculations. As mentioned in Section 2.4, the definition used in the literature for LEU+ can be tied to the upper limit on enrichment for a Category III facility. The LEU+ fuel, as shown in Table 2.2, is enriched to 9.95 w% ^{235}U , which would fall under the Category III limit. The HALEU fuel would require Category II facilities to achieve the 19.75 w% ^{235}U and 15.5 w% ^{235}U enrichment for the MMR and Xe-100 HALEU. Table 3.4 shows the SWU calculation values for each fuel type.

Table 3.4: SWU calculation values for each fuel type.

Variable	Value
MMR LEU+ x_p	0.0995
MMR HALEU x_p	0.1975
Xe-100 LEU+ x_p	0.0995
Xe-100 HALEU x_p	0.155
LEU x_p	0.045
x_f	0.00711
x_t	0.002

3.2.2 Energy Capacity

The reactor deployment schemes in this thesis meet the projected energy demand scenarios from the DOE and EIA outlined in Table 3.2. The reactors simulated herein have a static peak energy capacity, so the nuance in the fleet's ability to meet the demand comes from the deployment scheme and limitations in the fuel supply chain. This thesis discusses the realistic features of each scheme and compares the energy capacity with the demand scenarios to understand the relative performance of each deployment scheme.

3.2.3 Mass of Fuel

CYCLUS tracks the mass of material in each transaction. This thesis focuses on the cumulative mass of fuel, both fresh and used, that comes from deploying the reactors in each scenario. From the mass of fuel and fuel design, future work can convert these results into cost metrics, transportation indicators, and hypothetical repository space considerations.

3.3 Greedy Deployment

The *greedy deployment* scheme selects the largest reactor first until another reactor exceeds the demand—as outlined in 3.3. Then, it moves to the next largest reactor until the next deployment of the smallest capacity reactor exceeds the demand. This scheme is not a proxy for strategic decisions by individual actors, but it reveals the implications of deploying a minimal number of reactors to meet the demand.

Previous work from Bachmann et al. [7] employed a similar scheme to explore the deployment of advanced reactors in the U.S.. Both implementations are computationally efficient and allow for the exploration of the deployment of advanced reactors in a way that is not overly complex. This scheme is most useful for scenarios where the user is interested in comparing metrics relative to the number of specific reactors deployed outside of the context of the problem.

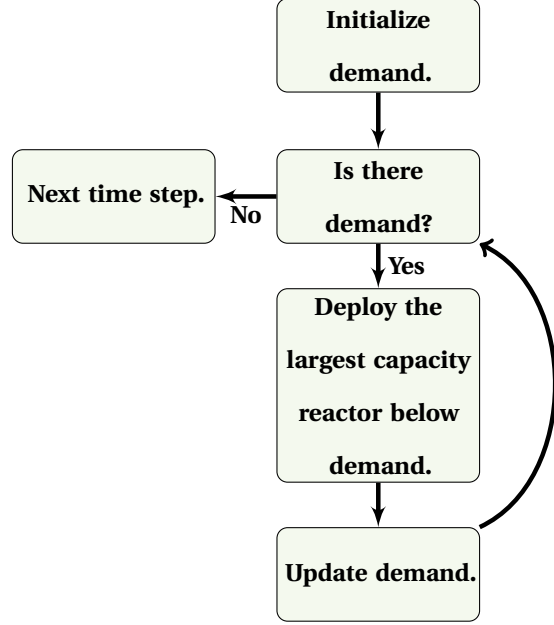


Figure 3.3: The greedy deployment diagram demonstrates a preference for larger power capacity reactors, and shows how the scheme could under-deploy if the remaining capacity is less than the size of the smallest reactor.

The *greedy deployment* does not attempt to capture the complexity of the deployment problem but rather to explore the implications of deploying a certain number of reactors. The scheme could mirror large actors in a market, but is likely not realistic. The scheme will deploy reactors until the demand is met within the amount of the smallest capacity reactor. Sections 3.3.1, 3.3.2, 3.3.3, and 3.3.4 show the *greedy deployment* results for the *no growth* scenario and the *double nuclear by 2050* scenario for each metric from Section 3.2.

3.3.1 Number of Reactors

As Section 3.1 mentions, one difference between the *no growth* scenario and the doubling scenario is that the transition for the *no growth* scenario will begin closer to 2050 instead of 2030. Figure 3.4 and 3.5 show the cumulative number of each reactor deployed in the *no growth* and *double by 2050* for the greedy scheme. This trend is reflected in Figures 3.4 and 3.5, where the MMRs, Xe-100s, and AP1000s start as the existing LWR fleet is retired. Comparing fuel enrichment deployments, Figures 3.4a and 3.5a are identical, which typifies the impact of the delayed transition in the *no growth* scenario.

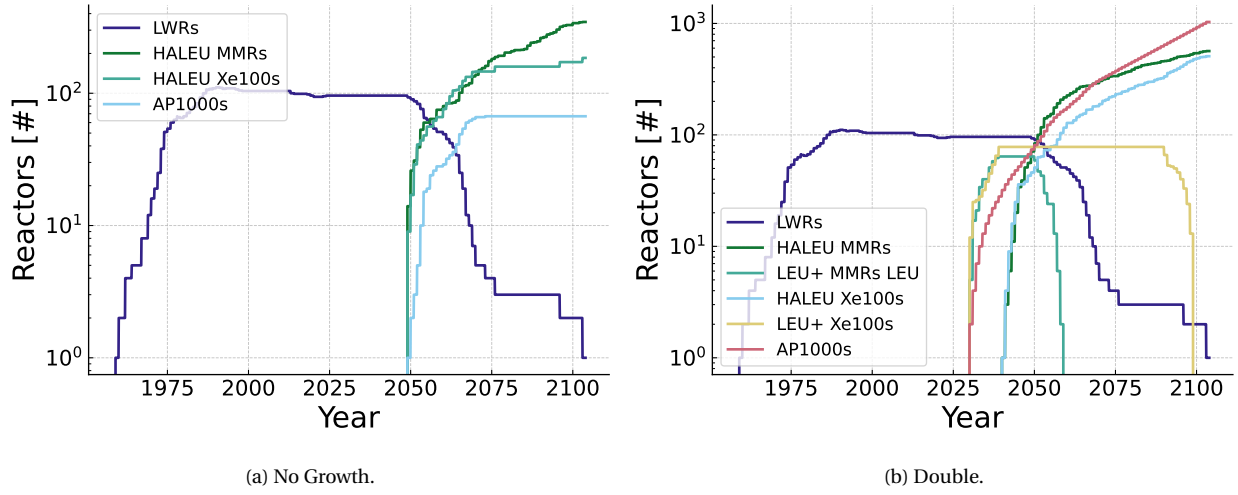


Figure 3.4: Greedy multi-fuel reactor deployment for the no growth (a) and double by 2050 (b) scenarios.

A direct consequence of the *greedy deployment* scheme is that, in the doubling scenario, the AP1000 is deployed the most over time, whereas the *no growth* scenario shows the opposite. Another consequence of the deployment scheme is that the deployment rate for the single-fuel enrichment deployment compared with the multi-fuel enrichment deployment is identical, and future work could investigate further implications of transitioning from one fuel type to another regarding operation. Simply meeting energy demand is not how utilities make decisions and is not the intended use case of the broad generation of new nuclear reactors; as this scenario models reactors solely for power production, this is an upper-bounding case for the energy demand met by designs like the MMR or Xe-100.

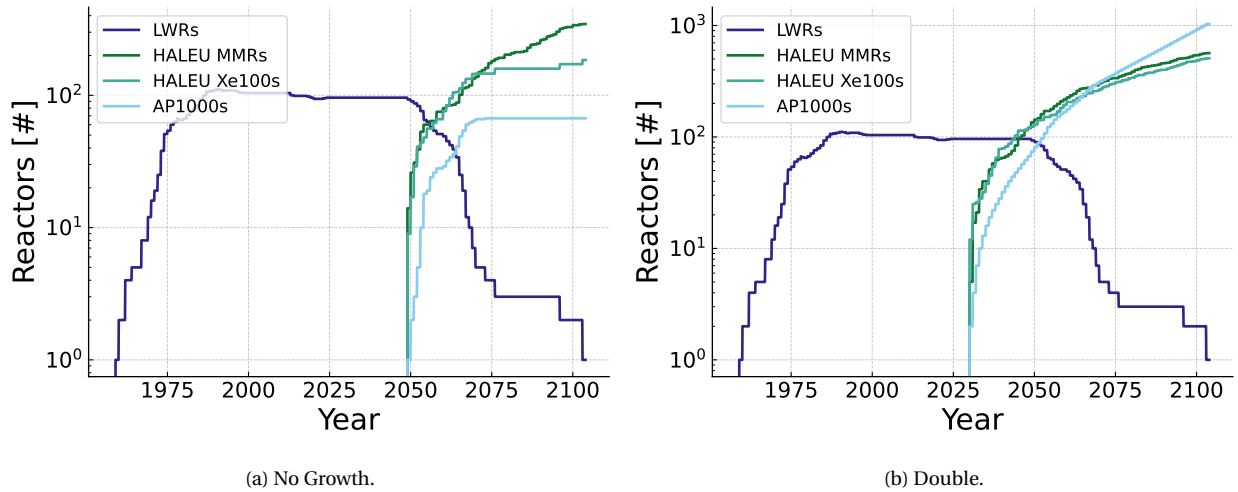


Figure 3.5: Greedy single-fuel reactor deployment.

Table 3.5 shows how the average number of reactors by design is not influenced by the interstitial period from 2030 to 2040 included in this thesis. Compared to the *no growth* scenario, the *double by 2050* scenario shows a significant increase in the average number of each design operating across the 2030-2104 timeline. Consequently, the average number of the AP1000s increases by 757% between the two growth scenarios, which is the largest increase of any design. The Xe-100 reactors show the second largest increase at 163%, followed by the MMR at 109%.

Table 3.5: Average greedy total operating reactors by design from 2030 to the end of the simulation.

Scenario	No Growth, Single	No Growth, Multiple	Double, Single	Double, Multiple
HALEU fueled MMRs	131.613	131.613	274.493	257.427
LEU+ fueled MMRs	-	-	-	17.067
HALEU fueled Xe-100s	94.04	94.04	246.88	184.48
LEU+ fueled Xe-100s	-	-	-	62.4
LEU fueled AP1000	38.667	38.667	331.387	331.387

3.3.2 SWU Results

Figure 3.6 shows the yearly SWU demand periodically spiking over time as enrichment production grows to meet the fuel demand for the fleet. When reactors begin operation in the depicted *no growth* scenario around 2050, the SWU demand for the AP1000 peaks above the other two reactors, while the demand from Xe-100s exceeds the demand from MMRs.

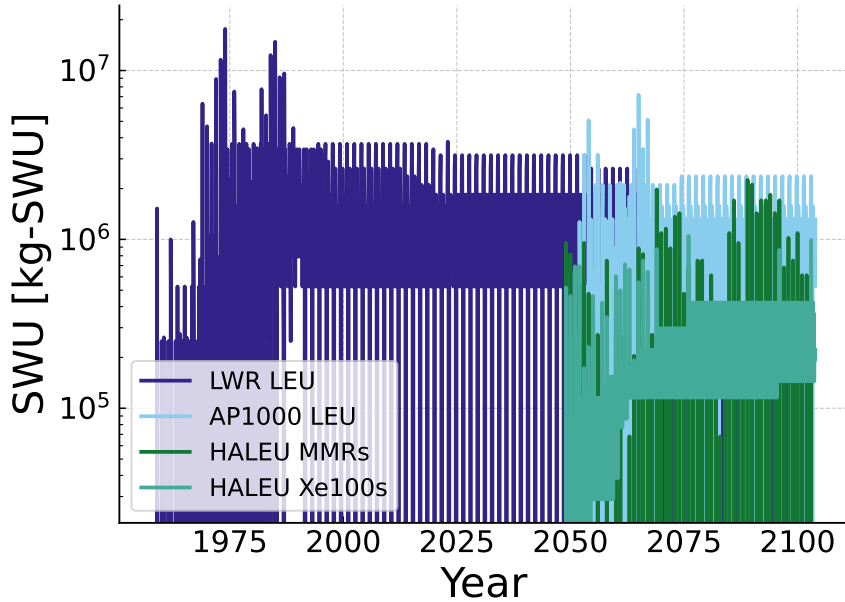


Figure 3.6: Greedy yearly SWU demand multi-fuel, no growth scenario by fuel type.

As the features of the yearly data are regular and dictated by the reactor's fuel cycle, Figures 3.7 and 3.8 visualize the total cumulative SWU demand for each type of fuel. The trend where the AP1000 peaks above SWU to the other reactors is exacerbated in the *double* by 2050 scenarios shown in Figures 3.7b and 3.8b, where the SWU from AP1000 LEU fuel rises quickly and eventually exceeds the total SWU for the existing fleet.

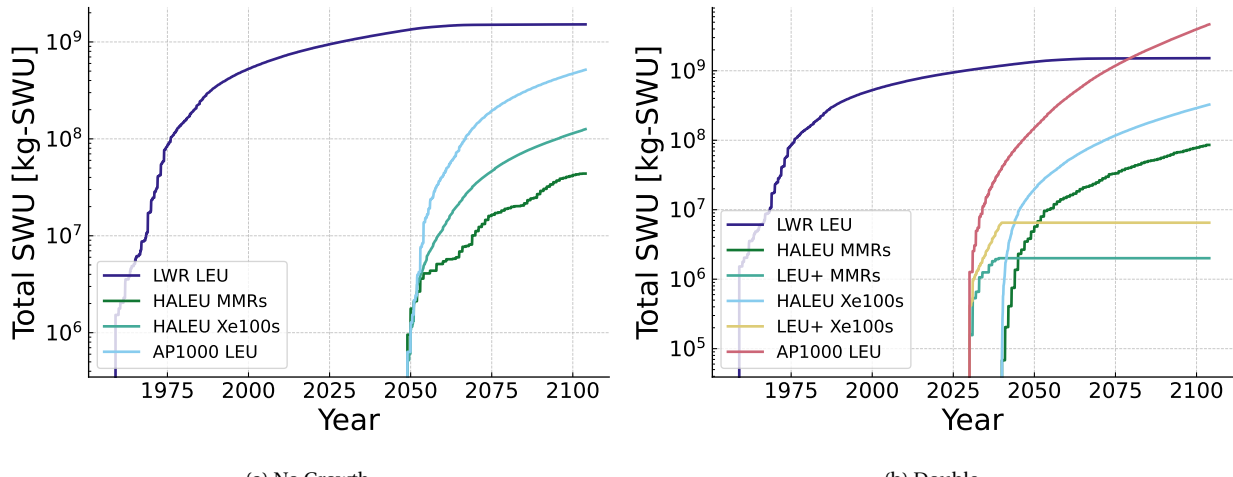


Figure 3.7: Greedy multi-fuel SWU by fuel type.

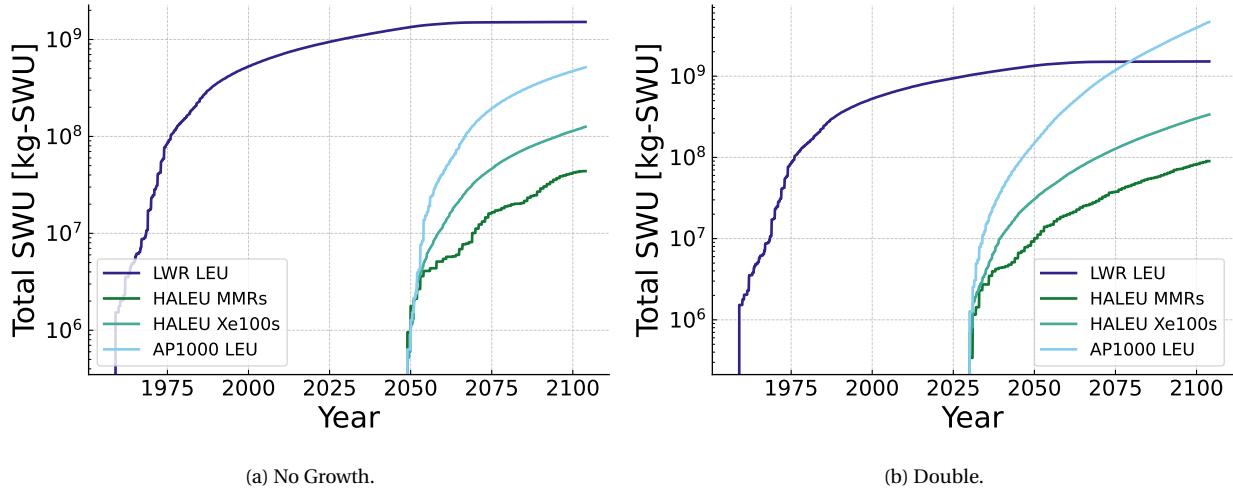


Figure 3.8: Greedy single-fuel SWU by fuel type.

Table 3.6 shows how the SWU demand for the MMR and Xe-100 reactors are the same in the single and multi-fuel enrichment deployments for the *no growth* scenarios, consistent with the reactor deployment trends in Section 3.3.1. The average SWU demand for the AP1000s increases by 800% from the *no growth* scenario to the *double by 2050* scenario, again consistent with the reactor deployment trends in the previous section. The average SWU demand for Xe-100 HALEU increases by 167%, while the SWU demand for MMR HALEU increases by 105% from the *no growth* scenario to the *double by 2050* scenario.

Table 3.6: Average greedy yearly SWU by fuel design in kSWU from 2030 to the end of the simulation.

Scenario	No Growth, Single	No Growth, Multiple	Double, Single	Double, Multiple
MMR HALEU	48.699	48.699	99.974	95.127
MMR LEU+	–	–	–	2.228
Xe-100 HALEU	139.926	139.926	374.323	362.312
Xe-100 LEU+	–	–	–	7.227
AP1000 LEU	573.989	573.989	5167.815	5167.815

3.3.3 Mass of Fresh Fuel Results

Figures 3.9 and 3.10 show the fresh fuel demand for the reactors in the *no growth* and *double by 2050* scenarios. The fresh fuel curves in each scenario follow the same pattern as the reactor deployment curves, as CYCLUS supplies fuel to each of the reactors as it is deployed.

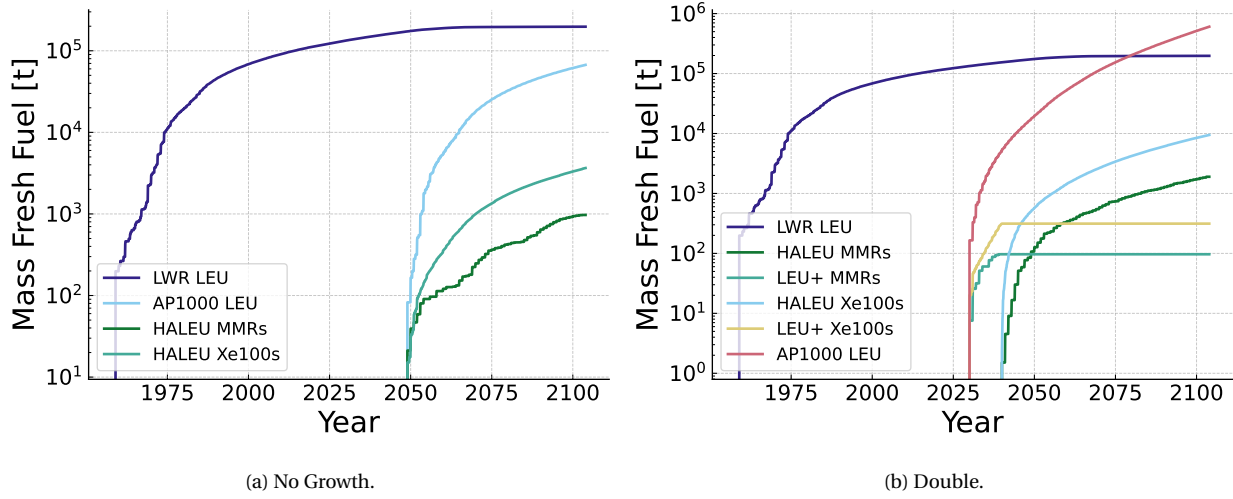


Figure 3.9: Greedy multi fresh fuel demanded by fuel type.

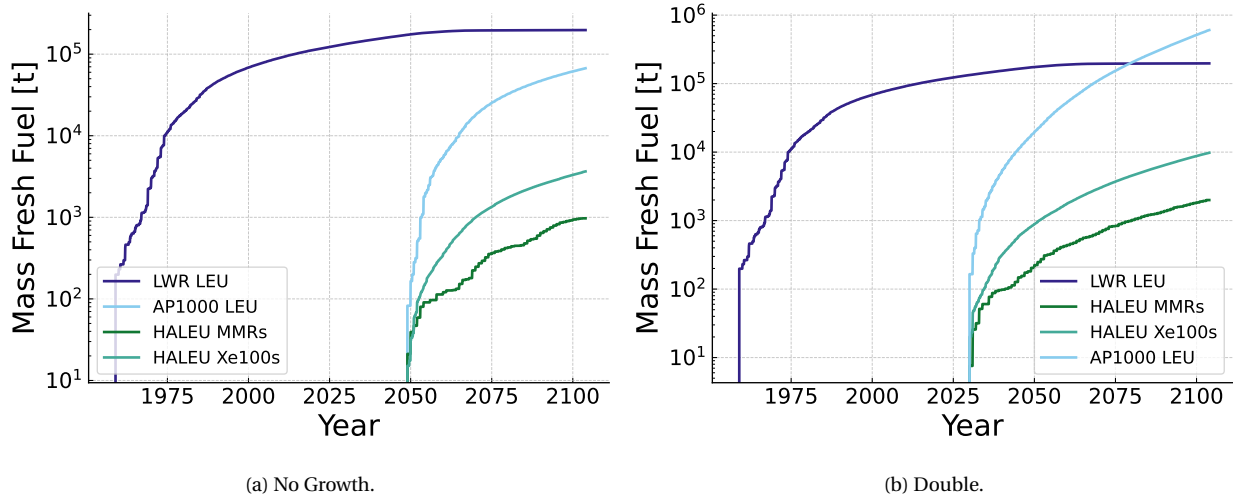


Figure 3.10: Greedy single fresh fuel demanded by fuel type.

Table 3.7 quantifies the average yearly fresh fuel demand by design in the *no growth* and *double* by 2050 scenarios. The AP1000 LEU shows the largest increase in average fresh fuel demand from the *no growth* scenario to the *double by 2050* scenario at 800%, followed by the Xe-100 HALEU at 159%. The MMR HALEU reactors show the smallest average increase in fresh fuel demand at 105%.

Table 3.7: Average greedy yearly fresh fuel by fuel design in tonnes from 2030 to the end of the simulation.

Scenario	No Growth, Single	No Growth, Multiple	Double, Single	Double, Multiple
MMR HALEU	1.079	1.079	2.216	2.108
MMR LEU+	–	–	–	0.107
Xe-100 HALEU	4.059	4.059	10.859	10.511
Xe-100 LEU+	–	–	–	0.348
AP1000 LEU	74.636	74.636	671.976	671.976

3.3.4 Mass of Used Fuel Results

Figures 3.11 and 3.12 describe the used fuel demand for the reactors in the *no growth* and *double by 2050* scenarios. The used fuel curves in each scenario lag the reactor deployment curves, as CYCLUS removes the used fuel after the given number of cycles from each operating, and eventually decommissioning, reactor.

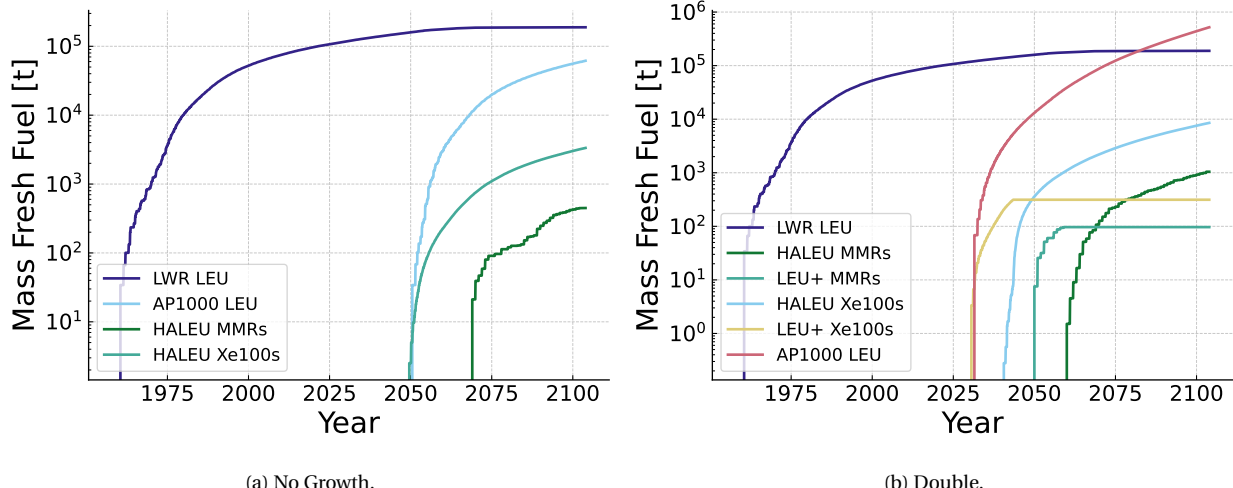


Figure 3.11: Greedy multi used fuel accumulation by fuel type.

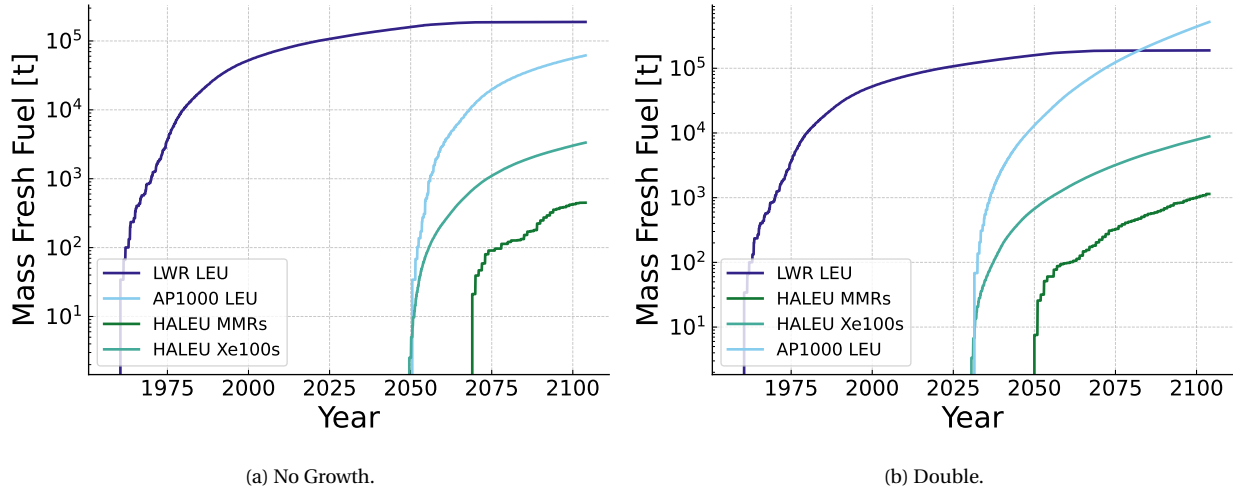


Figure 3.12: Greedy single used fuel accumulation by fuel type.

Table 3.8 itemizes the average yearly used fuel by design in the *no growth* and *double by 2050* scenarios. The average AP1000 LEU shows the largest increase in used fuel demand from the *no growth* scenario to the *double by 2050* scenario at 743%, followed by the Xe-100 HALEU at 164%. The average MMR HALEU reactors show the smallest increase in used fuel demand at 154%.

Table 3.8: Average greedy yearly used fuel by fuel design in tonnes from 2030 to the end of the simulation.

Scenario	No Growth, Single	No Growth, Multiple	Double, Single	Double, Multiple
MMR HALEU	0.499	0.499	1.267	1.160
MMR LEU+	–	–	–	0.107
Xe-100 HALEU	3.714	3.715	9.826	9.477
Xe-100 LEU+	–	–	–	0.348
AP1000 LEU	68.496	68.496	577.484	577.484

3.4 Random Deployment

Advanced reactor concepts, like the ones outlined in this thesis, are often designed for use cases ranging from industrial steam production to microgrid integration. Reactor deployment is a complex problem that requires a nuanced understanding of the energy market, regulatory environment, intended use of the technology, and the technical capabilities of the reactor.

This random deployment is a proxy for the complexity of the real-world problem; however, it does not include

the nuance of how individual deployments meet an end user's needs, which will drive the strategic decisions that utilities and ratepayers behind the meter make in their reactor choices. The random deployment scheme has the potential to capture some of the complexities in overall market development, but the extent to which it captures these details is not explored in this thesis.

The random deployment scheme is implemented by randomly selecting reactors from the list of deployable reactors until the demand is covered. Figure 3.13 illustrates this scheme, which shows the single loop in the logic from the top down. There is an irreducible demand that cannot be met because the power capacity is assumed to be constant. At its best, the random deployment scheme will meet the demand but has the potential to fall short of the demand by one of the smallest capacity reactors. This thesis implements a random rough case that deploys until the randomly selected reactor exceeds the demand to reduce the computational cost. This rough approximation is coupled with the greedy deployment scheme in the initially random, greedy deployment scheme in Section 3.5.

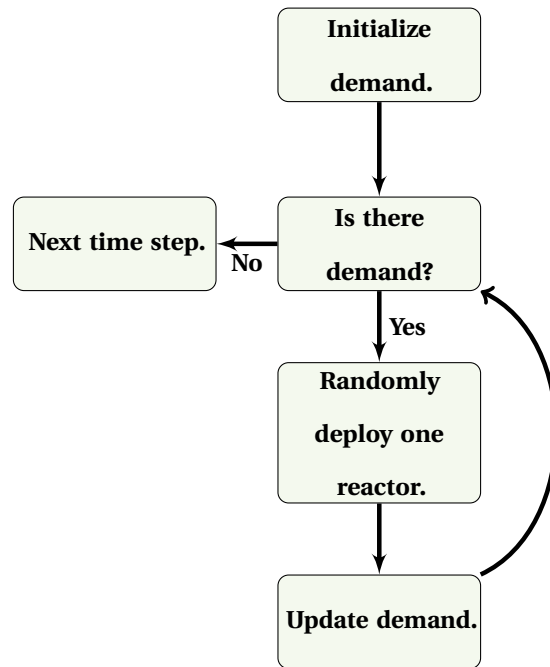


Figure 3.13: The random deployment diagram shows the method by which this scheme selects reactors at each time step.

The seed, which was set to 20240527121205 for every run for this scheme, for the random number generator is set by the date and time of the simulation to allow for the reproducibility of the results. This scheme is a proxy for aggregate decisions by actors and would fail to reliably capture individual actor decisions. This scheme is most useful for scenarios or timescales where there is a high degree of uncertainty in the deployment of reactors.

3.4.1 Number of Reactors

Figure 3.14 and 3.15 show the cumulative number of each reactor deployed in the *no growth* and *double by 2050* for the random scheme. The difference between the *no growth* and *double by 2050* scenarios in Figures 3.14 and 3.15 is that the *double by 2050* scenario requires new reactors to be deployed immediately during the transition. A consequence of the random reactor deployment scheme is that the reactors in Figures 3.14a and 3.14b grows similarly over time as they are sampled for deployment. This scheme has the potential to stochastically capture the complexity of deploying reactors in the real world but likely represents an extreme where utilities are not narrowing in on a single reactor design to reduce deployment costs.

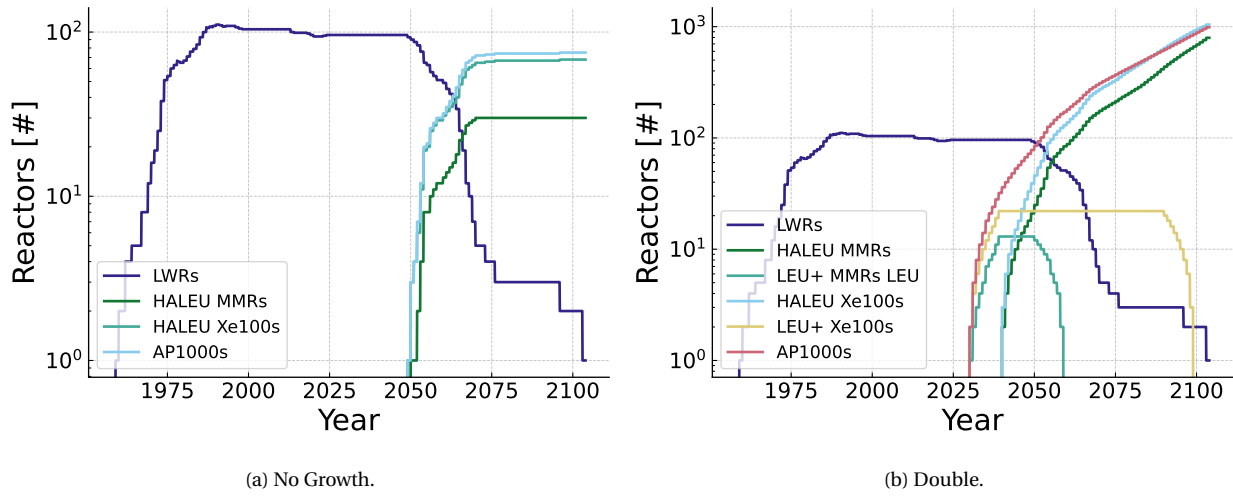


Figure 3.14: Multiple fuels random reactor deployment.

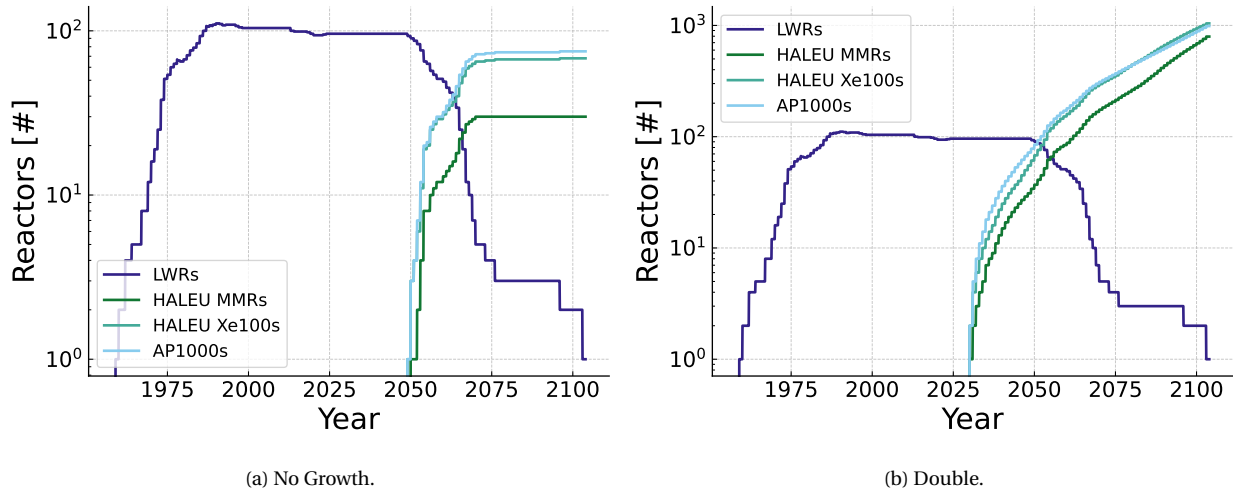


Figure 3.15: Single-fuel random reactor deployment.

Table 3.9 shows the average total number of reactors for the *no growth* and *double by 2050* scenarios in the single and multi-fuel enrichment deployments. There is a 740% increase in the AP1000s deployed from the *no growth* scenario to the *double by 2050* scenario. The average number of Xe-100 reactors show a 249% increase, while the MMR reactors show a 62% increase in the reactors deployed from the *no growth* scenario to the *double by 2050* scenario in the single-fuel enrichment deployment. Unlike the reactor deployment under the greedy scheme in Section 3.3.1 and the initially random then greedy scheme in Section 3.5.1, the random deployment scheme results for the single-fuel and multi-fuel enrichment deployments are not the same.

In the multi-fuel enrichment deployment, the AP1000 reactors show a 660% increase in the reactors deployed from the *no growth* scenario to the *double by 2050* scenario. The Xe-100 reactors show a 746% increase, while the MMR reactors show an 1138% increase in the reactors deployed from the *no growth* scenario to the *double by 2050* scenario.

Table 3.9: Average random total operating reactors by design from 2030 to the end of the simulation.

Scenario	No Growth, Single	No Growth, Multiple	Double, Single	Double, Multiple
HALEU fueled MMRs	131.613	17.267	213.707	210.24
LEU+ fueled MMRs	–	–	–	3.467
HALEU fueled Xe-100s	94.04	38.813	328.173	310.573
LEU+ fueled Xe-100s	–	–	–	17.6
LEU fueled AP1000s	38.667	42.72	324.68	324.68

3.4.2 SWU Results

Figure 3.16 visualizes the yearly SWU demand periodically spike as reactors begin operation in the depicted *no growth* scenario around 2050. The SWU demand for the AP1000 LEU rises above the other two reactors where the demand from Xe-100s overlaps heavily with the demand from MMRs. This trend is exacerbated in the *double by 2050* scenarios shown in Figures 3.7b and 3.8b, where the SWU for AP1000 LEU fuel rises quickly and eventually exceeds the total SWU for the existing fleet.

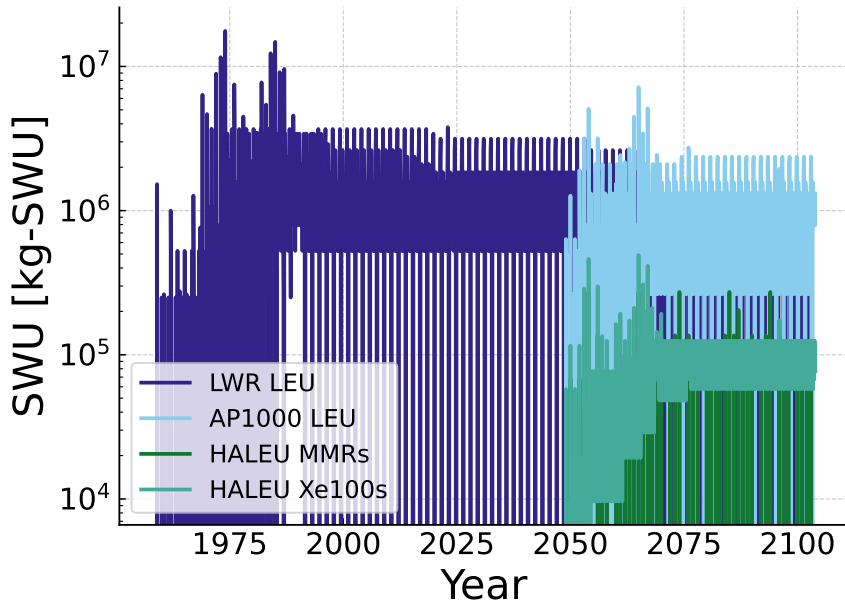


Figure 3.16: Random reactor yearly SWU demand by fuel type.

As the features of the yearly data are regular, dictated by the cycles of the reactors, and overlapping, Figures 3.17 and 3.18 visualize the total cumulative SWU demand.

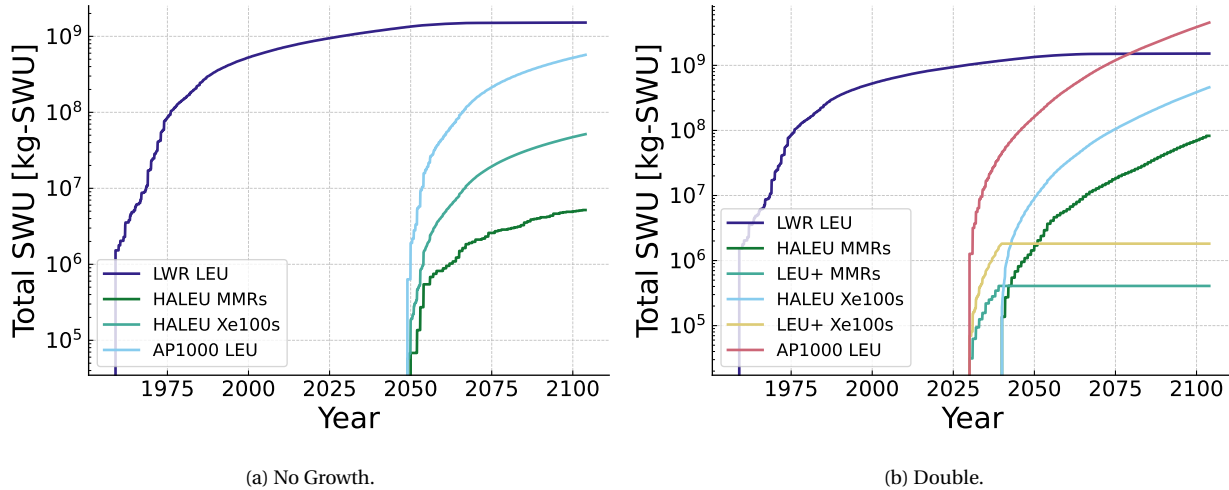


Figure 3.17: Random reactor multi-fuel SWU by fuel type.

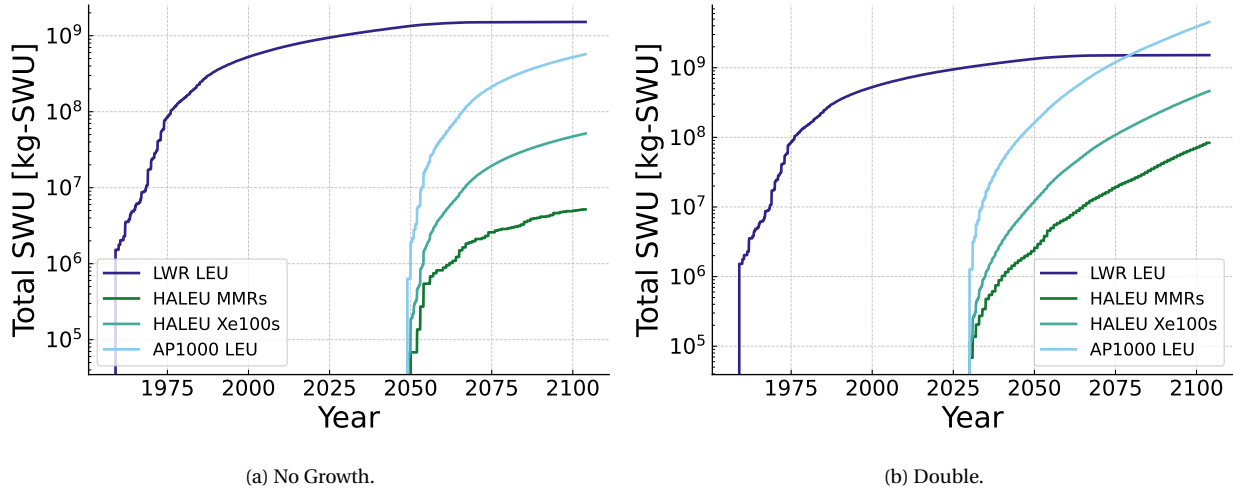


Figure 3.18: Random reactor single-fuel SWU by fuel type.

Table 3.10 shows the average total yearly SWU demand for the *no growth* and *double by 2050* scenarios in the single and multi-fuel enrichment deployments under the random deployment scheme. The Xe-100 reactors show a 796% increase in the average total yearly SWU demand from the *no growth* scenario to the *double by 2050* scenario in the single-fuel enrichment deployment. The MMRs show a 1511% increase in the average total yearly SWU demand from the *no growth* scenario to the *double by 2050* scenario in the single-fuel enrichment deployment. The AP1000 reactors show a 697% increase in the average total yearly SWU demand from the *no growth* scenario to the *double by 2050* scenario in the single-fuel enrichment deployment.

Table 3.10: Average random yearly SWU by fuel design in tonnes of SWU from 2030 to the end of the simulation.

Scenario	No Growth, Single	No Growth, Multiple	Double, Single	Double, Multiple
MMR HALEU	5.756	5.756	92.703	91.719
MMR LEU+	–	–	–	0.453
Xe-100 HALEU	57.327	57.327	513.746	510.388
Xe-100 LEU+	–	–	–	2.021
AP1000 LEU	634.554	634.554	5050.323	5050.323

3.4.3 Mass of Fresh Fuel Results

Figures 3.19 and 3.20 show the fresh fuel demand for the reactors in the *no growth* and *double by 2050* scenarios. The fresh fuel curves in each scenario follow the same pattern as the reactor deployment curves from Figures 3.14

and 3.15, as CYCLUS supplies fuel to each of the reactors as they deploy.

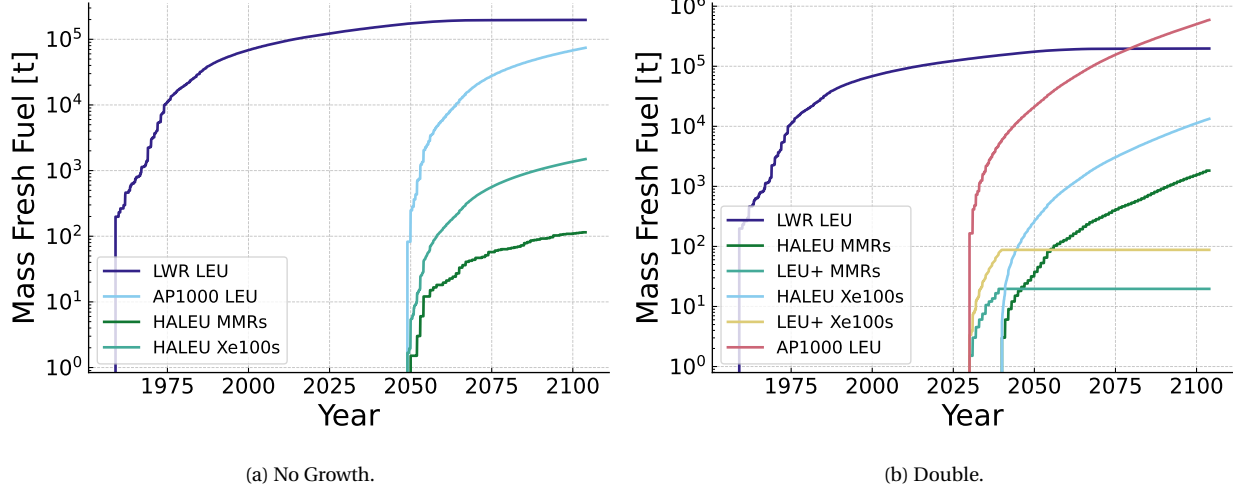


Figure 3.19: Random multi fresh fuel demanded by fuel type.

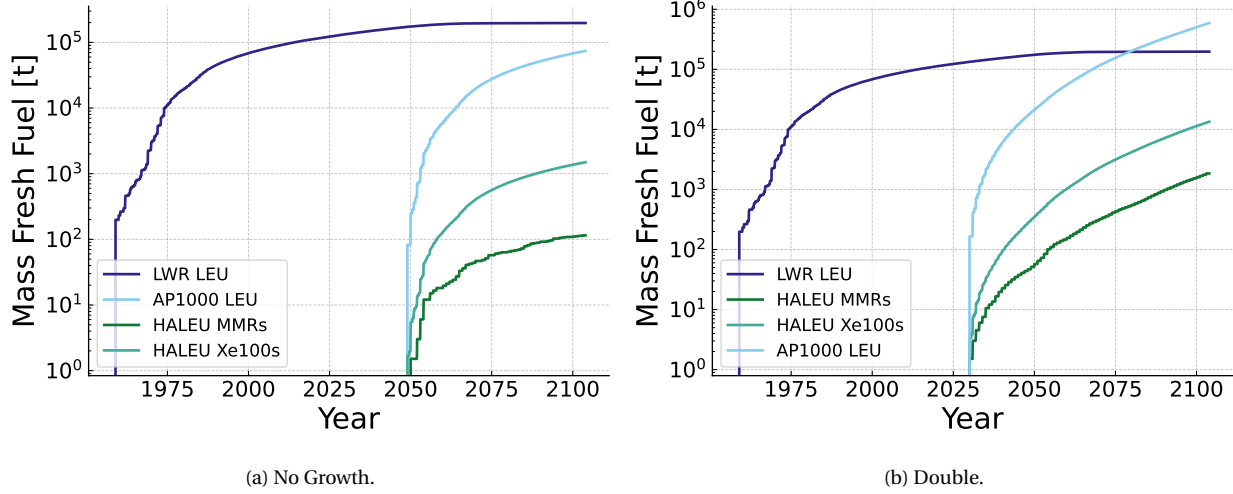


Figure 3.20: Random single fresh fuel demanded by fuel type.

Table 3.11 shows the average total yearly fresh fuel for the *no growth* and *double by 2050* scenarios in the single and multi-fuel enrichment deployments under the random deployment scheme. The Xe-100 reactors show a 796% increase in the average total yearly fresh fuel from the *no growth* scenario to the *double by 2050* scenario in the single-fuel enrichment deployment. The MMR reactors show a 1505% increase in the average total yearly fresh fuel from the *no growth* scenario to the *double by 2050* scenario in the single-fuel enrichment deployment. The AP1000 reactors show a 696% increase in the average total yearly fresh fuel from the *no growth* scenario to the *double by 2050* scenario in the single-fuel enrichment deployment.

Table 3.11: Average random yearly fresh fuel by fuel design in tonnes from 2030 to the end of the simulation.

Scenario	No Growth, Single	No Growth, Multiple	Double, Single	Double, Multiple
MMR HALEU	0.128	0.128	2.055	2.033
MMR LEU+	–	–	–	0.107
Xe-100 HALEU	1.663	1.663	14.904	14.806
Xe-100 LEU+	–	–	–	0.022
AP1000 LEU	82.512	82.512	656.698	656.698

3.4.4 Mass of Used Fuel Results

Figures 3.21 and 3.22 depict the used fuel accumulation for the reactors in the *no growth* and *double by 2050* scenarios. The used fuel curves in each scenario follow the reactor deployment curves with a lag corresponding to the cycle length of the reactor from Figures 3.14 and 3.15, as CYCLUS removes fuel from each reactor.

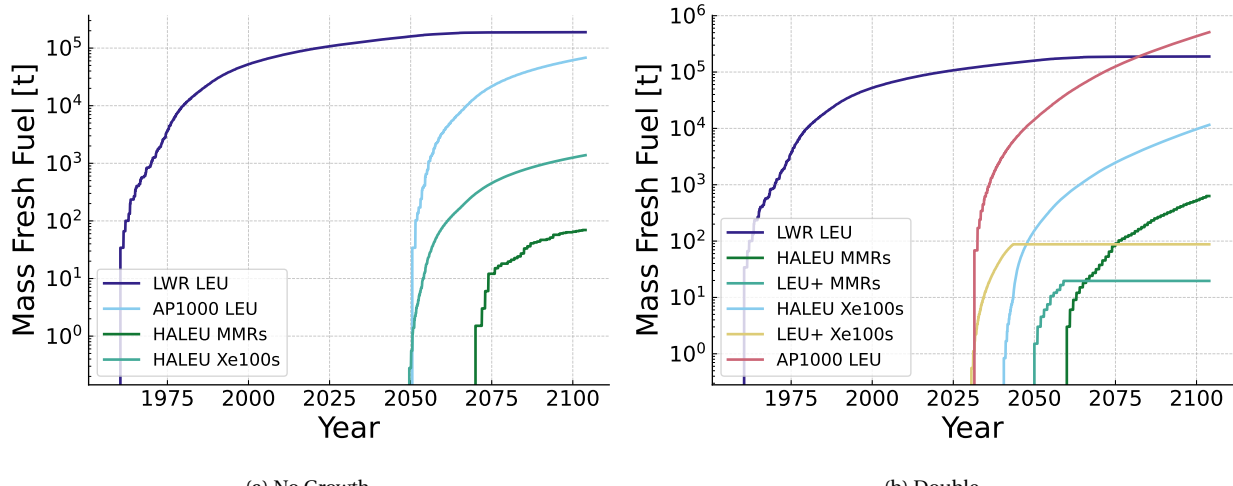


Figure 3.21: Random multi used fuel accumulation by fuel type.

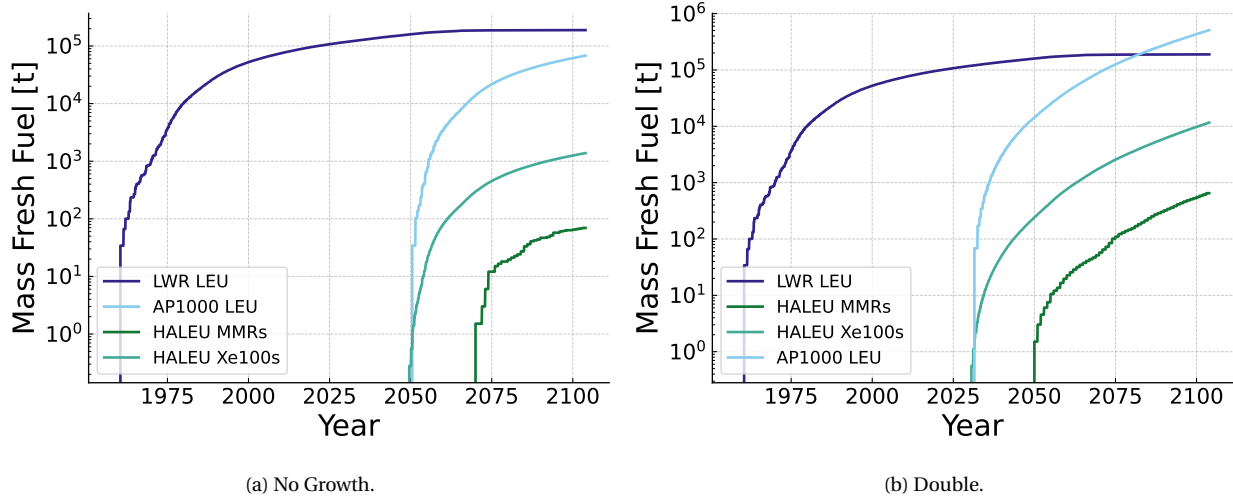


Figure 3.22: Random single used fuel accumulation by fuel type.

Table 3.12 shows the average total yearly used fuel for the *no growth* and *double by 2050* scenarios in the single and multi-fuel enrichment deployments under the random deployment scheme. The Xe-100 reactors show a 742% increase in the average total yearly used fuel from the *no growth* scenario to the *double by 2050* scenario in the single-fuel enrichment deployment. The MMR reactors show a 838% increase in the average total yearly used fuel from the *no growth* scenario to the *double by 2050* scenario in the single-fuel enrichment deployment. The AP1000 reactors show a 649% increase in the average total yearly used fuel from the *no growth* scenario to the *double by 2050* scenario in the single-fuel enrichment deployment.

Table 3.12: Average random yearly used fuel by fuel design in tonnes from 2030 to the end of the simulation.

Scenario	No Growth, Single	No Growth, Multiple	Double, Single	Double, Multiple
MMR HALEU	0.077	0.077	0.722	0.700
MMR LEU+	–	–	–	0.107
Xe-100 HALEU	1.536	1.536	12.930	12.833
Xe-100 LEU+	–	–	–	0.022
AP1000 LEU	75.638	75.638	566.239	566.239

3.5 Initially Random, Greedy Deployment

Combining the random and greedy deployment schemes allows us to inject uncertainty as to which reactor will be deployed at any given time while ensuring that the demand is met efficiently. This scheme does merely allows us to

leverage the strengths of both the random or greedy deployment.

This deployment scheme randomly deploys reactors until a reactor bigger than the remaining capacity is proposed for each year, then it fills the remaining capacity with a greedy algorithm. Figure 3.23 outlines, which shows the two loops (first random, then greedy) in the logic from the top down.

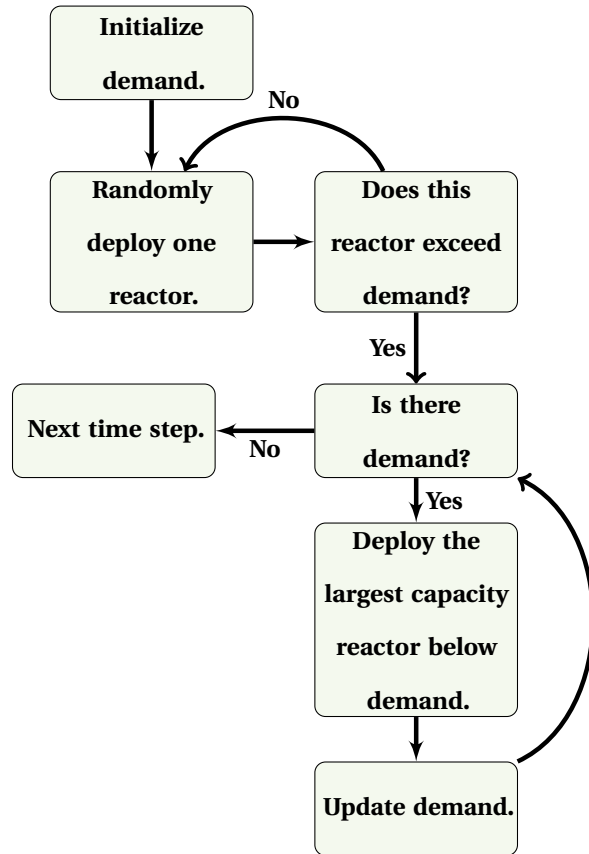


Figure 3.23: The initially random, greedy deployment diagram demonstrates how the random and greedy deployment schemes complement each other for a single time step.

This scheme combines random and greedy deployment schemes and inherits their realistic and unrealistic elements. The random deployment scheme captures some of the complexity of the deployment problem but does not guarantee the capture of the nuance of future user needs. The greedy deployment scheme captures the efficiency of the deployment problem but does not capture the complexity of the deployment problem.

The seed, which was set to 20240527121205 for every run for this scheme, for the random number generator is set by the date and time of the simulation, which allows for the reproducibility of the results. The degree to which this scheme captures features of the random or greedy deployment schemes varies with the number of reactors deployed in the random phase. Instead of randomly deploying until the demand is met, this implementation randomly deploys until the selected reactor exceeds the demand. This means that when the reactors are different

sizes, there is a chance that the random phase will deploy a reactor larger than the demand, and the greedy phase will make up more of the deployment.

3.5.1 Number of Reactors

Figure 3.24 and 3.25 show the cumulative number of each reactor deployed in the *no growth* and *double by 2050* for the greedy scheme. As with the random deployment scheme, they show that the share of reactors by design is much closer than the greedy deployment scheme. The reactors in the *no growth* scenarios (shown in Figures 3.24a and 3.25a) are deployed close to 2050, whereas the advanced reactors in the *double by 2050* scenarios (shown in Figures 3.24b and 3.25b) are deployed close to 2030.

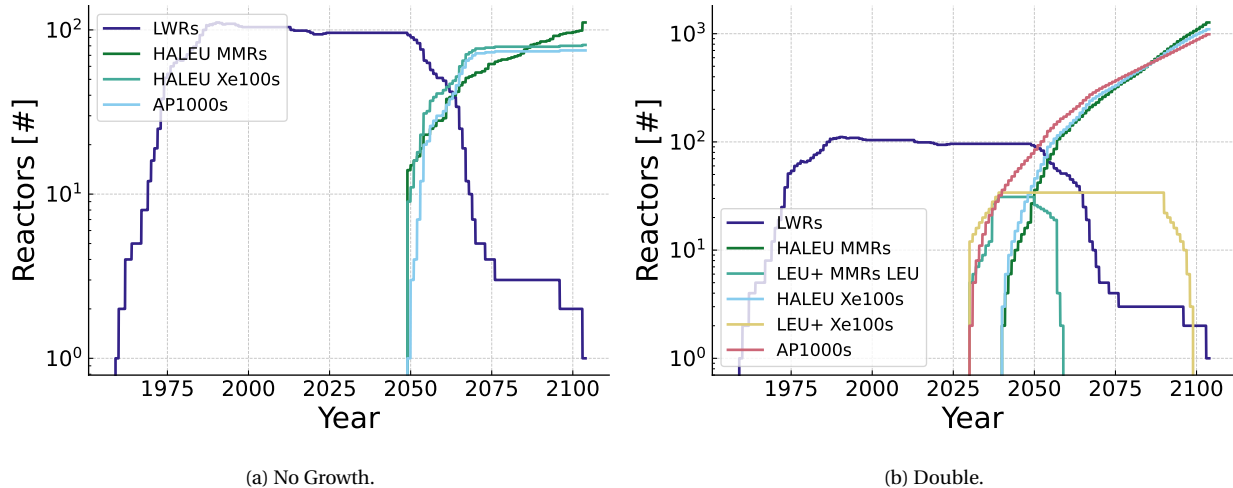


Figure 3.24: Multiple fuels initially random, then greedy reactor deployment.

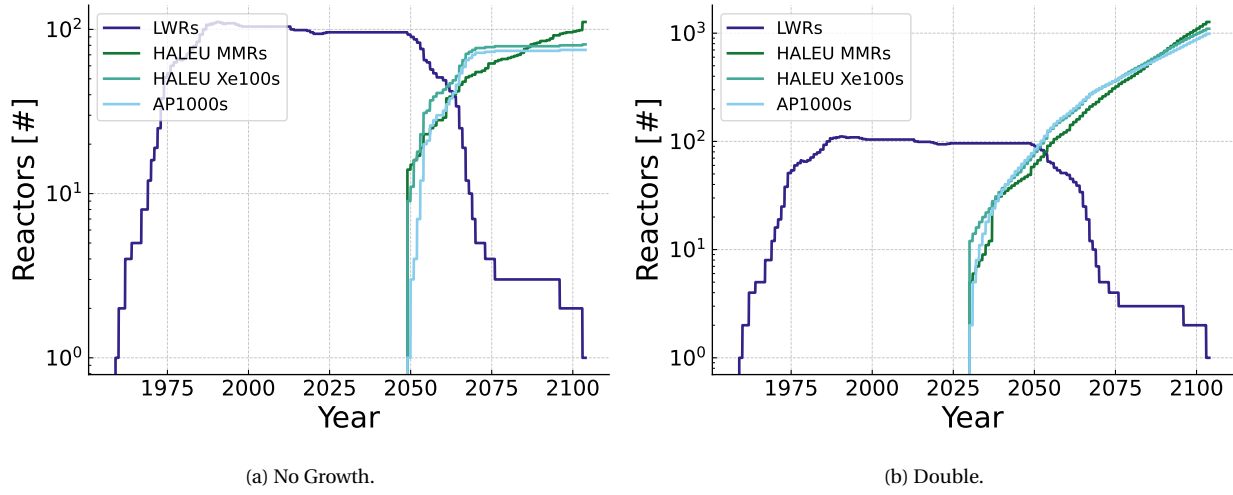


Figure 3.25: Single-fuel initially random, then greedy reactor deployment.

Table 3.13 shows the average total operating reactors by design for the *no growth* and *double by 2050* scenarios for the multi and single-fuel enrichment deployments. The HALEU fueled MMR and Xe-100 deployment is unchanged in the single and multi-fuel enrichment deployments for the *no growth* scenarios. The number of AP1000 reactors increases 660% from the *no growth* to the *double by 2050* scenario in the multi-fuel enrichment deployment. The number of HALEU fueled Xe-100 reactors increases 626%, while the number of HALEU fueled MMR reactors increases 649%.

Table 3.13: Average initially random, then greedy total operating reactors by design from 2030 to the end of the simulation.

Scenario	No Growth, Single	No Growth, Multiple	Double, Single	Double, Multiple
HALEU fueled MMRs	44.547	44.547	333.613	325.347
LEU+ fueled MMRs	—	—	—	8.267
HALEU fueled Xe-100s	47.52	47.52	344.88	317.68
LEU+ fueled Xe-100s	—	—	—	27.2
LEU fueled AP1000	42.72	42.72	324.68	324.68

3.5.2 SWU Results

Figure 3.26 shows the yearly SWU demand periodically spike as reactors begin operation in the depicted *no growth* scenario around 2050. The SWU demand for the AP1000 LEU rises above the other two reactors while the demand from Xe-100s overlaps heavily with the demand from MMRs. This trend is exacerbated in the *double by 2050*

scenarios shown in Figures 3.27b and 3.28b where the SWU for AP1000 LEU fuel rises quickly and eventually exceeds the total SWU for the existing fleet.

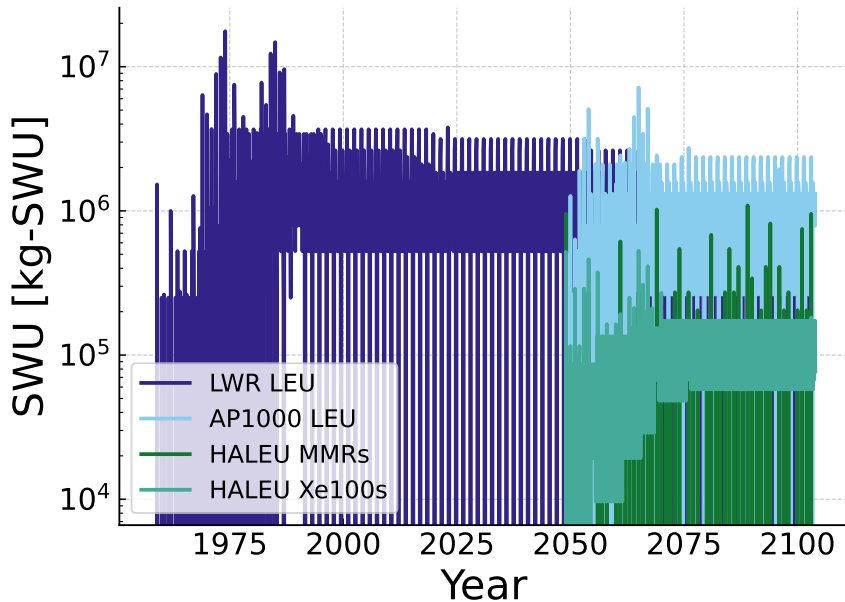
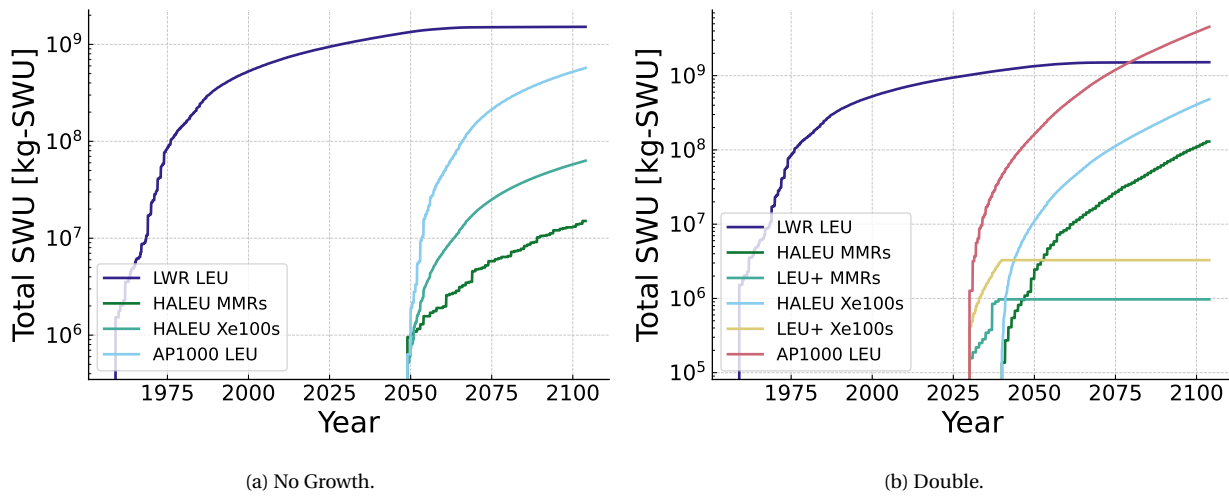


Figure 3.26: Initially random, then greedy yearly SWU demand by fuel type.

As the features of the yearly data are regular, dictated by the cycles of the reactors, and overlapping, Figures 3.27 and 3.28 visualize the total cumulative SWU demand.



(a) No Growth.

(b) Double.

Figure 3.27: Initially random, then greedy multi-fuel SWU by fuel type.

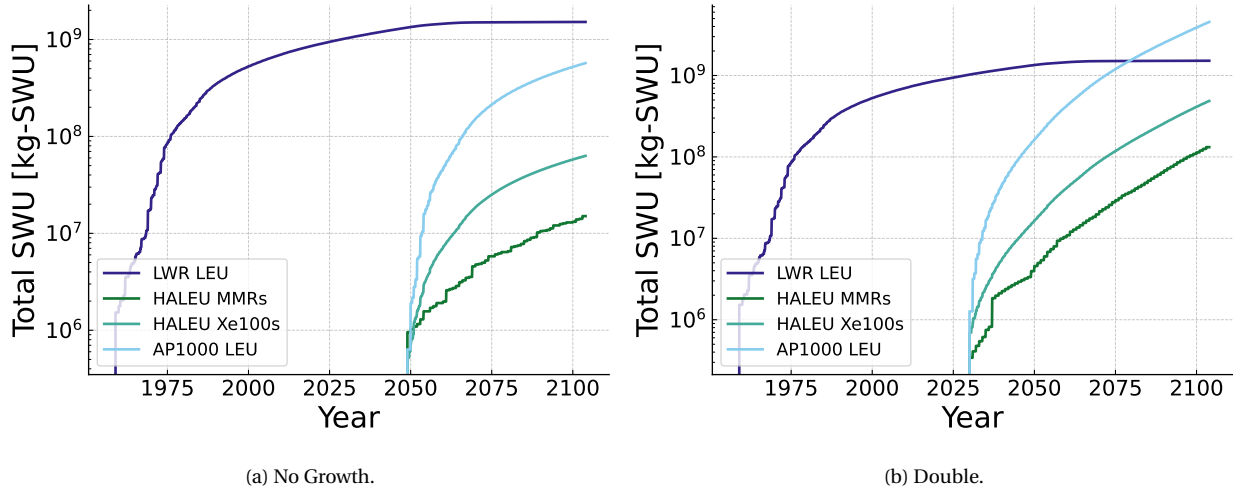


Figure 3.28: Initially random, then greedy single-fuel SWU by fuel type.

Table 3.14 shows the average yearly SWU for the *no growth* and *double* by 2050 scenarios for the multi and single-fuel enrichment deployments. The SWU demand for the MMR and Xe-100 reactors is the same in the single and multi-fuel enrichment deployments for the *no growth* scenarios, which is consistent with the reactor deployment trends in the Section 3.5.1. Across scenarios, the demand for SWU for AP1000 LEU fuel increases 696% from the *no growth* to the *double by 2050* scenario in the single-fuel enrichment deployment. The demand for SWU for HALEU fuel in the MMR and Xe-100 reactors increases 775% and 672% respectively from the *no growth* to the *double by 2050* scenario in the multi-fuel enrichment deployment.

Table 3.14: Average initially random, then greedy yearly SWU by fuel design in kSWU from 2030 to the end of the simulation.

Scenario	No Growth, Single	No Growth, Multiple	Double, Single	Double, Multiple
MMR HALEU	16.738	16.738	146.477	144.129
MMR LEU+	–	–	–	1.079
Xe-100 HALEU	70.066	70.066	540.613	534.559
Xe-100 LEU+	–	–	–	3.624
AP1000 LEU	634.553	634.553	5050.323	5050.323

3.5.3 Mass of Fresh Fuel Results

Figures 3.29 and 3.30 show the fresh fuel demand for the reactors in the *no growth* and *double by 2050* scenarios. The fresh fuel curves in each scenario follow the same pattern as the reactor deployment curves from Figures 3.24

and 3.25, as CYCLUS supplies fuel to each of the reactors as it they deploy.

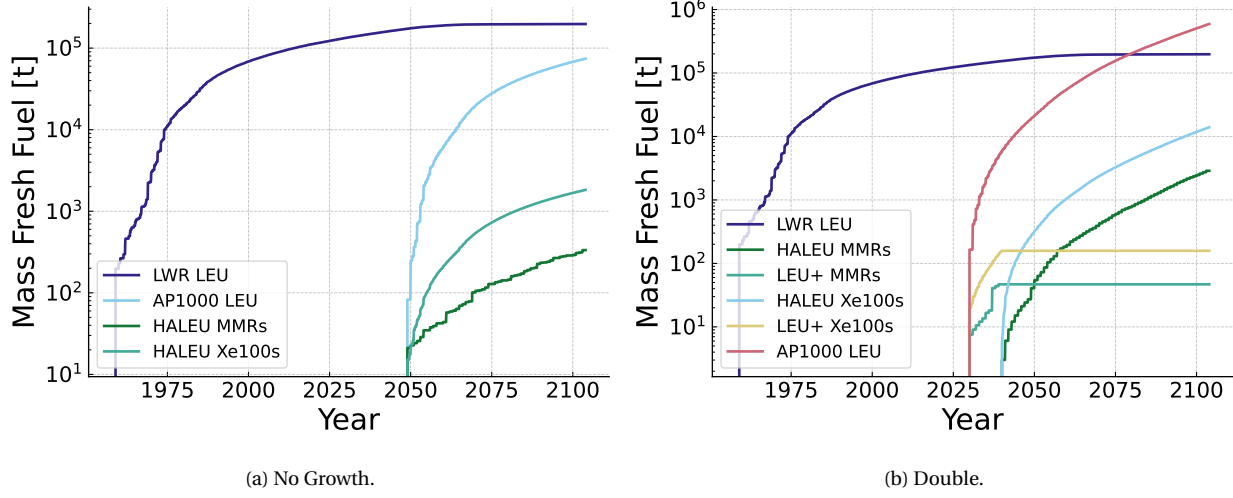


Figure 3.29: Initially random, then greedy multi fresh fuel demanded by fuel type.

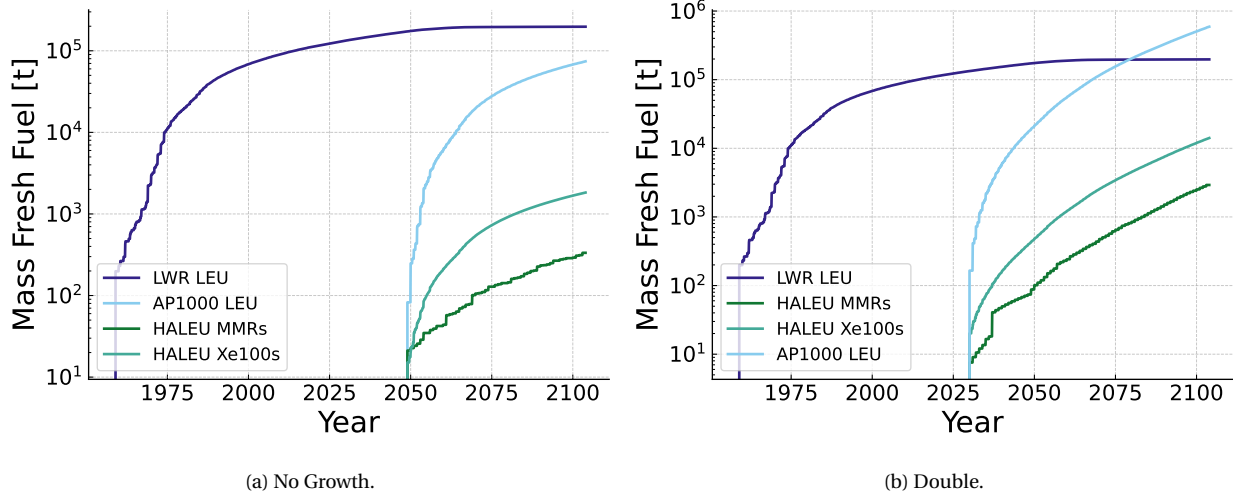


Figure 3.30: Initially random, then greedy single fresh fuel demanded by fuel type.

Table 3.15 shows the average yearly fresh fuel by design in tonnes for the *no growth* and *double by 2050* scenarios for the multi and single-fuel enrichment deployments. The fresh fuel demand for the reactors is the same in the single and multi-fuel enrichment deployments for the *no growth* scenarios, which is consistent with the reactor deployment trends in the Section 3.5.1. Across scenarios, the demand for fresh fuel for AP1000 LEU fuel increases 696% from the *no growth* to the *double by 2050* scenario in the single-fuel enrichment deployment. The demand for fresh fuel for HALEU fuel in the MMR and Xe-100 reactors increases 775% and 671% respectively from the *no growth* to the *double by 2050* scenario in the multi-fuel enrichment deployment.

Table 3.15: Average initially random, then greedy yearly fresh fuel by fuel design in tonnes from 2030 to the end of the simulation.

Scenario	No Growth, Single	No Growth, Multiple	Double, Single	Double, Multiple
MMR HALEU	0.371	0.371	3.247	3.194
MMR LEU+	–	–	–	0.052
Xe-100 HALEU	2.033	2.033	15.683	15.507
Xe-100 LEU+	–	–	–	0.176
AP1000 LEU	82.512	82.512	656.698	656.698

3.5.4 Mass of Used Fuel Results

Figures 3.31 and 3.32 depict the used fuel accumulation for the reactors in the *no growth* and *double by 2050* scenarios. The used fuel curves in each scenario follow the reactor deployment curves with a lag corresponding to the cycle length of the reactor from Figures 3.24 and 3.25, as CYCLUS removes fuel from each reactor.

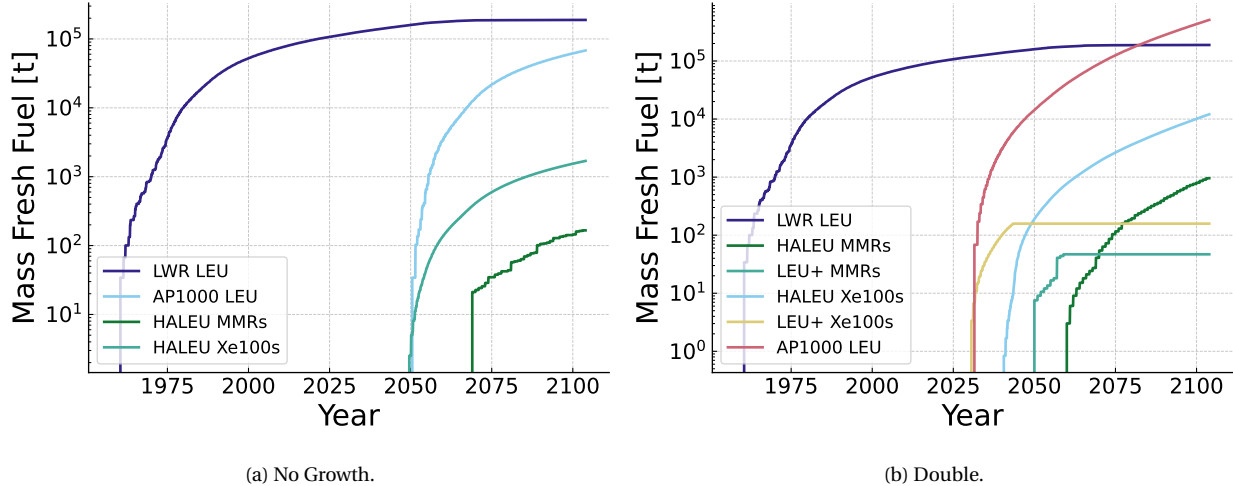


Figure 3.31: Initially random, then greedy multi used fuel accumulation by fuel type.

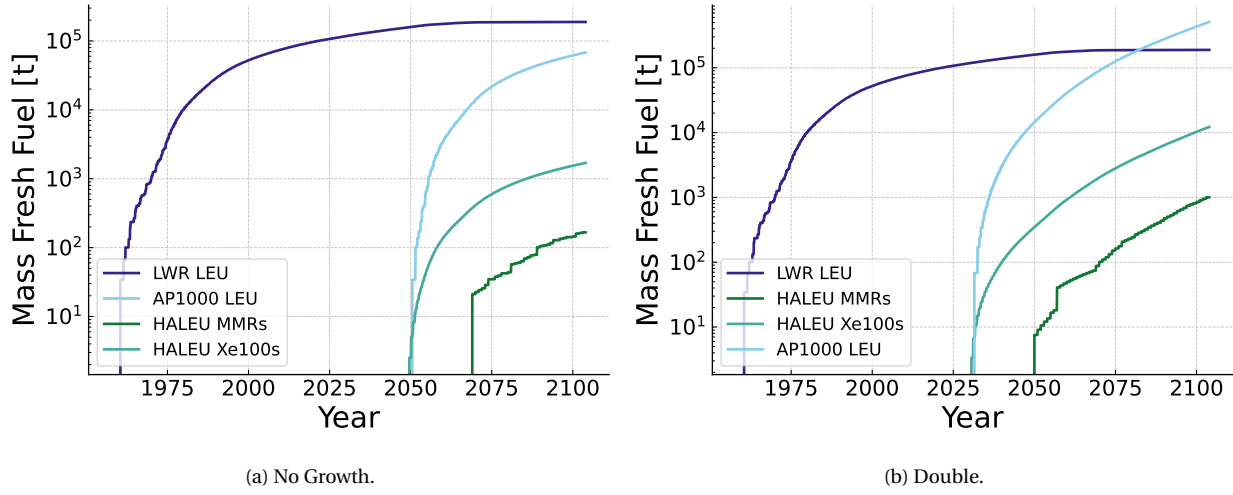


Figure 3.32: Initially random, then greedy single used fuel accumulation by fuel type.

Table 3.16 shows the average yearly used fuel by design in tonnes for the *no growth* and *double by 2050* scenarios for the multi and single-fuel enrichment deployments. The used fuel demand for the reactors is the same in the single and multi-fuel enrichment deployments for the *no growth* scenarios, which is consistent with the reactor deployment trends in the Section 3.5.1. Across scenarios, the demand for used fuel for AP1000 LEU fuel increases 649% from the *no growth* to the *double by 2050* scenario in the single-fuel enrichment deployment. The demand for used fuel for HALEU fuel in the MMR and Xe-100 reactors increases 503% and 620% respectively from the *no growth* to the *double by 2050* scenario in the multi-fuel enrichment deployment.

Table 3.16: Average initially random, then greedy yearly used fuel by fuel design in tonnes from 2030 to the end of the simulation.

Scenario	No Growth, Single	No Growth, Multiple	Double, Single	Double, Multiple
MMR HALEU	0.185	0.185	1.115	1.063
MMR LEU+	-	-	-	0.052
Xe-100 HALEU	1.882	1.882	13.549	13.419
Xe-100 LEU+	-	-	-	0.176
AP1000 LEU	75.638	75.638	566.239	566.239

Chapter 4

Reactor Power and Market Interactions

This chapter explores how altering the frequency with which the CYCAMORE reactor interacts with the Dynamic Resource Exchange (DRE) in CYCLUS impacts the computational efficiency of a simulation and how to make the power output from a reactor more realistic. The reactor archetypes are available on GitHub [59].

4.1 Archetypes and Time Management

Throughout the CYCLUS ecosystem, archetypes interact with the DRE and each other in a fixed, user-defined time step, forcing the entire simulation to operate on the smallest universal time step. For example, if a fabrication facility can produce material every 2 months but the enrichment facility can only provide material every 3 months, CYCLUS would need to use a 1-month time step to capture both. When the time step is smaller than the minimum for a given facility, that facility still participates in the DRE despite not needing to receive or send any materials. These, across hundreds of facilities, add inefficiencies when solving the transaction problem at each time step.

In the CYCLUS ecosystem there is an archetype called *PatternSink* wherein the user can alter the frequency at which the sink, often a repository, can accept the material. Figure 4.1 outlines an example scenario for this archetype with a simple A-B-C flow path. In this scenario, material is received from a source (A) to a reactor (B) with a final (C) sink that can only accept material at a specific frequency.



Figure 4.1: Simple A-B-C scenario.

The code alters how frequently the archetype updates its internal time step tracker. Figure 4.2 shows it appears, in Figure 4.2, as though multiple groups of material are received in one time step despite this archetype not having an idea of individual shipments. This archetype accomplishes the artificial restriction on accepting material by simply not updating the time step that the archetype is at until the next universal time step is met. Regardless of function, this is the only example of the timekeeping flexibility found in the ecosystem.

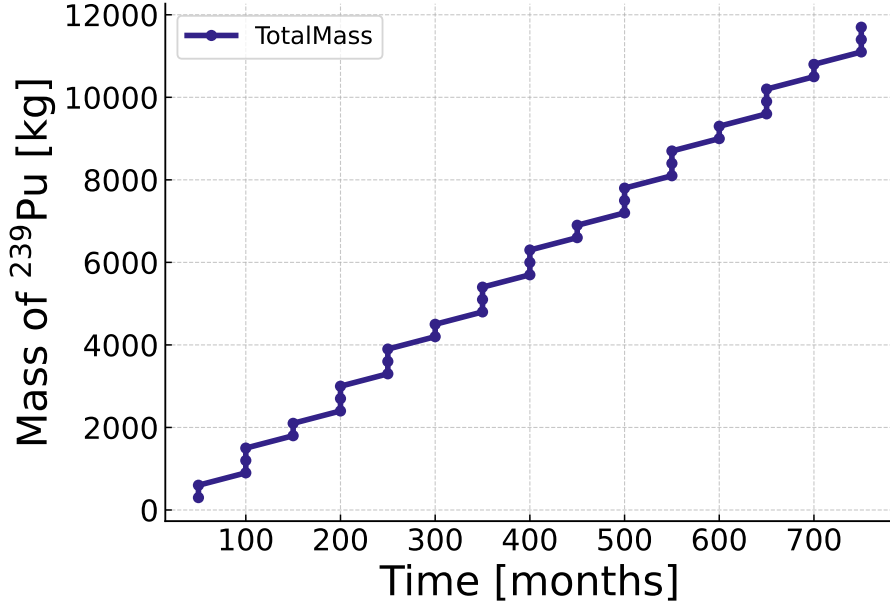


Figure 4.2: Acceptance of ^{239}Pu into the Sink with a frequency of 50 months using the *PatternSink* archetype.

While archetypes like *PatternSink* introduce new internal capabilities, they all inherit a set of base capabilities from the CYCLUS toolkit. The CYCLUS toolkit provides a modular and extensible framework for modeling nuclear fuel cycles (NFCs), allowing users to create custom archetypes that simulate various facilities and processes. These base capabilities standardize how archetypes create material buffers, interact with the DRE, and connect to the internal clock of the simulation, which are essential for coordinating the agents and commodities across their complex interactions within an NFC. This thesis examines the fundamental capabilities of the CYCLUS ecosystem and identifies time-intensive components of the current CYCMORE Reactor.

4.2 Trading On-Demand Reactor

As Section 4.1 discusses, CYCLUS simulations have a universal time step at which every facility operates. In each CYCLUS time step, every archetype undergoes three phases:

1. Tick: Agents respond to the current simulation state.
2. Exchange: This is where the market interactions happen with the DRE.
3. Tock: Agents reconcile their state.

For example, the CYCMORE reactor, when it refuels, will first identify which fuel is ready to be discharged in the Tick phase. Then, it will submit bids for new fuel and requests for somebody to take the used fuel away during the

Exchange phase. In the Tock phase, it loads the new fuel, and the old fuel is removed. From Tick to Tock, that's one time step, and the CYCMORE reactor, like other archetypes, operates on this universal time step and interacts with the DRE at every time step. This interaction is necessary for the reactor to receive fuel and to bid on material from other facilities; However, it is not necessary if the reactor does not need to refuel.

The basic structure of each time step is fundamental to aligning the material transactions and bids in the existing DRE, so a reduction in computational cost could come from checking whether or not it is time to refuel before engaging with the calculations that take place when the reactor needs to refuel. This thesis explores this reduction by building the Trading On-Demand (TOD) reactor, a modification on top of the CYCMORE reactor that calculates the time to refuel and skips the Tick and Tock phases if it is not time to refuel.

This thesis uses Valgrind's [60] Callgrind [61] tool to profile a source-reactor-sink scenario and establish which parts of the CYCMORE reactor code generate the most instructions. 52.27% of the 9,897,385,005 instructions come from the exchange manager in CYCLUS, and the reactor's Tock (which appends each time step) is the source of 13.26% of the instructions. The CYCMORE reactor's Tick (which pre-pends each time step) is the source of 4.66% of the instructions. For the TOD reactor, and the Tock was the source of 11.5% of the 9,519,845,814 instructions, while Tick was the source of 2.77% of the instructions.

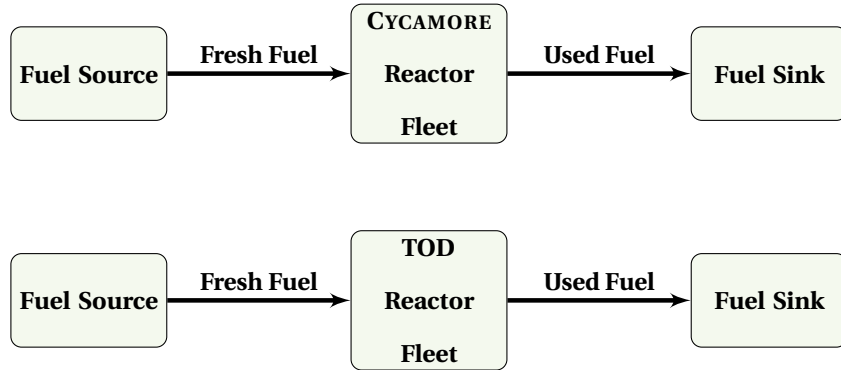


Figure 4.3: Simple A-B-C scenarios for the CYCMORE and TOD reactor archetypes.

In the scenarios from Figure 4.3, CYCLUS deploys 1000 reactors over the first ten time steps, and the reactors operate for three time steps before refueling for two. This scenario demonstrates an intensive deployment to exacerbate the differences between the two reactor archetypes. The mean, maximum, minimum, and standard deviation of the wall clock time, number of instructions, and instructions per cycle are in Table 4.1, measured across ten duplicate runs of the same source-reactor-sink scenario with statistics from the Linux tool Perf [62].

Table 4.1: TOD reactor and CYCAMORE reactor fleet simulation profiles showing the max, min, mean, and standard deviation of the wall time, number of instructions, and instructions per cycle.

Reactor	Metric	Mean	Max	Min	StDev
CYCAMORE Reactor	wall clock time [sec]	3.286	3.333	3.242	0.026
	Instructions	1.209×10^{10}	1.211×10^{10}	1.207×10^{10}	1.328×10^7
	Instructions per Cycle	0.800	0.808	0.791	0.005
TOD Reactor	wall clock time [sec]	3.166	3.195	3.142	0.016
	Instructions	1.174×10^{10}	1.176×10^{10}	1.167×10^{10}	2.692×10^7
	Instructions per Cycle	0.807	0.811	0.801	0.003

The results in Table 4.1 indicate an average speedup of 1.038 when using the TOD reactor compared with the CYCAMORE reactor. As Figure 4.4 indicates, these time results are significant outside their combined standard deviations.

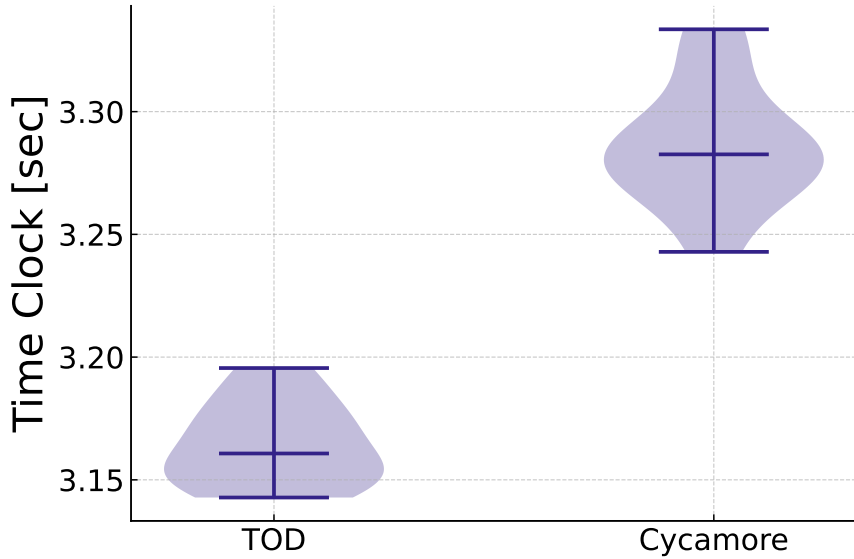


Figure 4.4: Wall clock time values for the TOD and CYCAMORE reactors.

The wall clock time values can vary by machine, architecture, and other demands during operation; however, the number of instructions issued using these archetypes, shown in Figure 4.5, is distinct between the TOD and CYCAMORE reactors and is specific to the code, not the machine. The distributions of instructions per cycle, presented alongside the instructions, overlap but indicate that the average TOD reactor simulation has a higher utilization than the CYCAMORE reactor.

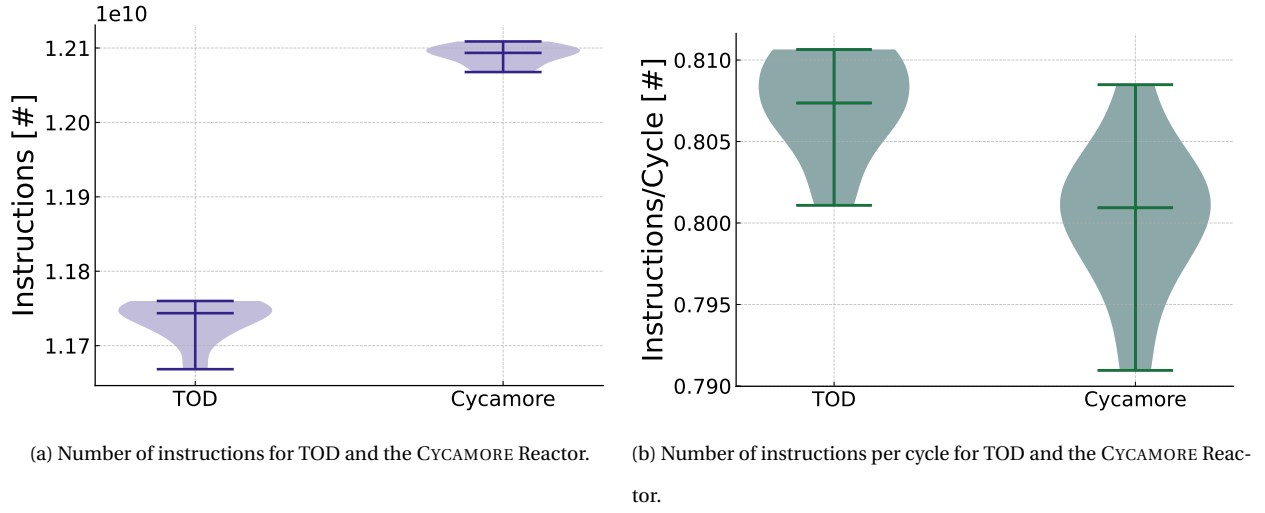


Figure 4.5: Comparing the number of instructions and instructions per cycle for the TOD and CYCAMORE reactors shows that TOD has a higher utilization.

These results are in line with our hypothesis, but are an initial step on improving the computational efficiency of simulations using a reactor in CYCLUS. The utilization is similar, and the number of instructions are similar; both of which could be improved by expanding this on-demand logic to the Exchange phase of each time step.

4.3 Dynamic Power Reactor

The U.S. Nuclear Regulatory Commission (NRC) publishes a daily Power Reactor Status report for each reactor under its jurisdiction [63]. These reports contain, amongst other things, the percentage of the total power at which the operators say the reactor operated. This reflects the reality that reactors do not operate at their total power capacity at all times, i.e., their capacity factor is not 1. Fuel cycle simulators can use the effective capacity factor to tell their model how much power to output over time, or they can use data over time to reflect real or imagined fluctuations. The CYCAMORE reactor assumes that the power is constant, and so, in the case of a fuel cycle simulation containing a small number of reactors or a full-fleet simulation over a short time, the power predicted by the CYCAMORE reactor and reality can diverge.

Section 3.1 describes one method of using energy demand to determine the number of reactors to deploy in the future, and such methods can be improved by incorporating realistic power fluctuations. If the reactors are producing more power in the simulation than they would in real life, the simulation will underestimate the number of reactors needed to meet the demand. Additionally, it will not be able to accurately reproduce historical data on the power availability from the fleet of reactors. Figure 4.6 shows real data from and a CYCAMORE representation of the single reactor operating at the Clinton Clean Energy Center (Clinton), with a reference unit power (i.e., net

power) of 1062 MWe according to the International Atomic Energy Agency (IAEA) Power Reactor Information System (PRIS) database [2], and compare it to the results from the CYCAMORE reactor modeled over the same time frame. This figure excludes the startup of the CYCAMORE reactor to ensure that it was operating on the same schedule as the data from the NRC suggest the reactor was operating on from the start of 2021 through the end of 2024.

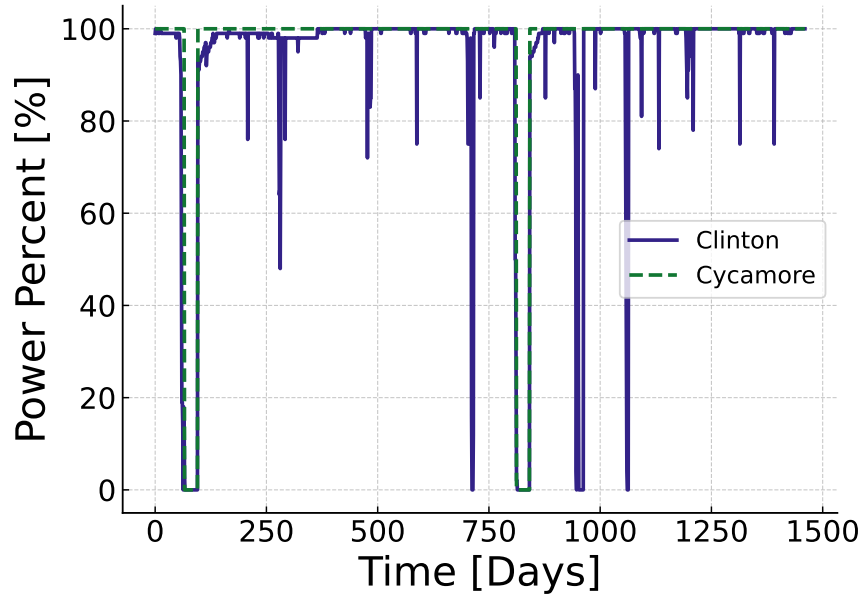


Figure 4.6: Clinton reactor daily capacity factor 2021-2024.

A simple numerical integration reveals that the total energy capacity of both reactors differs by just under 51 GWe with a percent difference of 3.52%; however, the two scenarios in Figure 4.6 were not equal on 908 days, or 62.2%, of the 1460-day simulation. This thesis introduces the Dynamic Power Reactor (DPR) to mirror this variability in power of an operating reactor to capture these temporal fluctuations. DPR functions the same way as the CYCAMORE reactor, except the user can input the percentage of the total capacity the reactor is outputting at any given time step.

Narrowing the scope of this study to 2024, this thesis uses DPR to replicate the capacity factor fluctuations of Clinton. The maximum difference between the reported values from the NRC [63] and the results from the CYCLUS simulation is 2.22×10^{-16} GWe, which is explainable by floating point error in calculations as this value matches a double point machine epsilon value. Figure 4.7 compares DPR to the CYCAMORE reactor. As the reactors are assumed to start operations before 2024, a buffer month in which the reactors receive fuel allows these results to align with reality. The vertical line indicates when 2024 begins, allowing Figure 4.7 to compare the NRC data with results from CYCLUS. Although the CYCAMORE reactor was able to reproduce the Clinton reactor's power output around refueling outages, the DPR is able to reproduce all of the fluctuations in power output even in years that did

not have a refueling outage.

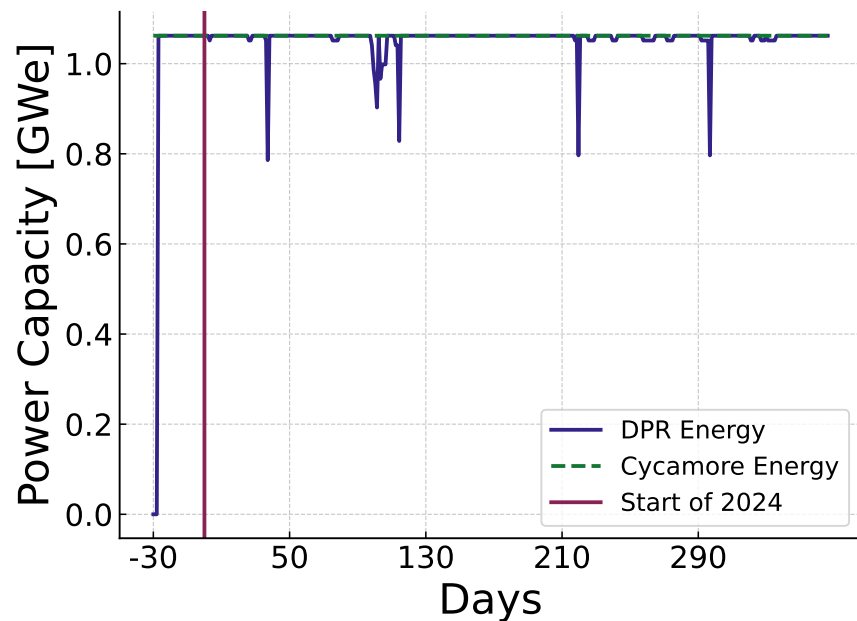


Figure 4.7: 2024 capacity factor of the CYCAMORE reactor and DPR.

Chapter 5

Conclusions

5.1 Transition Scenarios Conclusions and Limitations

This thesis characterizes bounding scenarios of reactor deployment as the United States (U.S.) transitions to a new fleet of nuclear reactors using an interstitial fuel cycle involving low-enriched uranium plus (LEU+) TRi-structural ISOtropic (TRISO) fuel. The results of this thesis show that the reactor deployment scheme has an understandable and identifiable impact on the separative work units (SWU) required to meet the energy demand.

The transition scenarios from this thesis develops a series of fuel cycles that include and contextualize the deployment of new nuclear reactors in the U.S. using TRISO fuels at high-assay low-enriched uranium (HALEU) and LEU+ enrichment levels. These fuel cycles meet the energy demand growths predicted by the U.S. Energy Information Administration (EIA) and the U.S. Department of Energy (DOE). The increase in demand assumes that nuclear energy's generation share remains constant over time. A 15% increase in demand means a 15% increase in nuclear energy capacity (as the EIA numbers [58] reflect the total energy demand, this conversion is only possible by assuming that the percentage share of nuclear capacity is the same). This assumption is not reflected in the demand scenarios from the DOE liftoff report [4], which are specific to nuclear deployment increases, and the number is agnostic to the total increase. The liftoff report scenarios are assumed to continue beyond the initial 2050 projection.

In this thesis, the Light Water Reactor (LWR) fleet deviates from reality by assuming that they all have regular 18-month cycles with regular 1-month outages. Related to this consistent cycle length, CYCLUS also assumes that the reactors have constant power outputs (when not in an outage) over their lifetime. Each LWR has an assembly size of 427.38589211618256 kg and a batch size of 80 assemblies, further normalizing the fleet. After 2024, no new LWRs will be built other than the AP1000s deployed under the various schemes.

The supply chain is not a limiting factor for new reactors, which allows these simulations to characterize the upper bound of what needs to be in place to achieve the projected deployment scenarios. Additionally, the fabrication and enrichment facilities for fuel are a black box, not factoring in variations in time, resources, or regulations associated with the fuels included.

The Micro Modular Reactor (MMR) and X-Energy Xe-100 (Xe-100) Serpent simulations are based on limited, publicly available information and do not rely on confidential or proprietary data, another limitation is they assume that when the reactors accept LEU+ fuel and operate with the same power levels and burnup rates. In Section 2.6 it was discussed that the intended use of many advanced reactors extends beyond simply meeting energy demand, so modeling them entirely in on-the-grid applications is not necessarily the only way they will deploy. These reactors could provide a range of services that can contribute to decarbonizing the economy.

Table 5.1 shows the average yearly percentage SWU increases from the *no growth* scenario to the *double by 2050* scenario, and the impacts of the deployment scheme are reflected in these values. Where the greedy scheme regularly prefers the highest capacity reactors, leading to the most significant increase in the SWU for AP1000 low-enriched uranium (LEU), the randomness in the other two schemes levels the reactor preferences and leads to more consistent increases across fuel types.

Table 5.1: Average yearly percentage SWU increases from the no growth scenario to the double by 2050 scenario.

Scheme	MMR HALEU	Xe-100 HALEU	AP1000 LEU
Greedy Deployment	105%	167%	800%
Random Deployment	1511%	796%	697%
Initially Random Greedy	775%	672%	696%

5.1.1 Future Work

This thesis could be expanded in various ways to contextualize the deployment of advanced reactors in the U.S.. Outside of simply removing the assumptions outlined above, two immediate additions to this thesis would be to incorporate isotope calculations for used fuel characterization and accumulation of isotopes of interest. This would allow for a more detailed understanding of the waste stream, the potential for recycling, and give insight into the security implications of the proposed systems. The second addition would be to compare the *no growth* and *double by 2050* nuclear scenarios to the triple nuclear scenario from the DOE liftoff report [4].

The next steps in expanding this thesis would be to translate the base metrics presented here (SWU, mass, energy, and deployment) into costs for fuel and energy to explore the impact of investment and supply chain dynamics on the ability of companies to invest in these technologies. The mass of used fuel would be a good starting point for repository space considerations and transportation costs. This thesis could leverage CYCLUS's ability to track latitude and longitude to understand the transportation time between facilities.

Section 2.4 on LEU+ highlights how the category of an enrichment facility is a critical component in the cost and logistics of a fuel cycle. SWU is a good starting point for understanding the relative effort required to deploy the

reactors, but the cost of that effort is a critical component of the deployment for making policy recommendations. SWU and masses of fuel can start to understand how international cooperation with nations that have existing enrichment facilities could help the U.S. meet its energy goals.

5.2 Reactor Power and Market Interaction Conclusions and Limitations

As Section 4.2 identifies, the CYCAMORE reactor enters the Tick and Tock phases of each time step whether or not it is time to refuel. This Section uncovered that for the Trading On-Demand (TOD) reactor both the Tick and Tock phases were the source of less instructions than those from the CYCAMORE reactor. Overall, the analysis shows that the TOD reactor archetype represents an alteration in the logic of the widely used CYCAMORE reactor that increases the utilization, decreases the number of instructions, and maintains consistent performance with the CYCAMORE reactor.

This reactor was demonstrated using a 2024 test case examining the power output of the Clinton Clean Energy Center (Clinton). Section 4.3 identified that the CYCAMORE reactor's constant power capacity results in a 3.52% difference between the cumulative power capacity of Clinton and the CYCAMORE reactor modeling Clinton. The Dynamic Power Reactor (DPR) is able to replicate historic and realistic power outputs from a reactor with the only differences between DPR and Clinton arising from floating point error below the machine epsilon.

5.2.1 Future Work

In the future, the TOD effort can be expanded to find other ways to reduce the number of instructions germane to the simulation. Profiling revealed that the Exchange method for the Dynamic Resource Exchange (DRE) was routinely a larger source of instructions than the Tick and Tock methods. Outside of the reactor, incorporating tools to bypass unnecessary interactions in other fuel cycle facilities would be the next step to allowing users to develop complex purchasing agreements restricted by external factors other than material availability.

The DPR is currently a stand-alone implementation of historical variation, and future work could contribute a method to generate realistic predictions of power capacity over time for the LWR fleet. There is also a need to apply this method to creating bounding cases for the advanced reactor fleet in Section 2.6, although each reactor model will exhibit different behavior that would require additional work to characterize. This bounding work could show the variation in power output in cases where reactors over perform their expected capacity factor, reproduce their expected capacity factor, and under perform their expected capacity factor. With this feature, the number of reactors deployed to meet demand can mirror the anticipated planning utilities will engage with. Outside of power capacity variation, the current scheme approximates the output and usage of fuel as constant over time, and

implementing a similar variability in the masses and burnups of fuel, as Section 2.3.1 discusses, would strengthen the conclusions of future CYCLUS simulations.

References

- [1] U.S. Energy Information Administration, "Statement on the Annual Energy Outlook and EIA plan to enhance long-term modeling capabilities," Jul. 2023. [Online]. Available: <https://www.eia.gov/pressroom/releases/press537.php>
- [2] I. A. E. Agency, "Power reactor information system (pris) database," 2024, accessed: 2024-09-30. [Online]. Available: <https://pris.iaea.org/>
- [3] US Energy Information Administration, "U.S. EIA: What is U.S. electricity generation by energy source?" Feb. 2024. [Online]. Available: <https://www.eia.gov/tools/faqs/faq.php>
- [4] Julie Kozeracki, Chris Vlahoplus, Ken Erwin, Alan Propp, Sonali Razdan, Rasheed Auguste, Tim Stuhldreher, Christina Walrond, Melissa Bates, Erica Bickford, Andrew Foss, Derek Gaston, Cheryl Herman, Rory Stanley, Billy Valderrama, Katheryn Scott, Tomotaroh Granzier-Nakajima, Paul Donohoo-Vallett, Tom Fanning, Brent Dixon, Abdalla Abou Jaoude, and Chris Lohse, "Pathways to Commercial Liftoff: Advanced Nuclear," *DOE Liftoff Report*, Sep. 2024. [Online]. Available: https://liftoff.energy.gov/wp-content/uploads/2024/09/LIFTOFF_DOE_AdvNuclear-vX6.pdf
- [5] EIA Electricity Supply & Uranium Statistics & Product Innovation Team, "2023 Domestic Uranium Production Report," US Energy Information Administration, Tech. Rep., May 2024. [Online]. Available: <https://www.eia.gov/uranium/production/annual/pdf/dupr2023.pdf>
- [6] K. D. Huff, M. J. Gidden, R. W. Carlsen, R. R. Flanagan, M. B. McGarry, A. C. Opotowsky, E. A. Schneider, A. M. Scopatz, and P. P. H. Wilson, "Fundamental concepts in the Cyclus nuclear fuel cycle simulation framework," *Advances in Engineering Software*, vol. 94, pp. 46–59, Apr. 2016. [Online]. Available: <http://www.sciencedirect.com/science/article/pii/S0965997816300229>
- [7] A. M. Bachmann, R. Fairhurst-Agosta, Z. Richter, N. Ryan, and M. Munk, "Enrichment dynamics for advanced reactor HALEU support," *EPJ Nuclear Sciences & Technologies*, vol. 7, p. 22, 2021. [Online]. Available: <https://www.epj-n.org/articles/epjn/abs/2021/01/epjn210024/epjn210024.html>
- [8] European Commission. Joint Research Centre., *GHG emissions of all world: 2021 report*. LU: Publications Office, 2021. [Online]. Available: <https://data.europa.eu/doi/10.2760/173513>
- [9] E. Papadis and G. Tsatsaronis, "Challenges in the decarbonization of the energy sector," *Energy*, vol. 205, p. 118025, Aug. 2020. [Online]. Available: <https://www.sciencedirect.com/science/article/pii/S0360544220311324>
- [10] D. S. Mallapragada, Y. Dvorkin, M. A. Modestino, D. V. Esposito, W. A. Smith, B.-M. Hodge, M. P. Harold, V. M. Donnelly, A. Nuz, C. Bloomquist, K. Baker, L. C. Grabow, Y. Yan, N. N. Rajput, R. L. Hartman, E. J. Biddinger, E. S. Aydil, and A. D. Taylor, "Decarbonization of the chemical industry through electrification: Barriers and opportunities," *Joule*, vol. 7, no. 1, pp. 23–41, Jan. 2023. [Online]. Available: <https://linkinghub.elsevier.com/retrieve/pii/S2542435122006055>
- [11] A. Farokhi Soofi, S. D. Manshadi, and A. Saucedo, "Farm electrification: A road-map to decarbonize the agriculture sector," *The Electricity Journal*, vol. 35, no. 2, p. 107076, Mar. 2022. [Online]. Available: <https://www.sciencedirect.com/science/article/pii/S1040619022000021>

- [12] D. Helm, "Energy policy: security of supply, sustainability and competition," *Energy Policy*, vol. 30, no. 3, pp. 173–184, Feb. 2002. [Online]. Available: <https://www.sciencedirect.com/science/article/pii/S0301421501001410>
- [13] G. B. Treasury, *Nationalised Industries: A Review of Economic and Financial Objectives*, ser. C (Series) (Great Britain. Parliament). H.M. Stationery Office, 1967. [Online]. Available: <https://books.google.com/books?id=XbInAQAAQAAJ>
- [14] M. V. Posner, "Fuel policy. A study in applied economics," *ETDEWEB World Energy Base*, Jan. 1973. [Online]. Available: <https://www.osti.gov/etdeweb/biblio/5240048>
- [15] F. A. Plazas-Niño, N. R. Ortiz-Pimiento, and E. G. Montes-Páez, "National energy system optimization modelling for decarbonization pathways analysis: A systematic literature review," *Renewable and Sustainable Energy Reviews*, vol. 162, p. 112406, Jul. 2022. [Online]. Available: <https://www.sciencedirect.com/science/article/pii/S1364032122003148>
- [16] S. Pfenninger, A. Hawkes, and J. Keirstead, "Energy systems modeling for twenty-first century energy challenges," *Renewable and Sustainable Energy Reviews*, vol. 33, pp. 74–86, May 2014. [Online]. Available: <https://www.sciencedirect.com/science/article/pii/S1364032114000872>
- [17] P. Laha and B. Chakraborty, "Energy model – A tool for preventing energy dysfunction," *Renewable and Sustainable Energy Reviews*, vol. 73, pp. 95–114, Jun. 2017. [Online]. Available: <https://www.sciencedirect.com/science/article/pii/S1364032117301193>
- [18] T. Hiraishi, B. Nyenzi, M. Gillet, J. Meijer, T. Pullus, T. Simmons, M. Tichy, A. C. Adi, M. Chandra, S. Emmanuel, J.-P. Fontelle, P. Fott, S. Lamotta, E. Lieberman, K. Mareckova, S. Amous, A. Olsson, I. Hossain, D. Gomez, M. Miroslav, M. Oi, U. Rajarathnam, S. Tuhkanen, J. Zhang, M. Walsh, S. Mowafy, and S. Eggleston, "Good Practice Guidance and Uncertainty Management in National Greenhouse Gas Inventories," Task Force on National Greenhouse Gas Inventorie, Intergovernmental Panel on Climate Change, Tech. Rep., May 2000. [Online]. Available: https://www.ipcc-nccc.iges.or.jp/public/gp/english/2_Energy.pdf
- [19] President Dwight. D. Eisenhower, "Atoms for Peace Speech," Jul. 1953, publisher: IAEA. [Online]. Available: <https://www.iaea.org/about/history/atoms-for-peace-speech>
- [20] IAEA, "List of Member States," Jun. 2016, publisher: IAEA. [Online]. Available: <https://www.iaea.org/about/governance/list-of-member-states>
- [21] P. Honnold, L. Crabtree, M. Higgins, A. Williams, R. Finch, B. Cipiti, D. Ammerman, C. Farnum, E. Kalinina, M. Ruehl, and K. Hawthorne, "PRO-X Fuel Cycle Transportation and Crosscutting Progress Report," Sandia National Laboratories, Tech. Rep. SAND2022-13387R, 1890069, 710373, Sep. 2022. [Online]. Available: <https://www.osti.gov/servlets/purl/1890069/>
- [22] NEA (2023), "Uranium 2022: Resources, Production and Demand," OECD Publishing, Paris, Biannual 29, 2023. [Online]. Available: https://www.oecd-nea.org/jcms/pl_79960/uranium-2022-resources-production-and-demand?details=true
- [23] U.S. Energy Information Administration, "Monthly Energy Review September 2024," U.S. Energy Information Administration, Tech. Rep. DOE/EIA-0035(2024/9), Sep. 2024. [Online]. Available: <https://www.eia.gov/totalenergy/Data/monthly/pdf/mer.pdf>
- [24] G. Li and J. Yao, "A Review of In Situ Leaching (ISL) for Uranium Mining," *Mining*, vol. 4, no. 1, pp. 120–148, Mar. 2024, number: 1 Publisher: Multidisciplinary Digital Publishing Institute. [Online]. Available: <https://www.mdpi.com/2673-6489/4/1/9>
- [25] B. M. T. Costa Peluzo and E. Kraka, "Uranium: The Nuclear Fuel Cycle and Beyond," *International Journal of Molecular Sciences*, vol. 23, no. 9, p. 4655, Jan. 2022, number: 9 Publisher: Multidisciplinary Digital Publishing Institute. [Online]. Available: <https://www.mdpi.com/1422-0067/23/9/4655>

- [26] I. Gurban and M. Laaksoharju, "Hydrochemical stability of groundwaters surrounding a spent nuclear fuel repository in a 100,000 year perspective," POSIVA OY, Finland, Tech. Rep. 951-652-107-X, 2001, pOSIVA-01-06 INIS Reference Number: 33020732. [Online]. Available: https://inis.iaea.org/collection/NCLCollectionStore/_Public/33/020/33020732.pdf?r=1
- [27] B. Hyland, G. Edwards, C. Kitson, and T. Chshyolkova, "Post-closure performance assessment of a deep geological repository for advanced heavy water reactor fuels," Canadian Nuclear Laboratories, Canada, Tech. Rep., 2013, aECL-CW-10192-CONF-001 INIS Reference Number: 49101296.
- [28] R. W. Carlsen, M. Gidden, K. Huff, A. C. Opotowsky, O. Rakhimov, A. M. Scopatz, and P. Wilson, "Cycamore v1.0.0," Figshare, June 2014. [Online]. Available: https://figshare.com/articles/software/Cycamore_v1_0_0/1041829
- [29] A. Yacout, J. Jacobson, G. Matthern, S. Piet, D. Shropshire, and C. Laws, "VISION—Verifiable Fuel Cycle Simulation of Nuclear Fuel Cycle Dynamics," *Waste Management*, 2006.
- [30] E. Schneider and A. Scopatz, "An Integrated Fuel Depletion Calculator for Fuel Cycle Options Analysis," battelle Energy Alliance, LLC, Tech. Rep. 12-4065, 1258475, Apr. 2016. [Online]. Available: <http://www.osti.gov/servlets/purl/1258475/>
- [31] S. E. Skutnik, N. C. Sly, and J. L. Littell, "CyBORG: An ORIGEN-Based Reactor Analysis Capability for Cyclus," in *Transactions of the American Nuclear Society*, ser. Fuel Cycle and Waste Management: General—II, vol. 115. Las Vegas, Nevada, United States: American Nuclear Society, Nov. 2016, pp. 299–301.
- [32] J. W. Bae, A. Rykhlevskii, G. Chee, and K. D. Huff, "Deep learning approach to nuclear fuel transmutation in a fuel cycle simulator," *Annals of Nuclear Energy*, vol. 139, May 2020. [Online]. Available: <https://www.sciencedirect.com/science/article/pii/S0306454919307406>
- [33] B. Feng, B. Dixon, E. Sunny, A. Cuadra, J. Jacobson, N. R. Brown, J. Powers, A. Worrall, S. Passerini, and R. Gregg, "Standardized verification of fuel cycle modeling," *Annals of Nuclear Energy*, vol. 94, pp. 300–312, Aug. 2016. [Online]. Available: <http://www.sciencedirect.com/science/article/pii/S0306454916301098>
- [34] S. Richards and B. Feng, "Application of sensitivity analysis in DYMOND/Dakota to fuel cycle transition scenarios," *EPJ Nuclear Sciences & Technologies*, vol. 7, p. 26, 2021, published: = <https://www.epj-n.org/articles/epjn/abs/2021/01/epjn210022/epjn210022.html>.
- [35] E. A. Schneider, C. G. Bathke, and M. R. James, "NFCSSim: A Dynamic Fuel Burnup and Fuel Cycle Simulation Tool," *Nuclear Technology*, vol. 151, no. 1, pp. 35–50, Jul. 2005.
- [36] O. Y. Amanda M. Bachmann and M. Munk, "An open-source coupling for depletion during fuel cycle modeling," *Nuclear Science and Engineering*, vol. 199, no. 5, pp. 1–14, 2024. [Online]. Available: <https://doi.org/10.1080/00295639.2024.2393940>
- [37] P. K. Romano, N. E. Horelik, B. R. Herman, A. G. Nelson, B. Forget, and K. Smith, "OpenMC: A state-of-the-art Monte Carlo code for research and development," *Annals of Nuclear Energy*, vol. 82, pp. 90–97, Aug. 2015. [Online]. Available: <https://www.sciencedirect.com/science/article/pii/S030645491400379X>
- [38] M. C. Regalbuto, "High-Assay Low Enriched Uranium Demand and Deployment Options 2020 HALEU Workshop Report," Idaho National Laboratory, Idaho National Laboratory, Tech. Rep. INL/EXT-21-61768, Jun. 2020. [Online]. Available: https://www.leidoseemg.com/haleuEIS.references/docs/Regalbuto%202020_HALEU%20Demand%20Deployment%20Options%202020%20Workshop.pdf
- [39] Nuclear Regulatory Commission, "10 CFR § 70.4 Definitions." Aug. 2017. [Online]. Available: <https://www.nrc.gov/reading-rm/doc-collections/cfr/part070/part070-0004.html>
- [40] J. López-Luna, J.-L. Francois, A. Castillo, and J. J. Ortiz-Servin, "Design of a 24-month equilibrium cycle of a bwr with extended low enrichment fuel using metaheuristic optimization techniques," *Annals of Nuclear Energy*, vol. 213, p. 111129, 2025. [Online]. Available: <https://www.sciencedirect.com/science/article/pii/S0306454924007928>

- [41] Framatome, "Press Release: Framatome's enhanced accident tolerant fuel assemblies first to complete lifecycle operations in U.S." 2024. [Online]. Available: <https://www.framatome.com/medias/worldwide-first-framatomes-enhanced-accident-tolerant-fuel-assemblies-first-to-complete-lifecycle-operations-in-us/>
- [42] A. M. Shaw and J. B. Clarity, "Impacts of leu+ and atf on fresh fuel storage criticality safety," Oak Ridge National Laboratory (ORNL), Oak Ridge, TN (United States), Tech. Rep., 02 2022. [Online]. Available: <https://www.osti.gov/biblio/1843694>
- [43] M. S. T. Price, "The Dragon Project origins, achievements and legacies," *Nuclear Engineering and Design*, vol. 251, pp. 60–68, Oct. 2012. [Online]. Available: <https://www.sciencedirect.com/science/article/pii/S0029549311010570>
- [44] F. B. Daniels, "Suggestions for a High-Temperature Pebble Pile," The University of Chicago Metallurgical Laboratory, Chicago, IL, Tech. Rep., Oct. 1944. [Online]. Available: <https://www.osti.gov/servlets/purl/4359817>
- [45] P. A. Demkowicz, B. Liu, and J. D. Hunn, "Coated particle fuel: Historical perspectives and current progress," *Journal of Nuclear Materials*, vol. 515, pp. 434–450, Mar. 2019. [Online]. Available: <https://www.sciencedirect.com/science/article/pii/S0022311518310213>
- [46] Bachmann, "MMR-like Serpent Model," Sep. 2023. [Online]. Available: <https://zenodo.org/records/8349385>
- [47] Z. Richter, "Isotopic fuel compositions in the sangamon200 model," Apr. 2022. [Online]. Available: <https://doi.org/10.5281/zenodo.6426312>
- [48] Ultra Safe Nuclear Corporation, "USNC Micro Modular Reactor (MMR™ Block 1) Technical Information," USNC, p. 36, 2021. [Online]. Available: [https://www.usnc.com/assets/media-kit/\[022989\]\[01\]%20MMR%20Technical%20Information%20Document.pdf?v=a7e3f7d8d5](https://www.usnc.com/assets/media-kit/[022989][01]%20MMR%20Technical%20Information%20Document.pdf?v=a7e3f7d8d5)
- [49] NuScale, "Chapter One Introduction and General Description of the Plant," Oct. 2018. [Online]. Available: <https://www.nrc.gov/reactors/new-reactors/design-cert/nuscale.html>
- [50] Susan A. Martinis, "Notice of Intent to Submit an Application for a Construction Permit for a Research & Test Reactor: ML21153A059," May 2021. [Online]. Available: <https://adamswebsearch2.nrc.gov/webSearch2/main.jsp?AccessionNumber=ML21153A059>
- [51] GFP Limited, "Project Description for the Micro Modular Reactor™ Project at Chalk River," Global First Power, Chalk River, Tech. Rep. CRP-LIC-01-001, Jul. 2019. [Online]. Available: <https://www.usnc.com/assets/media-kit/01%20CRP-LIC-01-001%20Rev%202%20Project%20Description.pdf?v=33d7ad7f2f>
- [52] Ultra Safe Nuclear Corporation, "USNC: Press & News, Media Kit," Oct. 2024. [Online]. Available: <https://www.usnc.com/tag/news/>
- [53] A. M. Bachmann, "Investigation of the impacts of deploying reactors fueled by high-assay low enriched uranium," Thesis, University of Illinois at Urbana-Champaign, Nov. 2023. [Online]. Available: <https://hdl.handle.net/2142/121987>
- [54] X-energy, "X-Energy Media Kit (Xe-100)," 2024. [Online]. Available: <https://x-energy.com/media/xe-100>
- [55] X-Energy, "X-Energy Media Kit (Triso-X)," 2024. [Online]. Available: <https://x-energy.com/media/triso-x>
- [56] Z. Richter, "ISOTOPIC AND REACTOR PHYSICS CHARACTERIZATION OF A GAS-COOLED, PEBBLE-BED MICROMEASURERACTOR," *UIUC Ideals*, 2022. [Online]. Available: <https://etd.ideals.illinois.edu/advisor/UJZchd2AwM/file/89111/RICHTER-THESIS-2022.pdf>
- [57] A. Bachmann, J. W. Bae, G. Chee, N. Ryan, R. Fairhurst, K. Huff, T. Kennelly, Olek, P. . Speaks, S. Dotson, K. Kleimenhagen, LukeSeifert, RhysMacMillan, FlanFlanagan, A. Scopatz, G. Westphal, P. Wilson, and S. M. Park, "arfc/transition-scenarios: Nathan's thesis," Apr. 2025. [Online]. Available: <https://doi.org/10.5281/zenodo.15213458>

- [58] U.S. Energy Information Administration, “Annual Energy Outlook 2023,” U.S. Energy Information Administration, Government, Mar. 2023. [Online]. Available: https://www.eia.gov/outlooks/aoe/pdf/AEO2023_Narrative.pdf
- [59] N. Ryan, “arfc/near: Release for zenodo,” Apr. 2025. [Online]. Available: <https://doi.org/10.5281/zenodo.15213139>
- [60] N. Nethercote and J. Seward, “Valgrind: a framework for heavyweight dynamic binary instrumentation,” in *Proceedings of the 28th ACM SIGPLAN Conference on Programming Language Design and Implementation*, ser. PLDI ’07. New York, NY, USA: Association for Computing Machinery, Jun. 2007, pp. 89–100. [Online]. Available: <https://dl.acm.org/doi/10.1145/1250734.1250746>
- [61] N. Nethercote, R. Walsh, and J. Fitzhardinge, “Building workload characterization tools with valgrind,” in *Proceedings of the 2006 IEEE International Symposium on Workload Characterization, IISWC 2006, October 25-27, 2006, San Jose, California, USA*. IEEE Computer Society, 2006, p. 2. [Online]. Available: <https://doi.org/10.1109/IISWC.2006.302723>
- [62] Linux Foundation, “perf,” <https://perf.wiki.kernel.org/>, 2025, version 6.8.12.
- [63] Nuclear Regulatory Commission, “Power Reactor Status Reports,” Jan. 2025. [Online]. Available: <https://www.nrc.gov/reading-rm/doc-collections/event-status/reactor-status/index.html>

Appendix A

LWRs Simulated

This thesis pulls publicly available information from the Power Reactor Information System (PRIS) database [2] to simulate the Light Water Reactor (LWR) fleet in the United States (U.S.). The PRIS database is a collection of information on nuclear power plants around the world, and is maintained by the International Atomic Energy Agency (IAEA). For the sake of completeness and replication of this thesis, Tables A.1, A.2, and A.3 include the LWR fleet simulated in this thesis and a notebook is available on GitHub [57] to pull the same information used herein.

Table A.1: LWR fleet simulated, A-Da.

Name	State	Type	Vendor	Core size	Startup date	License	Shut Down	Power cap
ANO 1	AR	PWR	B&W	177	1974	2034		836
ANO 2	AR	PWR	CE	177	1978	2038		988
Beaver Valley 1	PA	PWR	WE	157	1976	2036		908
Beaver Valley 2	PA	PWR	WE	157	1987	2047		905
Big Rock Point	MI	BWR	GE	84	1964		1997	67
Braidwood 1	IL	PWR	WE	193	1987	2046		1194
Braidwood 2	IL	PWR	WE	193	1988	2047		1160
Browns Ferry 1	AL	BWR	GE	764	1973	2033		1200
Browns Ferry 2	AL	BWR	GE	764	1974	2034		1200
Browns Ferry 3	AL	BWR	GE	764	1976	2036		1210
Brunswick 1	NC	BWR	GE	560	1976	2036		938
Brunswick 2	NC	BWR	GE	560	1974	2034		932
Byron 1	IL	PWR	WE	193	1985	2044		1164
Byron 2	IL	PWR	WE	193	1987	2046		1136
Callaway	MO	PWR	WE	193	1984	2044		1215
Calvert Cliffs 1	MD	PWR	CE	217	1974	2034		877
Calvert Cliffs 2	MD	PWR	CE	217	1976	2036		855
Catawba 1	SC	PWR	WE	193	1985	2043		1160
Catawba 2	SC	PWR	WE	193	1986	2043		1150
Clinton 1	IL	BWR	GE	624	1987	2026		1062
Columbia	WA	BWR	GE	764	1984	2043		1131
Comanche Peak 1	TX	PWR	WE	193	1990	2030		1205
Comanche Peak 2	TX	PWR	WE	193	1993	2033		1195
Cook 1	MI	PWR	WE	193	1974	2034		1030
Cook 2	MI	PWR	WE	193	1977	2037		1168
Cooper Station	NE	BWR	GE	548	1974	2034		769
Crystal River 3	FL	PWR	B&W	177	1976		2013	860
Davis-Besse	OH	PWR	B&W	177	1977	2037		894

Table A.2: LWR fleet simulated, Di-L.

Name	State	Type	Vendor	Core size	Startup date	License	Shut Down	Power cap
Diablo Canyon 1	CA	PWR	WE	193	1984	2024		1138
Diablo Canyon 2	CA	PWR	WE	193	1985	2025		1118
Dresden 1	IL	BWR	GE	464	1959	2029	1978	197
Dresden 2	IL	BWR	GE	724	1969	2029		894
Dresden 3	IL	BWR	GE	724	1971	2031		879
Duane Arnold	IA	BWR	GE	368	1974	2034	2020	601
Enrico Fermi 2	MI	BWR	GE	764	1985	2045		1115
Farley 1	AL	PWR	WE	157	1977	2037		874
Farley 2	AL	PWR	WE	157	1981	2041		883
Fitzpatrick	NY	BWR	GE	560	1974	2034		813
Fort Calhoun	NE	PWR	CE	133	1973		2016	482
Ginna	NY	PWR	WE	121	1969	2029		560
Grand Gulf 1	MS	BWR	GE	800	1984	2044		1401
Haddam Neck	CT	PWR	WE	157	1967		1996	560
Harris 1	NC	PWR	WE	157	1986	2046		964
Hatch 1	GA	BWR	GE	560	1974	2034		876
Hatch 2	GA	BWR	GE	560	1978	2038		883
Hope Creek	NJ	BWR	GE	764	1986	2046		1172
Humboldt Bay	CA	BWR	GE	184	1962		1976	63
Indian Point 1	NY	PWR	B&W	120	1962	2013	1974	257
Indian Point 2	NY	PWR	WE	193	1973	2024	2020	998
Indian Point 3	NY	PWR	WE	193	1975	2025		1030
Kewaunee	WI	PWR	WE	121	1973	2033	2013	566
La Crosse	WI	BWR	AC	72	1967		1987	48
LaSalle County 1	IL	BWR	GE	764	1982	2042		1137
LaSalle County 2	IL	BWR	GE	764	1983	2043		1140
Limerick 1	PA	BWR	GE	764	1985	2044		1134
Limerick 2	PA	BWR	GE	764	1989	2049		1134

Table A.3: LWR fleet simulated, Su-Q.

Name	State	Type	Vendor	Core size	Startup date	License	Shut Down	Power cap
Maine Yankee	ME	PWR	CE	217	1973		1996	860
McGuire 1	NC	PWR	WE	193	1981	2041		1158
McGuire 2	NC	PWR	WE	193	1983	2043		1158
Millstone 1	CT	BWR	GE	580	1970		1998	641
Millstone 2	CT	PWR	CE	217	1975	2035		869
Millstone 3	CT	PWR	WE	193	1986	2045		1210
Monticello	MN	BWR	GE	484	1970	2030		628
Nine Mile Point 1	NY	BWR	GE	532	1969	2029		613
Nine Mile Point 2	NY	BWR	GE	764	1987	2046		1277
North Anna 1	VA	PWR	WE	157	1978	2038		948
North Anna 2	VA	PWR	WE	157	1980	2040		944
Oconee 1	SC	PWR	B&W	177	1973	2033		847
Oconee 2	SC	PWR	B&W	177	1973	2033		848
Oconee 3	SC	PWR	B&W	177	1974	2034		859
Oyster Creek	NJ	BWR	GE	560	1969	2029	2018	619
Palisades	MI	PWR	CE	204	1971	2031		805
Palo Verde 1	AZ	PWR	CE	241	1985	2045		1311
Palo Verde 2	AZ	PWR	CE	241	1986	2046		1314
Palo Verde 3	AZ	PWR	CE	241	1987	2047		1312
Peach Bottom 2	PA	BWR	GE	764	1973	2053		1300
Peach Bottom 3	PA	BWR	GE	764	1974	2054		1331
Perry 1	OH	BWR	GE	748	1986	2026		1240
Pilgrim 1	MA	BWR	GE	580	1972	2032	2019	677
Point Beach 1	WI	PWR	WE	121	1970	2030		591
Point Beach 2	WI	PWR	WE	121	1971	2033		591
Prairie Island 1	MN	PWR	WE	121	1973	2033		522
Prairie Island 2	MN	PWR	WE	121	1974	2034		519
Quad Cities 1	IL	BWR	GE	724	1972	2032		908
Quad Cities 2	IL	BWR	GE	724	1972	2032		911

Table A.4: LWR fleet simulated, R-V.

Name	State	Type	Vendor	Core size	Startup date	License	Shut Down	Power cap
Rancho Seco	CA	PWR	B&W	177	1974		1989	873
River Bend 1	LA	BWR	GE	624	1985	2045		967
Robinson 2	SC	PWR	WE	157	1970	2030		741
Salem 1	NJ	PWR	WE	193	1976	2036		1169
Salem 2	NJ	PWR	WE	193	1981	2040		1158
San Onofre 1	CA	PWR	WE	157	1967		1992	436
San Onofre 2	CA	PWR	CE	217	1982		2013	1070
San Onofre 3	CA	PWR	CE	217	1982		2013	1080
Seabrook	NH	PWR	WE	193	1990	2050		1246
Sequoyah 1	TN	PWR	WE	193	1980	2040		1152
Sequoyah 2	TN	PWR	WE	193	1981	2041		1139
South Texas 1	TX	PWR	WE	193	1988	2047		1280
South Texas 2	TX	PWR	WE	193	1989	2048		1280
St. Lucie 1	FL	PWR	CE	217	1976	2036		981
St. Lucie 2	FL	PWR	CE	217	1983	2043		987
Summer 1	SC	PWR	WE	157	1982	2042		973
Surry 1	VA	PWR	WE	157	1972	2032		838
Surry 2	VA	PWR	WE	157	1973	2033		838
Susquehanna 1	PA	BWR	GE	764	1982	2042		1257
Susquehanna 2	PA	BWR	GE	764	1984	2044		1257
TMI 1	PA	PWR	B&W	177	1974	2034	2019	819
TMI 2	PA	PWR	B&W	177	1978	2038	1979	880
Trojan	OR	PWR	WE	193	1975		1992	1095
Turkey Point 3	FL	PWR	WE	157	1972	2052		837
Turkey Point 4	FL	PWR	WE	157	1973	2053		821
Vermont Yankee	VT	BWR	GE	368	1972	2032	2014	605
Vogtle 1	GA	PWR	WE	193	1987	2047		1150
Vogtle 2	GA	PWR	WE	193	1989	2049		1117
Vogtle 3	GA	PWR	WE	193	2023	2062		1117
Vogtle 4	GA	PWR	WE	193	2024	2063		1117

Table A.5: LWR fleet simulated, W-Z.

Name	State	Type	Vendor	Core size	Startup date	License	Shut Down	Power cap
Waterford 3	LA	PWR	CE	217	1985	2044		1168
Watts Bar 1	TN	PWR	WE	193	1996	2035		1157
Watts Bar 2	TN	PWR	WE	193	2016	2055		1164
Wolf Creek 1	KS	PWR	WE	193	1985	2045		1200
Yankee Rowe	MA	PWR	WE	76	1960		1991	167
Zion 1	IL	PWR	WE	193	1973		1997	1040
Zion 2	IL	PWR	WE	193	1973		1996	1040

Appendix B

Considered Deployment Schemes

In addition to the deployment schemes outlined in 3.3, 3.4, and 3.5, this chapter outlines others not included in the final analysis. I examined these schemes for their potential to capture the complexity of the deployment problem but were ultimately not included due to the egregious nature of approximation required to implement or the lack of a clear benefit over the other schemes for the questions explored in this work.

B.1 Capped Deployment

This scheme places a constant limit on the number of specific reactors deployed at any given time step. This is a simple way to model aggregate supply chain constraints that could limit vendors from deploying reactors freely. With the right constraints, this scheme would better succeed at roughly incorporating the limits of a workforce over a short to medium time scale. This thesis does not implement the capped deployment scheme as workforce constraints are outside the scope.

To use this deployment scheme, a user needs to understand the supply chain constraints that will limit the deployment of the reactors they are deploying. Figure B.1 illustrates the defining steps of the capped deployment scheme. The main loop in the logic is consistent with the greedy deployment scheme but adds a check to see if the current deployment exceeds the limit on that reactor. If it does, the reactor is removed from the list of reactors to be deployed in that time step.

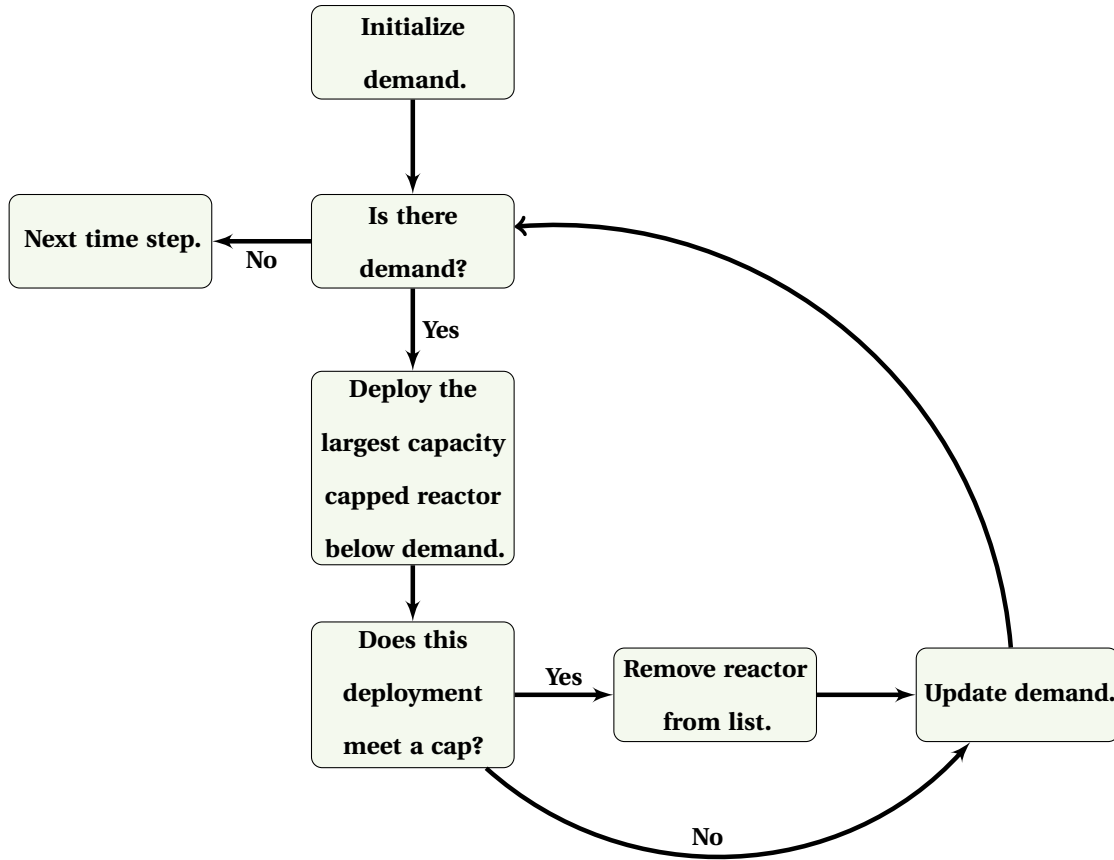


Figure B.1: Capped deployment diagram.

The realism of this deployment scheme mirrors some elements of the pre-determined distribution (this is a flat distribution after all), but the cap is a less granular way to account for supply chain constraints. This scheme is most useful for scenarios or timescales where there is a known limit on the workforce. The unrealistic element of this deployment scheme comes from two places: 1) the current implementation requires one reactor to be unrestrained (preferably the smallest reactor from the deployment standpoint); 2) the cap is a flat distribution, which is not a realistic representation of the supply chain constraints for most technologies.

When the unconstrained reactor is not the smallest power reactor, this scheme will fall below demand more so than when the unconstrained reactor is the smallest in power. This scheme has the potential to overperform by one reactor in the case where the unconstrained reactor is the smallest in power as it can over-deploy by one reactor's capacity in that case.

B.2 Pre-Determined Distribution Deployment

This deployment scheme allows users to incorporate the projections and commitments of ratepayers and utilities by setting a distribution over the simulation time. In this scheme, the distribution serves as a cap to the number of reactors deployed in a time step, and preferentially deploys reactors first to meet those caps. After completion, it deploys the remaining reactors without caps to meet the demand. In this way, it allows a user to incorporate knowledge of supply chain constraints for specific technologies without modeling the supply chain in detail.

To use this deployment scheme, a user needs some idea of the distribution of reactors deployed over the simulation time. Figure B.2 illustrates the defining steps of the pre-determined distribution deployment scheme. The main loop in the logic is consistent with the greedy deployment scheme but adds a check to see if the current deployment exceeds the limit on that reactor. If it does, the scheme removes the reactor from the list of deployable reactors in that time step. This scheme varies from the capped deployment scheme in that the distribution is not flat, but a more granular distribution that varies by year.

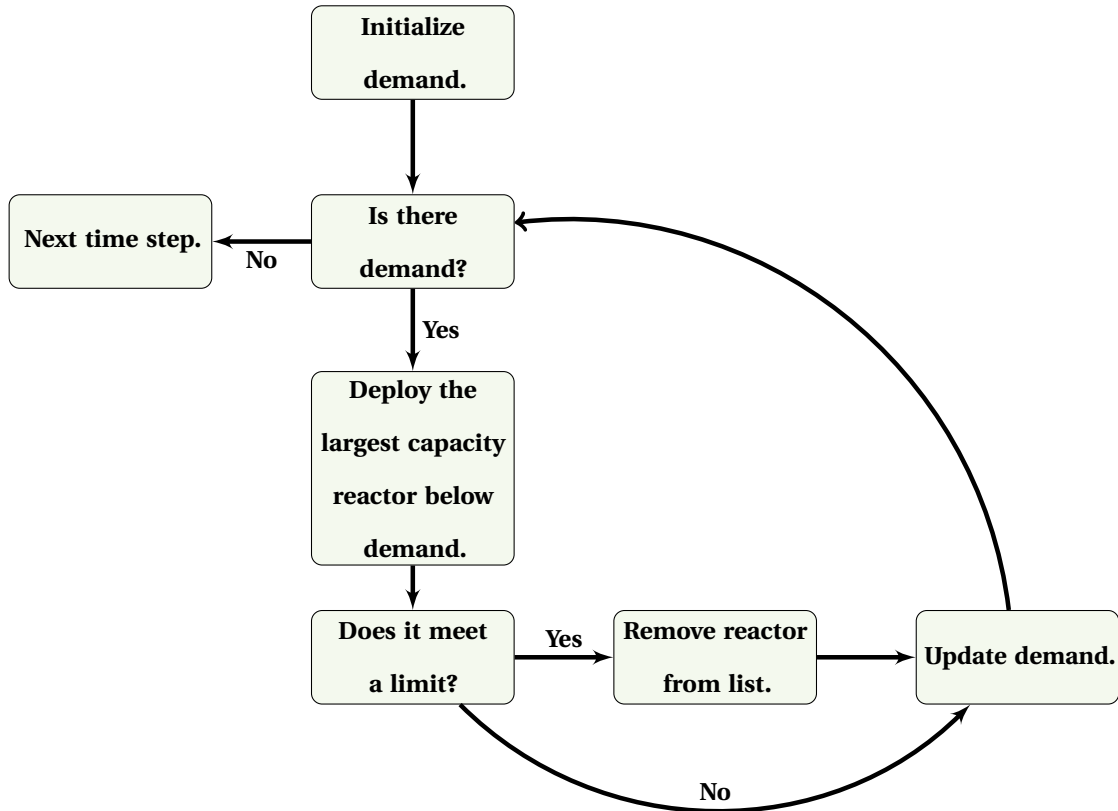


Figure B.2: Pre-determined distribution deployment diagram.

The realism of this deployment scheme mirrors some elements of the capped deployment, but the distribution is a more granular way to account for supply chain constraints. This scheme is most useful when there are known

commitments to specific technologies. It allows the user to indirectly incorporate the evolution of supply chains or workforce constraints over time, and to explicitly incorporate decisions from individual actors. If a user established the nuances of the supply chain constraints in other work, it could be incorporated through this scheme. Under and over-performance of this scheme is difficult to predict, as it depends on the distribution of reactors over time.